



## 저작자표시-비영리-변경금지 2.0 대한민국

이용자는 아래의 조건을 따르는 경우에 한하여 자유롭게

- 이 저작물을 복제, 배포, 전송, 전시, 공연 및 방송할 수 있습니다.

다음과 같은 조건을 따라야 합니다:



저작자표시. 귀하는 원저작자를 표시하여야 합니다.



비영리. 귀하는 이 저작물을 영리 목적으로 이용할 수 없습니다.



변경금지. 귀하는 이 저작물을 개작, 변형 또는 가공할 수 없습니다.

- 귀하는, 이 저작물의 재이용이나 배포의 경우, 이 저작물에 적용된 이용허락조건을 명확하게 나타내어야 합니다.
- 저작권자로부터 별도의 허가를 받으면 이러한 조건들은 적용되지 않습니다.

저작권법에 따른 이용자의 권리는 위의 내용에 의하여 영향을 받지 않습니다.

이것은 [이용허락규약\(Legal Code\)](#)을 이해하기 쉽게 요약한 것입니다.

[Disclaimer](#)

Doctoral Thesis

# Poly(carbyne)s Via Reductive C1 Polymerization

Collin Ryan Cahoon

Department of Chemistry

Graduate School of UNIST

2020

# Poly(carbyne)s Via Reductive C1 Polymerization

Collin Ryan Cahoon

Department of Chemistry

Graduate School of UNIST

# Poly(carbyne)s Via Reductive C1 Polymerization

A thesis/dissertation  
submitted to the Graduate School of UNIST  
in partial fulfillment of the  
requirements for the degree of  
Doctor of Philosophy

Collin Ryan Cahoon

October 22, 2020

Approved by



---

Advisor

Christopher W. Bielawski

# Poly(carbyne)s Via Reductive C1 Polymerization

Collin Ryan Cahoon

This certifies that the thesis/dissertation of Collin Ryan Cahoon is  
approved.


10. 22. 2020

signature  

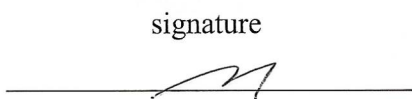

Advisor: Christopher W. Bielawski

signature  

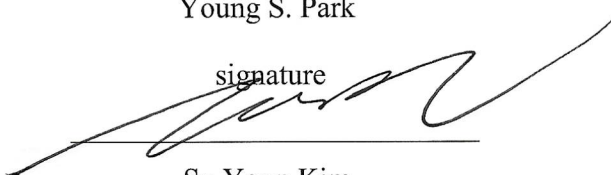

Hoi Ri Moon

signature  


Tae-Hyuk Kwon

signature  


Young S. Park

signature  


So Youn Kim

Portions of this thesis have been published in *Coordination Chemistry Reviews* (DOI: j.ccr.2018.06.017) on July 24, 2018 and in *Polymer International* (DOI: pi.6115) on September 7, 2020. Both Wiley and Elsevier allow article authors to include portions of said articles in a dissertation.

## Abstract

A C1 polymerization is a polymerization in which the backbone of the polymer is grown by one carbon atom for each monomer added to the chain. By polymerizing substituted C1 monomers, persubstituted polymers can be synthesized which contain functionalized pendant groups on each atom of the polymer's backbone. Often times, these persubstituted polymers are not easily synthesized through conventional polymerizations, and can show enhanced physical and/or chemical properties over conventional analogues. One class of C1 polymerizations utilizes carbyne precursors as monomers, which possess a geminal trifunctionalized carbon atom. When polymerized, all three geminal functional groups are replaced by new carbon-carbon bonds formed between monomers. Two of these new carbon-carbon bonds form the backbone of the polymer, with the third bond determining the polymers structure. The final bond can either be a sigma bond to a third monomer, creating a  $sp^3$  network polymer, or a pi bond to one of the other adjacent monomers, forming a highly unsaturated backbone.

To date, only four geminal trihalides, bromoform, chloroform, 1,1,1-trichloroethane, and trichlorotoluene, have been utilized as monomers in C1 carbyne polymerizations. Our work has greatly expand the scope of these polymerizations by varying both the reactive geminal functionalities as well as the pendant groups. Two new functionalities, fluorine and methyl ether, have been utilized as leaving groups in reductive poly(carbyne) synthesis, with trifluorotoluene and trimethyl orthobenzoate both polymerizing into poly(phenyl carbyne). Additionally, a number of ester and ketone containing monomers have successfully been polymerized into the first poly(carbynes) containing polar carbonyl groups. While these new monomers readily polymerized in the presence of Li, higher yields and molecular weights were obtained when an electron transfer agent, such as naphthalene, was also present in the reaction.

Interestingly, when different carbyne precursors are polymerized, we find a dichotomy in both the bonding structure of the polymer backbone as well as the polymerization mechanism. Monomers containing phenyl groups adjacent to the trifunctionalized atom undergo a chain-growth mechanism to give polymers with a branching  $sp^3$  backbone. Conversely, carbyne precursors containing carbonyl groups in the pendant chain exclusively polymerize via a step-growth mechanism to give polymers with unsaturated, linear backbones. In the case of polymers made from trichlorotoluene and pentyl trichloroacetate, the mechanism and final polymer architecture do not depend on reaction conditions, such as the use of an electron transfer agent, and are based solely on the monomer employed.

While the step-growth mechanism of poly(ester carbyne) is expected for a condensation polymerization, the chain condensation seen in the synthesis of poly(phenyl carbyne) is quite uncommon. The presence of a chain-growth mechanism suggests that growing chains of poly(phenyl carbyne) become activated towards further polymerization in comparison to their monomers. On the other hand, poly(ester carbyne)s experience the opposite effect upon polymerizing, becoming less reactive than their monomers. The changes in reactivity are likely caused by the steric and electronic differences which arise from replacing a C-Cl bond with another structural unit. The polymerization of poly(phenyl carbyne) is the first example of a chain condensation polymerization caused by "change of substituent" effects on a single carbon atom, and if the polymerization can be finely tuned, could lead to a controlled synthesis of poly(carbyne)s.





# Table of Contents

Abstract.....	V
List of Tables.....	IX
List of Figures.....	X
Chapter 1. Introduction to C1 Polymerizations.....	1
1.1 Introduction.....	1
1.2 C1 Polymerizations That Utilize Diazo-Containing Monomers.....	3
1.2.1 Copper Catalyzed Polymerizations.....	3
1.2.2 Lewis Acid Catalyzed Polymerizations.....	5
1.2.3 Gold Catalyzed Polymerizations.....	8
1.2.4 Palladium Catalyzed Polymerizations.....	12
1.2.5 Rhodium Catalyzed Polymerizations.....	20
1.3 C1 Polymerizations That Utilize Ylide Monomers.....	24
1.4 Stoichiometric C1 Polymerizations.....	26
1.5 Conclusions and Perspectives.....	28
1.6 References.....	30
Chapter 2. Optimization of Poly(phenyl carbyne) Synthesis and Characterization.....	37
2.1 Introduction .....	37
2.2 Results and Discussion.....	39
2.3 Conclusions.....	44
2.4 Experimental.....	45
2.5 Additional Data.....	47
2.6 References.....	48
Chapter 3. Synthesis and Characterization of New Poly(carbyne)s.....	50
3.1 Introduction.....	50

3.2 Results and Discussion.....	53
3.3 Conclusions.....	59
3.4 Experimental.....	59
3.5 Additional Data.....	63
3.6 References.....	84
 Chapter 4. Polymerization Mechanisms for Poly(carbyne)s.....	 87
4.1 Introduction.....	87
4.2 Results and Discussion.....	97
4.3 Conclusions.....	107
4.4 Experimental.....	108
4.5 Additional Data.....	111
4.6 References.....	114
 Chapter 5. Conclusions and Future Outlooks.....	 116
 Acknowledgements.....	 119

## List of Tables

<b>Table 1.1:</b>	Yields of poly(methyl methylene) as obtained from the polymerization of diazoethane using various metal foils (indicated).....	10
<b>Table 2.1:</b>	Effect of Monomer Concentration on Synthesis of Poly(phenyl carbyne).....	40
<b>Table 2.2:</b>	Effect of Temperature and Time on Synthesis of Poly(phenyl carbyne).....	41
<b>Table 2.3:</b>	Effect of Solvent on Synthesis of Poly(phenyl carbyne).....	42
<b>Table 3.1:</b>	Polymerization of various monomers.....	55
<b>Table 3.2:</b>	Spin Densities Measured for Various Poly(carbyne)s.....	58
<b>Table 3.S1:</b>	Variation of Monomer Concentration Used in the Polymerization of Pentyl Trichloroacetate.....	63
<b>Table 3.S2:</b>	Variation of the Temperature Used in the Polymerization of Pentyl Trichloroacetate.....	63
<b>Table 3.S3:</b>	Variation of Number of Equivalents of Li Used in the Polymerization of Pentyl Trichloroacetate.....	64
<b>Table 3.S4:</b>	Variation of the Naphthalene Concentration Used in the Polymerization of Pentyl Trichloroacetate.....	64

## List of Figures

<b>Figure 1.1:</b>	Structures of various polymers.....	1
<b>Figure 1.2:</b>	Polymerization of 2-butene.....	2
<b>Figure 1.3:</b>	Generalized examples of C1 polymerizations.....	3
<b>Figure 1.4:</b>	Mechanisms for the Lewis acid catalyzed polymerization of diazo compounds.....	7
<b>Figure 1.5:</b>	Reactions of carbonyl containing diazo compounds with boranes.....	8
<b>Figure 1.6:</b>	Mechanism of diazoalkane polymerization on gold surfaces.....	11
<b>Figure 1.7:</b>	Representative examples of Pd-catalyzed C1 polymerizations.....	13
<b>Figure 1.8:</b>	Mechanism for a Pd-catalyzed polymerization of a diazo compound.....	13
<b>Figure 1.9:</b>	Examples of diazo-containing monomers used in Pd-catalyzed C1 Polymerizations.....	14
<b>Figure 1.10:</b>	Insertion of an azo functional group into a growing polymer chain.....	16
<b>Figure 1.11:</b>	Pd complexes that have been used to catalyze C1 polymerizations.....	17
<b>Figure 1.12:</b>	Rh complexes used to catalyze the polymerization of ethyl diazoacetate.....	20
<b>Figure 1.13:</b>	Insertion of methyl diazoacetate into a growing polymer chain.....	23
<b>Figure 1.14:</b>	Insertion of dimethyloxosulfonium methylide into a borane.....	25
<b>Figure 1.15:</b>	Generalized example of “Grignard-like” C1 polymerization of geminal dihalides...	27
<b>Figure 1.16:</b>	Mechanism for Grignard-like C1 polymerizations of germinal dihalides.....	28
<b>Figure 1.17:</b>	General reaction scheme for poly(carbyne) synthesis.....	28
<b>Figure 2.1:</b>	<sup>1</sup> H-NMR of poly(phenyl carbyne).....	43
<b>Figure 2.2:</b>	Solid state <sup>13</sup> C CPMAS NMR of poly(phenyl carbyne).....	44

<b>Figure 2.S1:</b>	$^{13}\text{C}$ -NMR of poly(phenyl carbyne).....	47
<b>Figure 2.S2:</b>	EPR signal of poly(phenyl carbyne).....	47
<b>Figure 2.S3:</b>	FT-IR spectrum for poly(phenyl carbyne).....	48
<b>Figure 3.1:</b>	Theoretical scope of poly(carbyne) monomers.....	50
<b>Figure 3.2:</b>	Synthetic strategies for poly(methyl carbyne) and poly(hydrido carbyne).....	51
<b>Figure 3.3:</b>	Structures of potential poly(carbyne) monomers tested .....	54
<b>Figure 3.4:</b>	IR spectra recorded for pentyl trichloroacetate and its polymeric derivative.....	56
<b>Figure 3.5:</b>	$^{13}\text{C}$ NMR spectra recorded for decyl trichloroacetate before and after polymerization.....	57
<b>Figure 3.6:</b>	CPMAS NMR spectra recorded for the polymer obtained from decyl trichloroacetate.....	59
<b>Figure 3.S1:</b>	$^1\text{H}$ NMR spectrum of pentyl trichloroacetate.....	65
<b>Figure 3.S2:</b>	$^{13}\text{C}$ NMR spectrum of pentyl trichloroacetate.....	65
<b>Figure 3.S3:</b>	$^1\text{H}$ NMR spectrum of decyl trichloroacetate.....	66
<b>Figure 3.S4:</b>	$^{13}\text{C}$ NMR spectrum of decyl trichloroacetate.....	66
<b>Figure 3.S5:</b>	$^1\text{H}$ NMR spectrum of the polymer obtained from pentyl trichloroacetate.....	67
<b>Figure 3.S6:</b>	$^{13}\text{C}$ NMR spectrum of the polymer obtained from pentyl trichloroacetate.....	67
<b>Figure 3.S7:</b>	$^1\text{H}$ NMR spectrum of the polymer obtained from methyl trichloroacetate.....	68
<b>Figure 3.S8:</b>	$^{13}\text{C}$ NMR spectrum of the polymer obtained from methyl trichloroacetate.....	68
<b>Figure 3.S9:</b>	$^1\text{H}$ NMR spectrum of the polymer obtained from decyl trichloroacetate.....	69
<b>Figure 3.S10:</b>	$^{13}\text{C}$ NMR spectrum of the polymer obtained from decyl trichloroacetate.....	69
<b>Figure 3.S11:</b>	$^1\text{H}$ NMR spectrum of the polymer obtained from trichloroacetophenone.....	70

<b>Figure 3.S12:</b>	$^{13}\text{C}$ NMR spectrum of the polymer obtained from trichloroacetophenone.....	70
<b>Figure 3.S13:</b>	$^1\text{H}$ NMR spectrum of the polymer obtained from methyl orthobenzoate.....	71
<b>Figure 3.S14:</b>	$^{13}\text{C}$ NMR spectrum of the polymer obtained from methyl orthobenzoate.....	71
<b>Figure 3.S15:</b>	$^1\text{H}$ NMR spectrum of the polymer obtained from trifluorotoluene.....	72
<b>Figure 3.S16:</b>	$^{13}\text{C}$ NMR spectrum of the polymer obtained from trifluorotoluene.....	72
<b>Figure 3.S17:</b>	$^1\text{H}$ NMR spectrum of the polymer obtained from trichlorotoluene.....	73
<b>Figure 3.S18:</b>	$^{13}\text{C}$ NMR spectrum of the polymer obtained from trichlorotoluene.....	73
<b>Figure 3.S19:</b>	CPMAS NMR spectrum of the polymer obtained from pentyl trichloroacetate.....	74
<b>Figure 3.S20:</b>	CPMAS NMR spectrum of the polymer obtained from methyl trichloroacetate.....	74
<b>Figure 3.S21:</b>	CPMAS NMR spectrum of the polymer obtained from decyl trichloroacetate.....	75
<b>Figure 3.S22:</b>	CPMAS NMR spectrum of the polymer obtained from trichloroacetophenone.....	75
<b>Figure 3.S23:</b>	CPMAS NMR spectrum of the polymer obtained from methyl orthobenzoate.....	76
<b>Figure 3.S24:</b>	CPMAS NMR spectrum of the polymer obtained from trifluorotoluene.....	76
<b>Figure 3.S25:</b>	ATR FT-IR spectrum recorded for pentyl trichloroacetate.....	77
<b>Figure 3.S26:</b>	ATR FT-IR spectrum recorded for decyl trichloroacetate.....	77
<b>Figure 3.S27:</b>	FT-IR spectrum of the polymer obtained from pentyl trichloroacetate.....	78
<b>Figure 3.S28:</b>	FT-IR spectrum of the polymer obtained from methyl trichloroacetate.....	78
<b>Figure 3.S29:</b>	FT-IR spectrum of the polymer obtained from decyl trichloroacetate.....	79
<b>Figure 3.S30:</b>	FT-IR spectrum of the polymer obtained from trichloroacetophenone.....	79
<b>Figure 3.S31:</b>	FT-IR spectrum of the polymer obtained from methyl orthobenzoate.....	80
<b>Figure 3.S32:</b>	FT-IR spectrum of the polymer obtained from trifluorotoluene.....	80

<b>Figure 3.S33:</b>	SEC data of the polymer obtained from pentyl trichloroacetate.....	81
<b>Figure 3.S34:</b>	SEC data of the polymer obtained from methyl trichloroacetate.....	81
<b>Figure 3.S35:</b>	SEC data of the polymer obtained from decyl trichloroacetate.....	82
<b>Figure 3.S36:</b>	SEC data of the polymer obtained from trichloroacetophenone.....	82
<b>Figure 3.S37:</b>	SEC data of the polymer obtained from methyl orthobenzoate.....	83
<b>Figure 3.S38:</b>	SEC data of the polymer obtained from trifluorotoluene.....	83
<b>Figure 3.S39:</b>	SEC data of the polymer obtained from trichlorotoluene.....	84
<b>Figure 4.1:</b>	General reaction schemes for step-growth polymerizations.....	88
<b>Figure 4.2:</b>	Graphs of typical trends in step-growth polymerizations.....	89
<b>Figure 4.3:</b>	General reaction scheme for a chain-growth polymerization.....	91
<b>Figure 4.4:</b>	Graphs of the molecular weight vs.extent of conversion relationship for normal and living chain-growth polymerizations.....	92
<b>Figure 4.5:</b>	Mechanism for the living anionic polymerization of styrene.....	93
<b>Figure 4.6:</b>	Mechanism for the NMRP of styrene.....	94
<b>Figure 4.7:</b>	Mechanism for the GRIM polymerization of hexyl thiophene.....	95
<b>Figure 4.8:</b>	Basis and examples of chain-condensation arising from change of substituent effects.....	97
<b>Figure 4.9:</b>	Fundamental coupling reaction in poly(carbyne)s with examples.....	98
<b>Figure 4.10:</b>	Theoretical monomer consumption during poly(carbyne) formation for ideal step-growth and chain-growth polymerizations.....	99
<b>Figure 4.11:</b>	Graphs of monomer concentration vs. Eq. of Li added for trichlorotoluene and pentyl trichloroacetate, both with and without naphthalene present.....	100
<b>Figure 4.12:</b>	Graph of monomer concentration vs. extent of conversion for trichlorotoluene and pentyl trichloroacetate with the theoretical curve for an ideal step-growth polymerization.....	101

<b>Figure 4.13:</b>	Method in which change of substituent effect occurs in poly(carbyne) formation....	102
<b>Figure 4.14:</b>	Relationship between reduction potentials of poly(carbyne) monomers and dimers..	103
<b>Figure 4.15:</b>	Synthetic strategies for synthesizing dimers of trichlorotoluene and pentyl trichloroacetate.....	104
<b>Figure 4.16:</b>	Cyclic voltammograms for poly(carybne) monomers and their dimers.....	105
<b>Figure 4.17:</b>	Possible mechanisms for poly(carbyne) formation.....	106
<b>Figure 4.S1:</b>	$^1\text{H}$ NMR spectrum of 1,1,2,2-tetrachloro-1,2-diphenylethane.....	111
<b>Figure 4.S2:</b>	$^{13}\text{C}$ NMR spectrum of 1,1,2,2-tetrachloro-1,2-diphenylethane.....	111
<b>Figure 4.S3:</b>	$^1\text{H}$ NMR spectrum of Dimethyl 2,2,3,3-tetrachlorosuccinate .....	112
<b>Figure 4.S4:</b>	$^{13}\text{C}$ NMR spectrum of Dimethyl 2,2,3,3-tetrachlorosuccinate .....	112
<b>Figure 4.S3:</b>	$^1\text{H}$ NMR spectrum of Dipentyl 2,2,3,3-tetrachlorosuccinate .....	113
<b>Figure 4.S4:</b>	$^{13}\text{C}$ NMR spectrum of Dipentyl 2,2,3,3-tetrachlorosuccinate .....	113



# Chapter 1: Introduction to C1 Polymerizations

## 1.1 Introduction

Since the first half of the 20th century, synthetic polymers have become vital materials in contemporary society. Polyolefins in particular, such as poly(ethylene), poly(propylene), and poly(styrene) (see Figure 1), have become ubiquitous and frequently find utility in consumer goods, building materials, and medicine, among other applications. As reflected in the nomenclature, polyolefins are comprised of multiple, unsaturated alkenes (olefins) interconnected through a process wherein the length of the growing polymer chain increases by two carbon atoms per monomer addition cycle. Such processes may be classified as “C2 polymerizations” and, depending on the monomer employed, can be conducted using free radical, anionic, cationic, or transition metal-catalyzed polymerization techniques.<sup>1</sup>

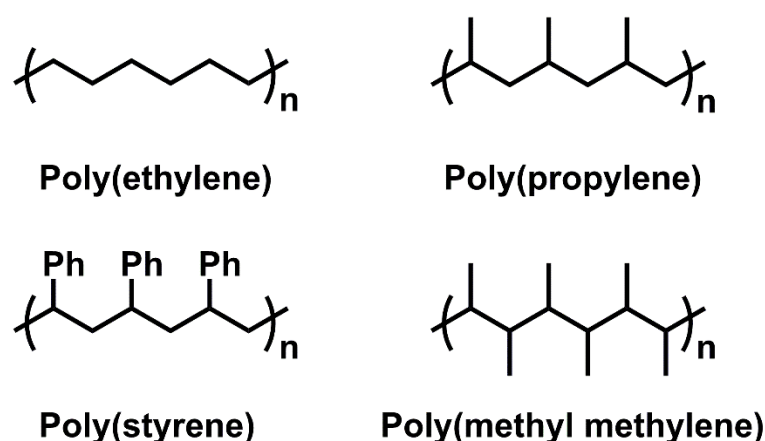


**Figure 1.** Structures of various polymers

While many polymers have been prepared using C2 polymerization methods, limitations exist that prevent certain structures from being realized. For example, persubstituted polymers, which feature pendant (non-hydrogen) substituents on every atom of the backbone, are often incompatible with known C2 polymerization techniques for steric and/or electronic reasons. Regardless, polymers with such

substitution patterns offer the potential to display relatively high densities of functional groups, adopt unusual architectures, or exhibit high crystallinities due to restricted bond rotation.

The prototypical example of a persubstituted polymer is poly(methyl methylene). While large quantities of poly(propylene) are synthesized every year, poly(methyl methylene) remains relatively unknown. Conventional polymerizations of 2-butene, a potential olefinic precursor to poly(methyl methylene), do not afford the persubstituted polymer as the major product; instead, a series of rearrangements result in the formation of one pendant methyl group for every three carbons atoms along the resulting polymer backbone (see Figure 2).<sup>2</sup> Similar isomerization phenomena are observed during the polymerizations of other internal olefins and, to the best of our knowledge, well-defined poly(alkyl methylene)s are not readily accessible through vinyl polymerization methodologies.<sup>3-5</sup>

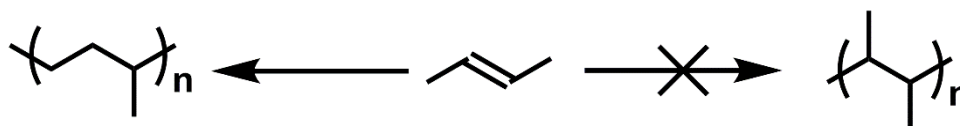


**Figure 2.** The polymerization of 2-butene typically results in rearrangement

“C1 polymerizations” offer access to poly(alkyl methylene)s and other persubstituted polymers.<sup>6</sup> As the name implies, C1 polymerizations grow polymer chains in one carbon atom increments during the propagation step. The monomers for such polymerizations are formally divalent carbenes or trivalent carbynes (see Figures 3a and 3b). Unfortunately, carbenes and carbynes are typically challenging to isolate and, as such, are generally introduced as their appropriate precursors or derivatives. Common examples include diazo compounds, ylides, geminal dihalides, trihalides, various transition metal complexes, and isocyanides (see Figure 3c). In some cases, C1 polymerizations are accompanied by the condensation of small molecules (byproducts), which may serve to drive the reactions. Additionally, many C1 monomers require activation, predominately through metal<sup>6-8</sup> or Lewis acid<sup>6, 8-10</sup> catalysts. In the former, polymerizations can be initiated through the addition of either stoichiometric or catalytic quantities of metal.

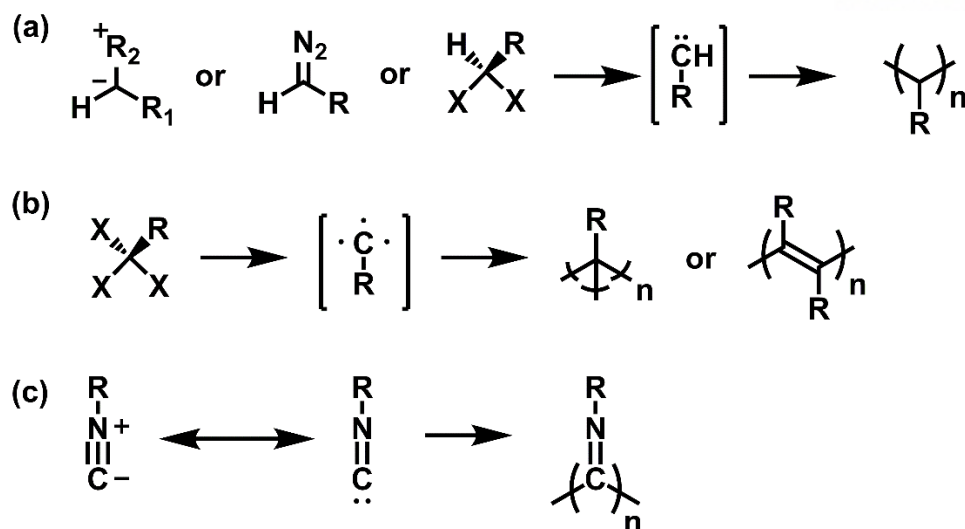


**Figure 3.** Generalized examples of C1 polymerizations as conducted using (a) carbene, (b) carbyne, or (c) isocyanide precursors as monomers.

Herein we describe the use of various carbene and carbyne precursors in C1 polymerizations. The following three sections will focus on the polymerizations of diazo compounds and ylides which are among the most common monomers used in C1 polymerizations. The sections are further divided according to the catalysts used to facilitate such chemistry. Discussions will begin with copper, which was the first metal employed to catalyze the polymerization of diazo compounds. Later subsections will describe the use of other catalysts, including Lewis-acids, gold, palladium, and rhodium. The penultimate section will briefly discuss C1 polymerizations that have been conducted using stoichiometric quantities of metals. Finally, concluding remarks as well as some perspectives for the field will be offered. Throughout the chapter, emphasis will be placed on the scope of the polymerization chemistry, mechanistic insight, and potential opportunities for further development.

## 1.2 C1 Polymerizations That Utilize Diazo-Containing Monomers

### 1.2.1 Copper-Catalyzed Polymerizations

In 1948, it was reported that treating an ethereal solution of diazomethane with copper powder resulted in the formation of poly(methylene), a C1 analog of poly(ethylene), in about 10% yield after 24 hours.<sup>11</sup> Spectral analysis of the polymer using infrared (IR) spectroscopy displayed signals characteristic of a polymer made entirely of methylene groups, and the molecular weight of the polymer was determined to be 20 kDa using dilute solution viscometry. Various Cu(II) salts, including copper

stearate, citrate, succinate, or benzoate, were also reported to afford poly(methylene) from diazomethane and, while the yields were similar to those obtained using copper powder, the polymers produced were of relatively lower molecular weight.<sup>12, 13</sup>

A similar reaction using diazoethane and copper powder in a 5:1 ratio afforded poly(methyl methylene) with a molecular weight of 5.8 kDa in over 80% yield.<sup>11</sup> Similar to diazomethane, diazoethane was also polymerized using a variety of Cu(I) and Cu(II) and yielded similar quantities of polymers with molecular weights of 7.2 kDa and 2.5 kDa, respectively. Reduction of the initial monomer concentration from 0.12 M to 0.06 M increased the molecular weights of the polymeric product to as high as 14 kDa. Relatively high yields were reported with copper stearate, which also enabled the use of monomer to catalyst ratios that were as high as 10,000.<sup>13</sup> The IR spectra recorded for the polymers obtained from diazoethane were reported to differ from the data acquired for poly(methylene) and were consistent with the presence of methyl pendant groups on every carbon atom of the polymer.

Using copper powder, Ray and coworkers reported that the polymerization of 1-diazopropane gave poly(ethyl methylene) with a molecular weight of 7 kDa in a 95% yield.<sup>11</sup> Again, IR was used to identify the unique signals from the ethyl pendant groups. Attempts to polymerize longer or secondary alkanes, such as 1-diazobutane or 2-diazopropane, with copper powder did not afford polymer. However, 1-diazobutane was subsequently polymerized in a 92% yield by Mesrobian and coworkers in 1955 using Cu(II) stearate, although molecular weight information was not provided.<sup>13</sup> While no subsequent reports of polymerizations of higher diazoalkanes with copper have been reported to the best of our knowledge, Liu and coworkers relatively recently (2002) described the polymerization of allyl diazoacetate using copper powder.<sup>14</sup> The polymer was shown to have a molecular weight of 3 kDa, as determined by size exclusion chromatography (SEC), and a nuclear magnetic resonance (NMR) spectroscopic analysis revealed that the polymer retained the ester and olefin functional groups found in the monomer.

Several mechanisms have been proposed for the copper-catalyzed polymerization of diazoalkanes, and the active species is generally considered to be in the +1 oxidation state.<sup>15</sup> One proposal involves Cu(I)-stabilized free radicals as the propagating species; however, the addition of radical scavengers to such copper-catalyzed reactions were reported to not effect on the molecular weights or yields of the polymer products.<sup>12, 13</sup> Another proposal relies on a cationic chain-growth mechanism, although the presence of nucleophiles is not seen to prematurely terminate the polymerization reaction as is seen in similar polymerizations.<sup>15</sup> Chain propagation via insertion of the

monomer into a Cu-alkyl bond has also been proposed. Such a mechanism is similar to those described for other catalysts that utilize diazoalkanes as monomers and is discussed in more detail below.

In recent years, the paucity of publications using copper-catalyzed diazoalkane polymerizations may be due to the development of catalytic systems that display more desirable outcomes. For example, diazomethane treated with boron trifluoride was reported to form a poly(methylene) with a molecular weight over 3.3 MDa with 30%.<sup>16</sup> Gold catalysts also appear to outperform copper as nearly quantitative yields of poly(methylene) can be obtained, and a broader scope of monomers may be used (*vide infra*). However, copper may hold economic benefits compared to gold or other metals, and the resurgence of copper catalysts for organic transformations<sup>17-19</sup> has led to the development of commercially available copper catalysts that could promote C1 polymerization reactions.

## 1.2.2 Lewis Acid-Catalyzed Polymerizations

The first reports of a Lewis-acid catalyzed polymerization of diazo compounds came from Meerwein in 1948.<sup>20</sup> He reported that the addition of diazomethane to a room temperature ether solution of various boronic esters produced an insoluble polymer with the chemical formula  $(CH_2)_n$ . Repeating the reactions at 0 °C, Buckley reported the formation of a polymer spectroscopically identical (by IR and X-ray diffraction) to poly(methylene) prepared using a copper catalyst.<sup>21</sup> The poly(methylene) was soluble in boiling tetralin and was analyzed through dilute solution viscosity to give a molecular weight estimated at 200 kDa. The reaction of diazomethane with boron trifluoride at 0 °C was found to progress in a violent manner and produced an even larger polymer of up to 3 MDa.<sup>16</sup> While boron trifluoride was found to be the most reactive Lewis-acid toward diazomethane, a large number of boron compounds were found to catalyze the polymerization of diazomethane, including trace amounts of boronic esters found in silicone grease.<sup>22, 23</sup>

While Buckley was unsuccessful in synthesizing homopolymers from larger diazoalkanes with boronic esters, he showed diazoalkanes up to 1-diazododecane polymerized as a copolymer with diazomethane.<sup>21</sup> As is expected, these copolymers had increasing solubility and decreasing crystallinity as the length and content of the larger alkyl component increased. Use of a trinaphthyl boron catalyst was also reported to lead to diazomethane copolymers with diazoethane and diazoisobutane which reached molecular weights up to 70 kDa.<sup>24</sup> The first successful homopolymerization of higher diazocompounds using a Lewis-acid catalyst was achieved by using  $BF_3$  and resulted in the formation of poly(ethylidene)<sup>25</sup> and poly(benzylidene).<sup>26</sup> When polymerized at 0 °C, poly(methyl methylene) of 5 kDa was formed, but further cooling of the polymerization to -115 °C increased the molecular weight

up to 20 kDa. More recently,  $\text{BF}_3$  was used as a catalyst to produce polymers with paracyclophane side chains. Both racemic and chiral (S and R) versions of the monomer, 4-diazomethyl[2.2]paracyclophane were prepared and successfully polymerized at  $-78^\circ\text{C}$  leading to the isolation of polymers of less than 1.2 kDa in 13 – 20% yields. Interestingly, UV-Vis spectra of these polymers showed a strong bathochromic shift compared to both [2.2.]paracyclophane as well as the C2 polymer equivalent, poly(4-vinyl[2.2]paracyclophane). This was attributed to transannular  $\pi$ - $\pi$  interactions which occur due to the dense packing of the aromatic side chains in the C1 polymer.<sup>27</sup>

A number of mechanisms have been proposed for the Lewis-acid catalyzed polymerization of diazo compounds, and it is generally considered that multiple might be operative based on the Lewis acid used. The first mechanism, proposed by Kantor, was initiated through the complexation of a diazo monomer to the  $\text{BR}_3$  complex, followed by liberation of nitrogen to form the carbocation (Figure 4, a).<sup>16</sup> Propagation occurred through nucleophilic attack by another monomer onto the carbocation chain end, followed by liberation of nitrogen from the new end group. Feltzin and Davies both proposed a similar mechanism that differed from Kantor's in that propagation occurred through an  $\text{S}_{\text{N}}2$  reaction on the chain end, with a diazo monomer liberating and replacing the  $\text{N}_2$  functionality at the end of a growing chain.<sup>13, 23</sup> In all three cases, termination occurs through the loss of a proton and formation of an alkene end group. Finally, an insertion mechanism was proposed by Bawn which differed considerably from the other two. This mechanism consisted of complexation of a diazo monomer to the  $\text{BR}_3$  followed by insertion of the monomer into the B-R bond (in the case of initiation) or growing polymer chain (in the case of propagation) with a concerted loss of  $\text{N}_2$  (Figure 4, b).<sup>26</sup> Termination, in this case, was caused by the loss of  $\text{N}_2$  from a complexed monomer followed by hydride transfer mediated through formation of a 5 membered ring. This leads to an unsaturated polymer end group as well as reforming of a  $\text{BR}_3$  species. This mechanism is similar to those proposed for other more modern C1 polymerizations.

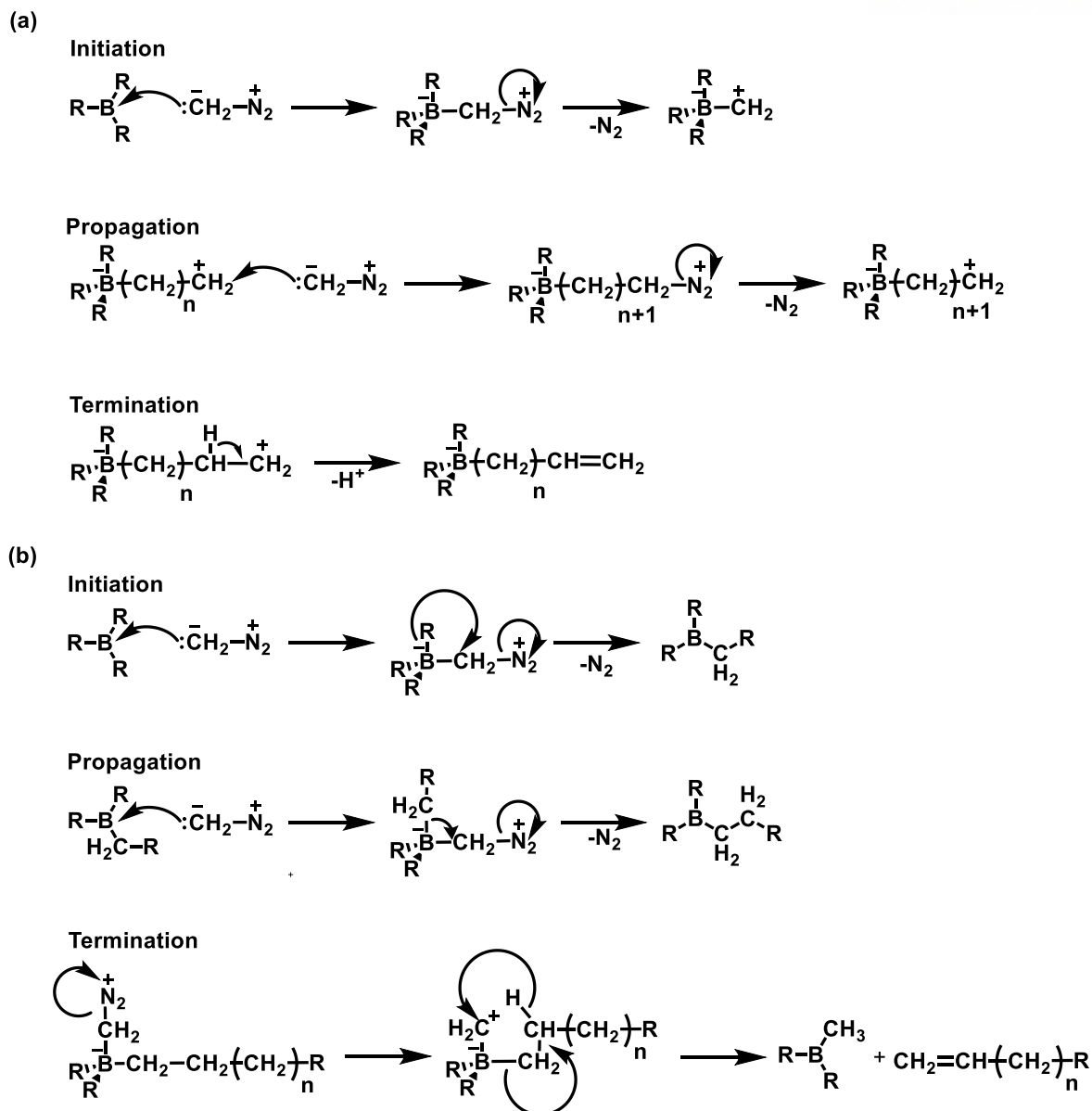


**Figure 4.** Cationic (a) and insertion (b) mechanisms for the Lewis acid-catalyzed polymerization of diazo compounds.

In comparison to alkyl diazo compounds, polymerization of polar carbonyl-containing diazo compounds by Lewis acids is substantially more difficult. Carbonyl-containing diazo compounds including esters, ketones, and aldehydes have been observed to undergo single insertions into the C-B bond of alkyl boranes, however further insertions are not seen.<sup>28-31</sup> This has been reported to occur due to the formation of a stable O-boron enolate, which occurs from isomerization of the complex after insertion of the diazo compound.<sup>32</sup> When the compound is exposed to aqueous conditions, the complex is hydrolyzed and the carbonyl-containing addition product is isolated. Shea found that borane ( $\text{BH}_3$ ) was able to catalyze multiple insertions of ethyl diazoacetate (EDA) leading to a mixture of products

ranging from ethyl acetate to hexamers, with dimer being the primary product (38%).<sup>33</sup> Computational experiments showed that the C-boron enolate was more stable than the O-boron enolate for all insertion products after the first insertion due to interactions between boron and the carbonyl of the  $\gamma$ -carbonyl.

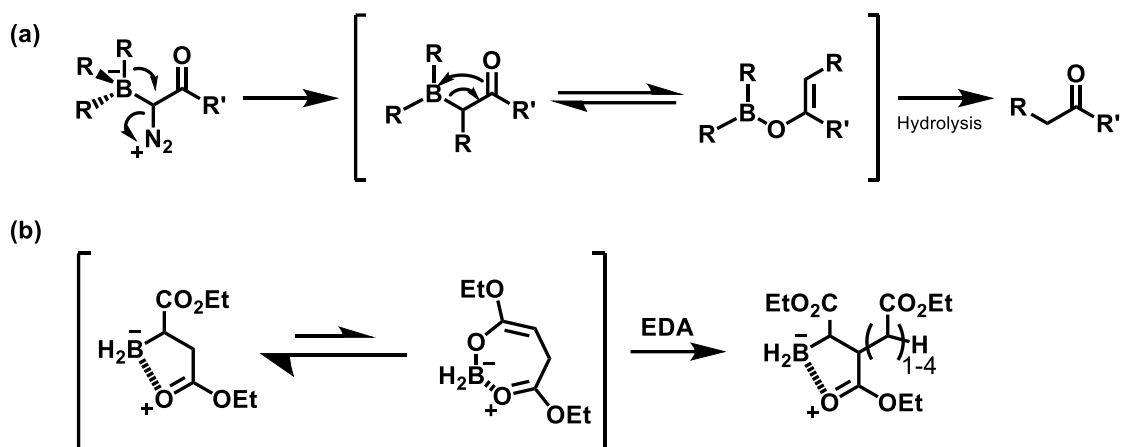


**Figure 5.** The reaction of carbonyl-containing diazo compounds with boranes (a) often results in a single insertion due to keto-enol tautomerism. Shea showed that EDA was able to form a stable C-boron enolate after two insertions, and was able to achieve products which had undergone 6 insertions (b).

Diazoketones were successfully polymerized by Inoue through the use of trialkyl aluminum and diisobutylaluminum hydride (DIBAL).<sup>34</sup> Polymerization of (*E*)-1-diazo-3-nonen-2-one and (*E*)-1-diazo-4-phenyl-3-butene-2-one led to the isolation of polymers with  $M_n$  values between 2-5 kDa in yields up to 50%, however the polymer backbone was found to contain up to 33% azo and ethylidene groups. The polymerization mechanism proposed was similar to the one proposed by Bawn, with the diazocompounds iteratively inserting in between the metal-carbon bonds. The azo addition process was proposed to occur when a terminal nitrogen atom of the monomer inserts into the growing polymer chain instead of undergoing expulsion. Reductive cleavage of the acyl groups was thought to be responsible for the formation of ethylidene groups in the backbone.

### 1.2.3 Gold Catalyzed Polymerizations

Saini and Nasini reported the first use of gold to synthesize poly(alkyl methylene)s in 1956. They reported that a quantitative yield of poly(methylene) was obtained when  $\text{AuCl}_3$  was added to an



ethereal solution of diazomethane.<sup>35</sup> The resulting polymer was determined by dilute solution viscometry to exhibit a molecular weight of 5 kDa. Higher diazoalkanes, up to 1-diazobutane, also underwent polymerization and yielded oligomers (ca. 1 kDa) under similar conditions. Polymer yields could be increased from approximately 10–30% to quantitative when the solvent system was switched from ether to *n*-octane.<sup>36</sup> Even larger diazoalkanes, up to 1-diazoctane, were also reported to polymerize in *n*-octane and afforded polymers in yields between 30 and 70%. Molecular weights between 3.5 and 8.5 kDa, as determined by vapor phase osmometry (VPO), were reported for these polymers. The polymerization of these larger diazoalkanes produced a crystalline fraction in addition to an amorphous material.<sup>35</sup> The crystalline component was only present when the polymerization was performed in ether, and made up approximately 5% and 1-2% of the total yield for poly(methyl methylene) and poly(ethyl methylene) or poly(propyl methylene), respectively. The increased crystallinity was attributed to stereoregular positioning of the alkyl sidechains along the backbone, as confirmed via X-ray diffraction analyses.

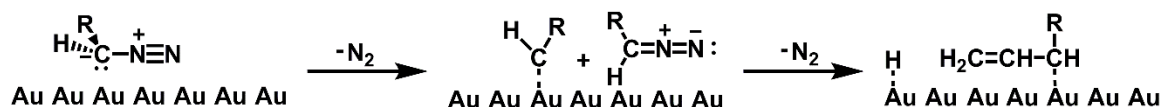
In all of the cases described above, the transformation of AuCl<sub>3</sub> to a colloidal gold through reduction was reported to occur immediately upon introduction to the diazoalkane solution. For example, the addition of AuCl<sub>3</sub> to an ethereal solution of diazomethane led to the formation of a red colloid that contained gold particles with a diameter of about 13 nm, as determined by electron microscopy.<sup>35</sup> After the polymerization reaction reached completion, the gold particles were recovered and washed to remove residual AuCl<sub>3</sub>. Subsequent addition of a freshly prepared solution of diazomethane to the gold particles led to further polymerization and afforded polymers in similar yields and molecular weights. Collectively, these observations indicated that the metallic gold particles, and not the AuCl<sub>3</sub>, were the active catalysts for these polymerizations. Diazomethane and diazoethane were also polymerized with gold foils, which supported the notion that metallic gold may be the catalytically active species in these reactions. While various other metal foils were used to catalyze the polymerization of diazoethane (see Table 1), only gold afforded crystalline polymer.<sup>35</sup>

**Table 1.** Yields of poly(methyl methylene) as obtained from the polymerization of diazoethane using various metal foils (indicated).

Metal	Yield (%)	Metal	Yield (%)
Cu	90	Pt	27
Ti	67	Co	26
Fe	64	Zn	25
Mg	57	Cd	22
W	45	Au	14
Ni	38	Cr	13
V	31	Al	7
Mn	30	Mo	3
Ta	30		

In 1963, Nasini and Trossarelli proposed a mechanism for the gold-catalyzed polymerization of diazoalkanes (see Figure 6).<sup>37</sup> The mechanism begins with the adsorption of a diazoalkane molecule onto the metal, which was reported to result in the formation of a bond between the interacting carbon and gold atoms and the expulsion of nitrogen gas. Subsequent attack of another diazoalkane molecule on the adsorbed monomer, followed by nitrogen loss and migration of a hydrogen atom to gold, gives an unsaturated species that initiates the polymerization reaction. Propagation occurs with insertion of another monomer into the Au–C bond along with the release of nitrogen, increasing the length of the polymer by one carbon unit. Termination occurs when hydrogen recombines with the polymer end-group via reductive elimination.

### Initiation



### Propagation

### Termination

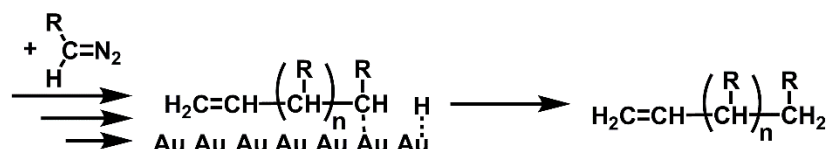


**Figure 6.** A proposed mechanism of a diazoalkane polymerization as catalyzed by a gold surface.

In 1997, Allara et. al. used surface techniques such as ellipsometry and atomic force microscopy to further elucidate the mechanism of poly(methylene) growth on gold surfaces.<sup>38</sup> Polymer formation was found to be initially localized in nanoclusters around high energy defect sites on the gold. These high energy sites were proposed to catalyze the complexation and decomposition of diazomethane to gold-bound carbenes. Combination of two carbenes led to formation of biradical “excited” ethene molecules that initiated the polymerization of surface-bound monomers and effectively resulted in the growth of polymer chains. Termination was reported to occur through a disproportionation process that resulted in the formation of vinyl and methyl end-groups. Finally, as full surface coverage was reached, the polymerization stopped and poly(methylene) films of up to 100 nm thickness were formed.

In 2002, Guo and Jennings investigated the effects of mixed-metal surfaces on growing diazomethane films.<sup>39</sup> A variety of gold films, modified with varying surface concentrations of Ag or Cu, were used to catalyze the growth of poly(methylene). A 60% coverage of Cu or Ag on the Au surface led to thicker film formation than those seen on just gold, with films being 250 and 150 nm thicker, respectively. Additionally, at a 90% surface concentration of Cu, a more pronounced effect was seen, with the films produced being thicker than those formed on pure copper. Higher coverages of Ag resulted in an opposite effect, wherein growth was limited when compared to the film with 60% Ag coverage. The different effects of Cu and Ag on polymer growth were attributed to the metals performing different roles in the polymerization system. At low concentrations of Ag, the active atoms may be spread apart and function as defect sites on the Au to initiate polymerization chemistry. In contrast, higher concentrations of Ag may facilitate the formation of densely packed ad-layers that effectively block the Au and thus prevent polymerization. The combination of Cu and Au may be

synergistic, however, with the former stabilizing methyldiene units on the surface and the latter minimizing surface oxidation.

In order to introduce polar functionality, Bai and Jennings later (2005) used Au surfaces to grow copolymers of diazomethane and ethyl diazoacetate.<sup>40</sup> Ethyl diazoacetate did not polymerize on gold by itself, but up to 5% incorporation of the ester functional group was achieved in copolymerizations. Regardless, the film thickness varied linearly with ethyl diazoacetate concentration and films of up to nearly 800 nm were formed within 24 hours. The enhanced growth rate was attributed to a co-catalytic effect of ethyl diazoacetate intermediates complexed to gold near the growing chain. Further functionalization of the films was successfully achieved through post-synthetic modification as hydrolysis led to the formation of carboxylic acid groups on the surface<sup>41</sup> and further transformation afforded derivatives that featured pendant amines.<sup>42</sup> The carboxylic acid- and amino-functionalized films were found to be hydrophobic when neutral but became charged and hydrophilic when subjected to basic or acidic media, respectively.

Gold has been successfully used to produce polymers from a number of diazoalkanes. In some cases, the polymers produced are unique and have not yet been synthesized through any other process (e.g., poly(butyl methylene)).<sup>36</sup> The production of higher molecular weight polymers, as well as the successful homopolymerization of monomers containing polar functionalities, remain areas of opportunity. Considering that AuCl<sub>3</sub> appears to undergo reduction in situ to metallic gold colloids, the use of derivatives that exhibit increased solubilities and/or facilitate catalyst formation may offer improved control over the polymerization reactions or provide insight into the underlying mechanisms.

## 1.2.4 Palladium-Catalyzed Polymerizations

In 2003, Inoue reported the first C1 polymerization using a homogenous palladium complex.<sup>43</sup> The study used diazoacetates as monomers, which had historically not been used due to strong complexation between the metal catalyst and the carbonyl group on the monomer. Methyl diazoacetate (**1**) and ethyl diazoacetate (**2**) were successfully polymerized using PdCl<sub>2</sub> and pyridine or triethylamine in a mixture of DCM and toluene at 55 °C (see Figure 7). While the yields were quantitative, low molecular weights were seen with degrees of polymerization (DP) less than 10 as determined by SEC. Moreover, increasing the monomer-to-catalyst ratio had no effect on molecular weight.

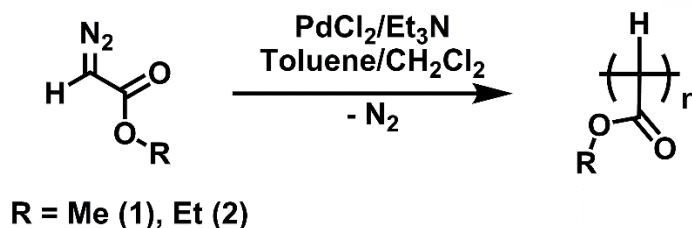
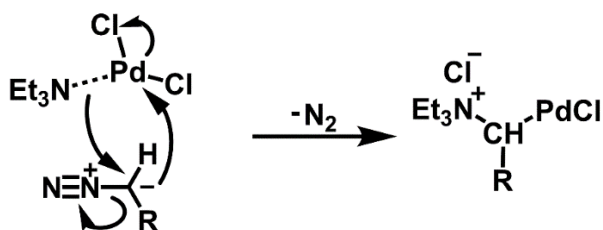


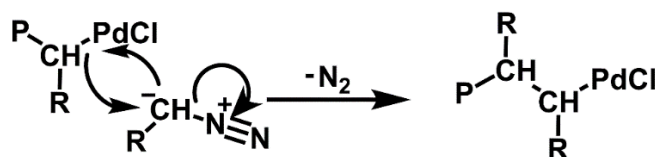
**Figure 7.** Representative examples of Pd-catalyzed C1 polymerizations.

The authors proposed an insertion mechanism for the polymerization similar to that seen for other diazoacetate/ metal systems (see Figure 8).<sup>43</sup> Initiation occurs with a simultaneous nucleophilic attack by an amine on the  $\alpha$ -carbon of the diazoacetate and the release of  $\text{N}_2$  with formation of a new Pd-C bond. Propagation occurs through subsequent nucleophilic attack by another monomer, leading to the monomer being inserted into the Pd-C bond. Multiple methods of termination occur in these polymerizations and are determined by the catalyst used (*vide infra*). In the case of  $\text{PdCl}_2$ -catalyzed polymerizations, it was proposed that two polymer chains growing on the same Pd center undergo reductive elimination to form a new C-C bond. The presence of amino groups on both ends of the polymer, as determined by matrix assisted laser desorption/ionization (MALDI) mass spectrometry supported this theory.

#### Initiation



#### Propagation



#### Termination

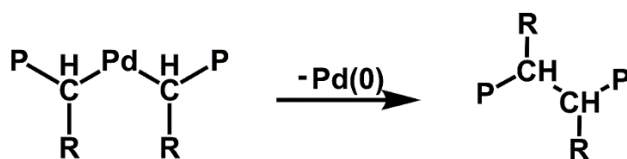


**Figure 8.** Proposed mechanism for a Pd-catalyzed polymerization of a diazo compound. P = polymer.

Subsequently, Inoue, Ihara, and coworkers have worked extensively to expand the scope of monomers amenable to Pd-catalyzed C1 polymerizations (see Figure 9). In subsequent reports [PdCl<sub>2</sub>(MeCN)<sub>2</sub>] was used in lieu of PdCl<sub>2</sub> because of its higher solubility. Additionally, higher yields and molecular weights were obtained when the reactions were performed at an elevated temperature (80 °C) and/or the amino additives were excluded. In the latter case, weak nucleophilic species present in solution such as MeCN or H<sub>2</sub>O were responsible for initiating the polymerizations. Under the aforementioned reaction conditions, monomers containing linear (**11–15**) or cyclic ketones (**18–19**), amides (**21, 22**), ferrocenyl groups (**27, 52**), and multiple diazo groups (**25–27**) were successfully polymerized.<sup>44–46</sup>

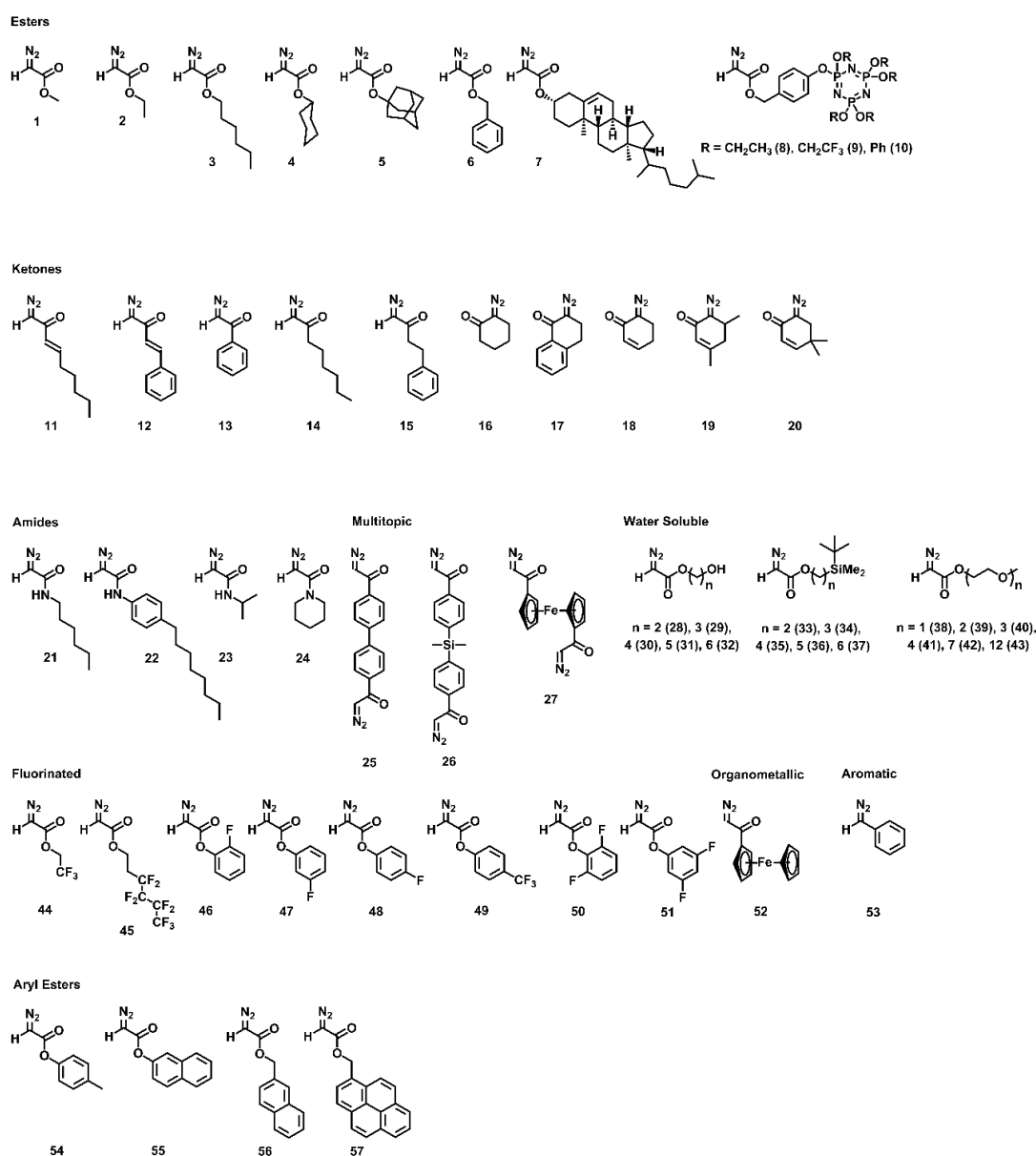


**Figure 9.** Examples of diazo-containing monomers used in Pd-catalyzed C1 polymerizations.

Monomer structure, particularly for the ketone-containing derivatives, was found to greatly influence the quality of polymers formed using  $[\text{PdCl}_2(\text{MeCN})_2]$ . For example, monomers **11** and **12**, containing linear  $\alpha,\beta$ -unsaturated diazoketones, afforded polymers with molecular weights of 2.40 and 1.74 kDa in approximately 37 and 63% yields, respectively.<sup>44</sup> However, the diazoketones **14** and **15**, which lacked the double bond, were found to be less active towards polymerization and yielded approximately 13 and 16%, respectively, of relatively low molecular weight polymers (up to 0.89 kDa). Similar effects were observed when cyclic diazoketones were polymerized with  $[\text{PdCl}_2(\text{MeCN})_2]$ . While **18** was polymerized in approximately 24% yield and afforded a polymer with a molecular weight of 1.4 kDa, the saturated and aromatic analogs **16** and **17** did not undergo homopolymerization.<sup>46</sup>

Monomers with bulky functional groups also retarded the activity of the  $[\text{PdCl}_2(\text{MeCN})_2]$  catalyst. For example, subjecting the 3,5-disubstituted monomer **19** to the catalyst afforded a 9% yield of a 0.9 kDa polymer whereas the 4,4-disubstituted monomer **20** was unreactive.<sup>46</sup> The pendant phenyl group of 2-diazoacetophenone (**13**) also effectively hindered propagation as a polymer with a molecular weight of 0.42 kDa was obtained in 25% yield.<sup>44</sup> Bulky diazoacetamides also showed a reduced activity towards polymerization. For example, low molecular weight polymers (up to 1.89 kDa) in yields of up to 11% were obtained when amides **21** and **22** were used as monomers.<sup>45</sup> Analogues that featured relatively bulky substituents, such as *N*-isopropyl (**23**) or piperidinyl groups (**24**), did not undergo homopolymerization.

To prepare relatively high molecular weight polymers, monomers that feature multiple diazo groups (e.g., **25**, **26**, or **27**) were polymerized in the presence of a (monotopic) diazo compound (e.g., **2**, **11**, or **12**).<sup>47</sup> For example, when **25** or **26** was copolymerized with **11** in increasing feed ratios, the molecular weights of the resulting materials were significantly higher (up to 50 kDa) than the values reported for the homopolymers of **11**. At feed ratios exceeding 25%, the copolymers became insoluble. The formation of higher molecular weight and/or insoluble materials is consistent with the formation of crosslinked polymer networks.

Elemental analysis of polymers prepared using ketone or amide containing monomers contained higher nitrogen contents than expected. This fact was attributed to the incorporation of azo groups into the polymer backbone, which was confirmed through the observation of characteristic Raman signal at  $1560\text{ cm}^{-1}$ .<sup>48</sup> The inclusion of azo groups into the polymer was thought to occur in a fashion similar to what is proposed with diazoacetates and alkyl aluminum compounds (see Figure 10).<sup>44</sup> The azo content varied based on monomer employed, with linear diazoketones showing less than 5% incorporation while cyclic ketones and amides contained up to 25% of the azo linkage in the polymer backbone.<sup>44-46</sup>

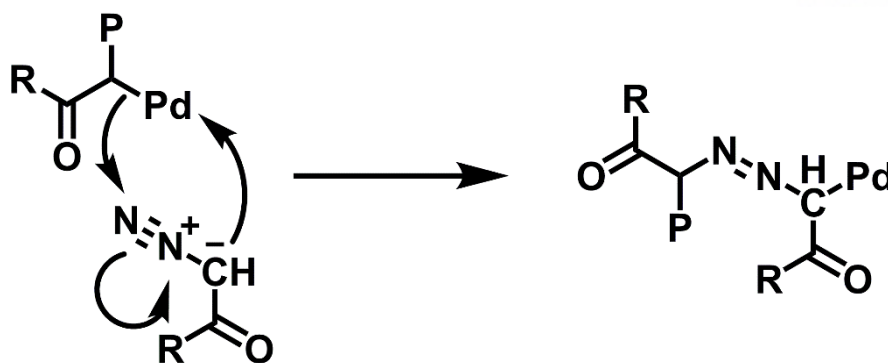


**Figure 10.** Proposed pathway leading to the insertion of an azo functional group into a growing polymer chain. P = polymer.

In an attempt to further improve molecular weights and yields of polymers, Inoue and coworkers experimented with a number of other Pd-based (see Figure 11). Palladium complexes supported by N-heterocyclic carbenes (NHCs) (e.g., [IMesPd(NQ)]<sub>2</sub> (**58**) and [IPrPd(NQ)]<sub>2</sub> (**59**), where NQ is naphthoquinone) were among the first catalysts reported after [PdCl<sub>2</sub>(MeCN)<sub>2</sub>].<sup>49</sup> The corresponding polymerization reactions were performed by adding the monomer to a solution of the catalyst and either NaBPh<sub>4</sub> or NaBAr<sup>F</sup><sub>4</sub> (**62** or **63**, respectively) in THF at room temperature. Polymerizations were initiated through oxidation of the Pd(0) to Pd(II) through addition of borates. Use of the NHC catalyst led to isolation of polymers with molecular weights of up to 40 kDa in yields between 30-40% when ethyl diazoacetate<sup>49</sup> or other diazoacetyl esters (**3-7**) were used as monomers.<sup>50</sup> Higher monomer to catalyst ratios had limited effects on increasing the molecular weight of the polymer produced, however, suggesting early termination was still occurring in the polymerization system. MALDI mass spectrometry data indicated the end-groups of the polymers were unsaturated, which was consistent with early termination via  $\beta$ -hydride elimination. Regardless, use of carbene ligands led to improvements in molecular weights and purity, as no azo linkages were seen in the final polymer.

When NHC ligands with bulky groups were paired with bulky monomers, poor catalyst performance was observed. When [IMesPd(NQ)]<sub>2</sub> (**58**) was used as a catalyst, monomers with sterically large side groups, such as 1-adamantyl diazoacetate (**5**), afforded significantly lower yields of polymer (13%) and in lower molecular weights (3.6 kDa) than those obtained with comparatively less bulky monomers, such as *n*-hexyl diazoacetate (**3**) (68%; 26 kDa).<sup>50</sup> Additionally, polymers prepared using [IPrPd(NQ)]<sub>2</sub> (**59**), which features bulky isopropyl groups near the metal center, were obtained in lower yields. For example, cyclohexyl diazoacetate (**4**) was polymerized in a 41% yield when **58** was used as a catalyst but in only 14% with **59**.



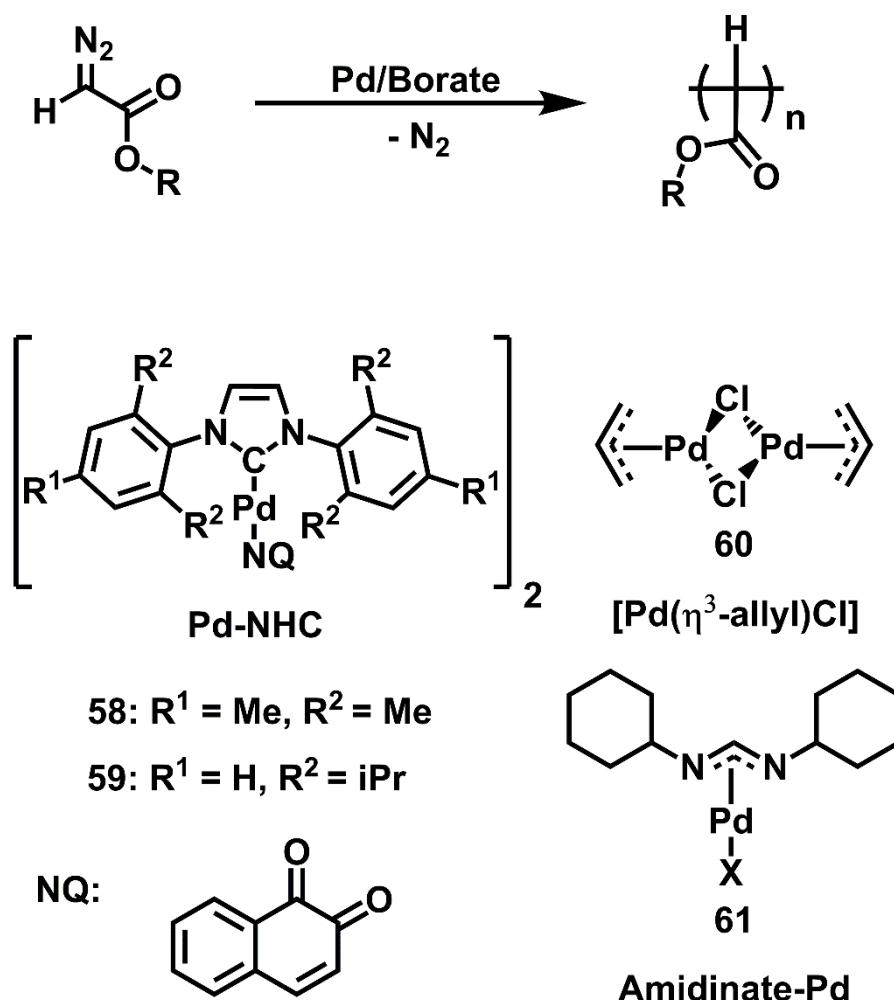


**Figure 11.** Examples of Pd complexes that have been used to catalyze C1 polymerizations.

More recently, the  $[\text{Pd}(\eta^3\text{-allyl})\text{Cl}]_2$  complex (**60**) was investigated as a catalyst for the polymerization of diazoacetates.<sup>51</sup> In addition to being less bulky when compared to the aforementioned NHCs, the allylic ligand outperformed  $\text{PdCl}_2$ , leading to improved molecular weights and the yields when compared to the latter. Using a 100:1 monomer-to-catalyst ratio, ethyl diazoacetate (**2**) and benzyl diazoacetate (**6**) afforded the corresponding polymers with molecular weights of up to 7.7 and 11.9 kDa and in yields of 75 and 66%, respectively. At larger ratios of benzyl diazoacetate to catalyst, however, molecular weights increased by diminishing amounts. Similar to the previous cases, the lack of a significant molecular weight increase was attributed to early chain termination. MALDI end-group analysis suggested that in addition to the expected protonolysis from quenching the polymerization reaction with acid, termination also occurred through backbiting to form cyclic structures and the insertion of solvent. Even with a lack of control over termination, the allylic Pd catalyst afforded higher

molecular weight polymers than previously seen and was subsequently used to synthesize different types of functional polymers.

Ihara and coworkers used the  $[\text{Pd}(\eta^3\text{-allyl})\text{Cl}]_2$  catalyst to prepare a series of polymers from bulky cyclophosphazene-based monomers (i.e., **8**, **9**, and **10**).<sup>52</sup> When **8** and the catalyst were dissolved in THF at room temperature, only dimer was isolated. However, by cooling the solution to -20 °C and adding NaBPh<sub>4</sub>, polymers with molecular weights of up to 13.8 kDa were isolated in yields of up to 79%. Mass spectrometric analysis of the resulting polymers showed the presence of the expected phenyl and hydrogen end-groups from the initiation and termination (acid quenched) reactions, respectively, and signals stemming from cyclic backbiting or THF insertion were not observed. A linear relationship between the polymer molecular weight and monomer conversion was also seen. Collectively, the data were consistent with a controlled polymerization, where the bulky side groups prevented chain termination during propagation. Indeed, block copolymers were successfully synthesized by first adding a 20-fold excess of **10** to the catalyst to afford a polymer with a molecular weight of 5.4 kDa. After purification, the polymer was then added to a solution of **9** which, after 13 hours, yielded a block copolymer that exhibited a molecular weight of 25.0 kDa and a low polydispersity index of 1.15.

A series of aryl diazoesters (**54–57**) were also polymerized using the  $[\text{Pd}(\eta^3\text{-allyl})\text{Cl}]_2$  /NaBPh<sub>4</sub> system.<sup>53</sup> Adding monomer in a 100-fold excess relative to the catalyst afforded a polymer with a molecular weight of about 7 kDa and in yields exceeding 70% when the reactions were conducted for 16 hours in THF at room temperature. Due to the fluorescent activity of the pyrenyl side chains, the polymer formed from **57** was further investigated for its optical. Compared to poly(1-pyrenylmethyl methacrylate), its C2 equivalent, the C1 polymer from **57** exhibited significantly enhanced  $\pi$ - $\pi$  interactions due to the increased density of aromatic sidechains. The enhancement of these interactions led to increased excimer formation and thus may hold potential for use in optoelectronic applications.

Both the  $[\text{Pd}(\eta^3\text{-allyl})\text{Cl}]_2$  and NHC-Pd catalysts were used to prepare alcohol-functionalized polymers which were soluble in water.<sup>54</sup> Hydroxy-containing diazoacetates (**28–32**) were polymerized as the free alcohol and silyl-protected forms (**33–37**) to give polymers in yields up to about 60% and with molecular weights of ca. 8 kDa. While higher yields were generally obtained when the alcohols were protected, extra steps were required to add and remove the protecting groups. In addition to exhibiting good solubility in water, the polymer containing a pentyl ester chain (**31**) was found to display a lower critical solution temperature (LCST): when a 0.5 wt.% solution of the polymer in water was heated above 20 °C, the polymer rapidly precipitated from solution; subsequent cooling to below 20 °C resulted in re-dissolution. The scope of these water-soluble polymers was subsequently expanded through the incorporation of ethylene glycol sidechains of varying lengths (**38–43**).<sup>55</sup> The corresponding

C1 polymers exhibited higher LCSTs and ion conductivities than their corresponding C2 analogs, which was attributed to the higher densities of the pendant functional groups in the former.

More recently, a series of fluorinated polymers were prepared from functionalized diazoacetate monomers, including partially fluorinated alkyl esters (**44**, **45**) as well as monosubstituted (**46–49**) and disubstituted (**50**, **51**) aryl esters.<sup>56</sup> Trifluoroethyl diazoacetate (**44**) was polymerized using the  $[\text{Pd}(\eta^3\text{-allyl})\text{Cl}]_2$  catalyst and afforded a polymer with a molecular weight of 18.8 kDa in yields of up to 65%. Solutions of the polymer displayed an upper critical solution temperature (UCST) in toluene, chloroform, and DMSO. Nonafluorohexyl diazoacetate (**45**) also underwent polymerization but was found to be insoluble as a homopolymer. The aryl esters **50** and **51** were polymerized using the same catalyst to give polymers with molecular weights that ranged from 4.6 to 13.6 kDa in yields between 27 and 87%. In general, the polymers exhibited good solubilities in typical organic solvents, with the exception of those containing *ortho*-fluorine substituents (**46** and **50**), which were only soluble in DMSO. Several of these polymers were amenable to post-polymerization modification. For example, treatment of polymers of **49** or **51** with an amine led to the removal of the aryl groups and resulted in formation of the corresponding amides and/or imides.

In 2017, a Pd catalyst with an amidinate ligand (**61**) was reported to afford polymers from ethyl diazoacetate with molecular weights of up to 45 kDa, albeit in isolated yields of 44%.<sup>57</sup> Likewise, methyl diazoacetate (**1**) was also polymerized using this catalyst to afford polymers with molecular weights of up to 26.2 kDa in 56% yield. Polymers with molecular weights of nearly 98 kDa were obtained when bulky monomers (**3** or **6**) were employed but in yields of less than 10%. NMR signals recorded for polymers prepared using the amidinate catalyst were reported to be relatively narrow and attributed to a relatively high degree of ordered tacticity. The ability to prepare high molecular weight polymers with potentially high stereoregularity renders the amidinate-Pd system attractive for further investigation.

Since 2002, a number of different palladium catalysts have been used to polymerize a wide variety of diazo compounds, including functionalized derivatives. While the molecular weights of the polymers produced using these catalysts are generally not as high as those obtained from B- or Rh-catalyzed polymerizations (*vide infra*), the scope of amenable monomers is relatively large. Moreover, in many cases, the C1 polymers prepared using Pd catalysts have been shown to exhibit improved properties over their C2 analogs. An ability to synthesize polymers with high degrees of stereoregularity has also been demonstrated. Considering the breadth of Pd catalysts that are now commercially available, including those that contain chiral ligands, opportunities to further enhance the polymerization of diazo-based monomers may be within reach. For example, the development of

catalysts that resist early chain termination phenomena may facilitate access to a broader range of high molecular weight polymers.

### 1.2.5. Rhodium-Catalyzed Polymerizations

In 2006, de Bruin and coworkers reported a series of Rh complexes supported by cyclooctadiene and *N,O*-bidentate ligands (**62**–**65**) that catalyzed the polymerization of ethyl diazoacetate and enabled access to polymers with molecular weights that exceeded 100 kDa in 10-50% yield (see Figure 12).<sup>58</sup> In general, the reactions were performed at room temperature for 14 hours. However, the polymer molecular weights were increased to 190 kDa when the reaction was conducted at -20 °C in chloroform for 7 days. For comparison, the same reaction afforded a polymer with a molecular weight of 133 kDa when conducted at room temperature in only 14 hours, yet the yields of the two reactions were similar (45-50%). The high molecular weights of the polymers produced may be due in part to a relatively low initiation efficiency (~3%) and the yields may be affected by the competitive formation of low molecular weight species (e.g., dimethyl maleate or fumarate and oligomers).<sup>59</sup>

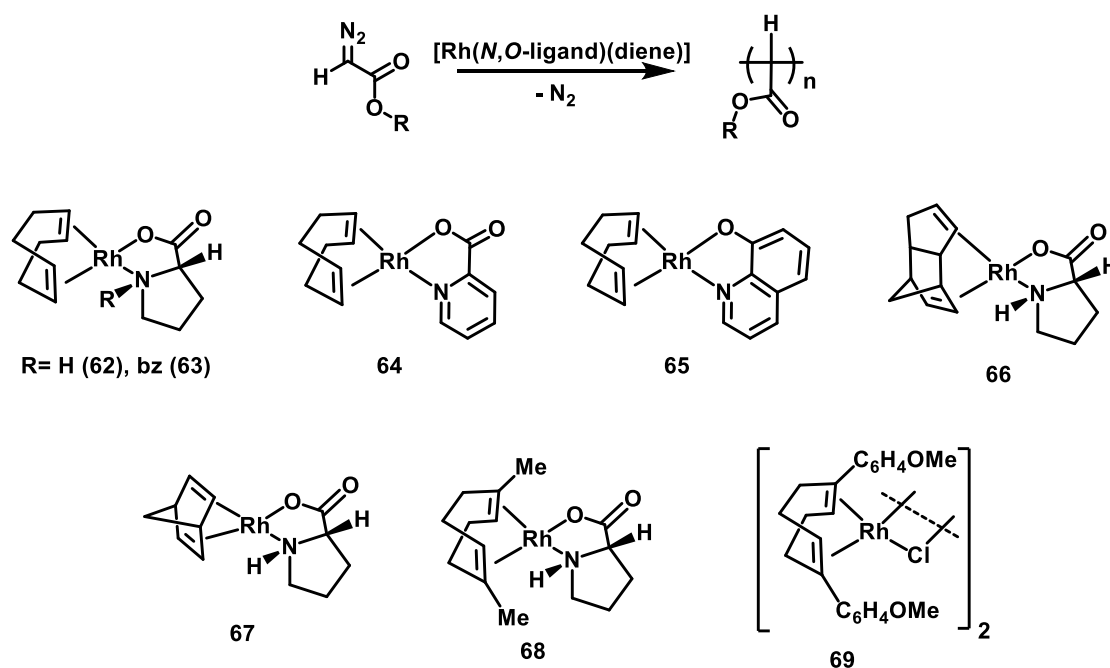


**Figure 12.** Examples of Rh complexes that have been used to catalyze the polymerization of ethyl diazoacetate. bz = benzyl group.

Remarkably, the polymers prepared using Rh were isolated as white solids instead of viscous oils as often obtained from other catalysts. Furthermore, the polymers produced from ethyl diazoacetate

using Rh-based catalysts appeared to be stereoregular and exhibited relatively sharp NMR signals when compared to spectral data recorded for polymers prepared using other catalysts.<sup>58</sup> The stereochemistry of the polymers was determined to be syndiotactic based on comparisons with isotactic poly(dialkyl fumarate)s.<sup>59, 60</sup> Differential scanning calorimetry (DSC) analysis of the polymers revealed distinct phase changes at 100 and 75 °C upon heating and cooling, and further studies demonstrated that these signals were due to a transition between semi-crystalline and liquid-crystalline (LC) states.<sup>61</sup> The LC phase was reported to originate from the self-assembly of the polymers into rigid rod-like aggregates that adopted triple-helix structures, as determined by scanning tunneling microscopy (STM), wide and small angle X-ray scattering (WAXS and SAXS), and solid state NMR spectroscopy.<sup>62</sup>

Subsequent work was directed toward optimizing the catalyst to increase the yields of high molecular weight polymer. Although variation of the *N,O*-donor ligand on the catalyst did not appear to exhibit a significant effect on the molecular weight or polydispersity of the polymer produced, catalyst **62**, which was supported by an *l*-proline-based ligand, afforded substantially higher yields than other catalysts.<sup>59</sup> These results indicated that the *N,O*-ligand may play a key role in forming the active catalyst, but may not be involved in mediating propagation as it may undergo dissociation during the initiation process. The diene ligand (e.g., 1,5-cyclooctadiene), however, appeared to remain ligated to the Rh center during the polymerization and influenced the reaction. For example, when the 1,5-cyclooctadiene ligand was replaced with dicyclopentadiene (i.e., conversion of **62** to **66**), a polymer with a relatively high molecular weight of 540 kDa was obtained in a yield of 30% under otherwise identical conditions. The use of norbornadiene-based catalyst **67** gave a polymer with a molecular weight of 350 kDa in 5% yield.

An even greater enhancement was achieved through the use of a more sterically hindered ligand, 1,5-dimethyl-1,5-cyclooctadiene, as yields of up to 80% and polymers with molecular weights of up to 670 kDa were obtained with catalyst **68**.<sup>63</sup> In order to achieve higher molecular weights and yields, however, dry samples of the catalyst had to be aged in an oxygen environment for up to 40 days. When freshly prepared catalyst **68** was used to polymerize ethyl diazoacetate, the yields of the polymer were 30% with an additional 35% of low molecular weight oligomer being collected. Reactions using the aged catalysts on the other hand produced almost no olefinic dimers and substantially less oligomer. Further studies were conducted to ascertain the effect of ageing. When samples of freshly prepared and aged catalysts were examined using NMR spectroscopy, it was determined that the former featured two diastereomers whereas the latter was comprised almost entirely of one diastereomer. Moreover, electron paramagnetic resonance (EPR) studies of the aged catalyst revealed the presence of a Rh-oxo complex which was designated as the reaction product between oxygen and the ‘missing’ diastereomer. Subsequent analysis by electrospray ionization mass spectroscopy (ESI-MS) revealed that cationic

[(2,6-dimethyl-cycloocta-2,6-dien-1-yl)Rh(III)OH] is the active polymerization catalyst and its formation was deciphered through a series of DFT calculations.<sup>64</sup>

The formation of side products in the Rh-catalyzed polymerizations of ethyl diazoacetate was investigated through a series of kinetic studies. In situ NMR analyses of polymerizations using **62** showed that 75% of the monomer had been consumed within 1 hour.<sup>59</sup> Hence, it was concluded that dimer and oligomer production may occur early in the reaction, and that formation rates approach zero within a relatively short period of time. After the first hour, only high molecular weight polymer is formed, albeit at a relatively slow rate, until the monomer is consumed. Collectively, these results indicate that two separate species may be operative: one is relatively active and leads to the formation of olefin and oligomer before deactivating, and the other is less active, yet affords stereoregular, high molecular weight polymer.

Several studies were subsequently conducted to further investigate the initiation, propagation, and termination mechanisms of Rh-catalyzed polymerization reactions of diazo compounds.<sup>59, 64-67</sup> End-group analysis was performed using MALDI mass spectrometry of oligomeric products obtained from the polymerizations of ethyl diazoacetate with various Rh catalysts.<sup>67</sup> The high molecular weight products proved challenging to analyze due to their broad molecular weight distributions and large sizes, so oligomers were used as models. The primary end-groups detected were hydrogen atoms and alkoxy groups along with a small fraction of unsaturated termini. The presence of the alkoxy end-groups was attributed to initiation through insertion of a monomer into the Rh-OR bond of the activated catalyst.<sup>64</sup> In contrast, the hydrogen termini were ascribed to protonolysis due to adventitious water or alcohols (solvent stabilizers) present in the reaction mixture. The observation of olefinic end-groups was consistent with a termination process that involved  $\beta$ -hydride elimination, which may occur preferentially in low molecular weight oligomers. Based on these results, it was surmised that different termination mechanisms may be operative and stem from the formation of different active Rh-based species. In the case of polymerizations catalyzed by oxidized samples of **68**,  $\beta$ -hydride elimination was not observed and thus chain termination may occur primarily via protonolysis.<sup>64</sup> The lack of  $\beta$ -hydride elimination paired with the substantial decrease in oligomers formed further supports the hypothesis that two active species are present wherein one affords high molecular weight polymer and the other facilitates oligomerization.

Density functional theory (DFT) calculations were also performed to investigate the propagation step using a neutral [(cyclooctadiene)Rh(I)(polymeryl)] complex as the catalyst, methyl diazoacetate as the monomer, and a trimeric oligomer of methyl diazoacetate as a model for a growing polymer chain (see Figure 13).<sup>59</sup> From the computational data it was proposed that propagation begins

with methyl diazoacetate coordinating to a Rh center attached to a polymer, similar to the mechanism proposed for the Pd-catalyzed diazoacetate polymerizations. Subsequent loss of nitrogen leads to the formation of a carbene bound to the Rh center and insertion of the carbene into the growing chain completes the propagation step, with a  $\beta$ -carbonyl coordinating to the Rh center to form a catalytic resting state. Stereoregulation was proposed to proceed in a chain end control manner and may stem from steric effects between the incoming monomer and the polymer chain attached to the metal center.

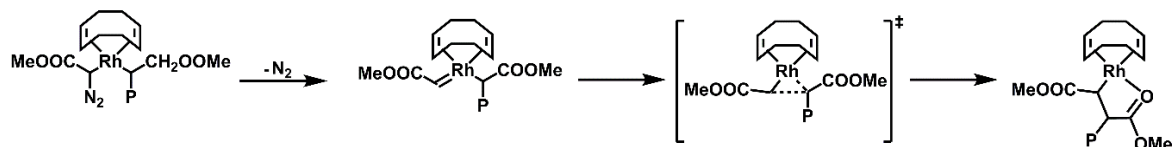


**Figure 13.** Proposed mechanism for the insertion of methyl diazoacetate into a growing polymer chain. P = polymer.

Subsequent calculations were performed using similar monomer and polymer chain models but with cationic [(2,6-dimethyl-cycloocta-2,6-dien-1-yl)Rh(III)(polymeryl)] as the active catalyst.<sup>65</sup> While the coordination, carbene formation, and insertion steps of the polymerization mechanism remained fundamentally similar to those described above, key details were gleaned from the data. The energy barrier for  $\beta$ -hydride elimination was found to be higher than that of propagation or protonolysis, which was in good agreement with experimental results. Additionally, significantly reduced propagation rates were calculated when monomer was inserted in an isotactic configuration which effectively explains the formation of polymers with high syndiotacticities. The deactivation may also explain the low initiation efficiencies since non-syndiotactic oligomers formed during the early phases of the reaction may grow relatively slowly when compared to their syndiotactic analogues.

Efforts have also been directed toward the homopolymerization of diazomethane as well as the copolymerization of diazomethane and ethyl diazoacetate using various Rh catalysts.<sup>68</sup> Treatment of diazomethane with Rh-diene catalysts **62** or **68** yielded primarily ethene, a product of dimerization, as well as low molecular weight oligomers ( $DP \approx 6$ ) of poly(methylene). NMR analysis of the oligomers revealed that the expected methyl end-groups existed in a 1:1 ratio with terminal olefins. The large concentration of unsaturated end-groups as well as the low degree of polymerization were consistent with rapid chain termination of the growing polymer via  $\beta$ -hydride elimination. Copolymerizations of diazomethane and ethyl diazoacetate were successful, although the high rates of  $\beta$ -hydride elimination required that the diazomethane be added 10 minutes after the polymerization had been initiated. Indeed, gradual addition of diazomethane afforded copolymers with greater incorporation of methylene, albeit with relatively low yields and molecular weights. Regardless, copolymers with compositions between



4 and 26 mol% of methylene were reported, and polymers with molecular weights of up to 250 kDa were obtained in yields of up to 29%. The slow addition of diazomethane prevented the formation of large blocks of poly(methylene), which are prone to termination as described above. Such strategy led to polymer architectures that were characterized as “blocky” and featured randomly dispersed, relatively short homopolymeric segments of ethyl 2-ylideneacetate (EDA) and methylene units. At ratios of diazomethane to ethyl diazoacetate greater than 1:4, poly(methylene) contents of up to 80 mol% were achieved although the molecular weights were found to be  $\leq 1$  kDa and the yields were  $< 10\%$ .

Poly(EDA-*co*-methylene)s with molecular weights of up to 350 kDa were obtained when copolymers were prepared from mixtures of ethyl diazoacetate and dimethyl sulfoxonium methylide ylide.<sup>69</sup> Homopolymerizations of the ylide using **62**, **66**, or **67** as a catalyst afforded polymers with molecular weights of up to 4 kDa and in yields of up to 77%. When the ylide was added to an ongoing polymerization of ethyl diazoacetate, high molecular weight block copolymers of up to 648 kDa were formed with poly(methylene) contents of up to 58 mol%. The highest yield (18%) of polymer was obtained when the sterically congested Rh-diene **69** was used to polymerize a 1:1 mixture of dimethyl sulfoxonium methylide ylide and ethyl diazoacetate. The copolymers produced from these reactions exhibited a structure that consisted of a block of syndiotactic poly(EDA) connected to a block of primarily poly(methylene), as determined from DSC and NMR spectroscopy.

Rh-catalyzed polymerizations of diazo compounds produce the largest ester-functionalized C1 polymers to date. Moreover, steady improvements to the catalyst design have increased the molecular weights and yields of the polymers produced. Additionally, Rh-based catalysts often afford C1 polymers with regular tacticity. The high molecular weights and high stereoregularity should give rise to polymers that exhibit a range of attractive properties, including self-assembly characteristics and abilities to adopt unique morphologies.<sup>62</sup> While a variety of monomers have been used in Rh-catalyzed polymerizations, further exploration of different catalyst/monomer combinations could greatly expand the scope of the polymerization chemistry. Additionally, the mechanistic details that have been gathered thus far may lead to the development of catalysts that provide new isotactic and/or syndiotactic polymers, or controlled mixtures thereof.

### 1.3 C1 Polymerizations That Utilize Ylide Monomers

In 1966, it was reported that alkyl boranes could be extended by one methylene unit through the addition of stoichiometric amounts of dimethyloxosulfonium methylide.<sup>70</sup> Homologation was thought to occur through complexation of the methyl ylide to the boron followed by migration of an R group to the ylide and release of DMSO, in an insertion process similar to diazoacetate polymerizations seen



above (figure 14). In addition to the homologated product, which was collected in about 70% yield for various alkyl boranes, doubly and triply homologated products were also isolated in about 25 and 5% yields, respectively.



**Figure 14.** Complexation and insertion of dimethyloxosulfonium methylide into a borane.

Shea was the first to utilize the borane mediated homologation of ylides to make poly(methylene) in 1997, a reaction which he termed “polyhomologation”.<sup>71</sup> Polyhomologation was achieved by simply increasing the ratio of ylide to borane in the solution, and when run in THF at 40 °C complete conversion was seen in 10 minutes. Some precipitation was seen during the reaction, however, attributed to the relatively low solubility of large ( $n > 30$ ) alkanes in THF. Because of the precipitation, higher PDI values were observed than what was expected. Repeating the reactions in heated (70 – 80 °C) toluene fixed the solubility issues and led to the polymerization of the ylides in a living manner. Poly(methylene) synthesized in this manner had D.P. values incredibly close to the expected values (i.e. expected D.P. 50, 117, and 232; found D.P. 48, 108, 231) and low PDIs (1.04 – 1.17).<sup>72</sup> The living nature of this polymerization was proven through the formation of block copolymers, with perdeuterio dimethyloxosulfonium methylide being incorporated into the poly(methylene) after an aliquot of dimethyloxosulfonium methylide was already polymerized.

The aforementioned polymers contained alkyl and hydroxyl endgroups due to the use of triethyl borane as a catalyst and sodium hydroxide or hydrogen peroxide as a quenchant.<sup>71</sup> Through the use of various other organoborane catalysts synthesized through the hydroboration of their alkene precursors, polymers were readily synthesized with a variety of  $\alpha$  endgroups. Of particular interest are those containing fluorescent aryl groups, biologically active molecules, amines, poly(ethylene glycol) spacers, and olefins.<sup>73, 74</sup>  $\omega$ -functionalization can also be achieved by reacting the tris(polymethylene) boranes with various organic reagents to produce end groups such as hydrogen, amines, halogens, and carbon-metal bonds.<sup>10</sup>

Use of  $\omega$ -, as well as  $\alpha$ -, functionalization has been used to create poly(methylene) with varying topologies using relatively mild conditions. Reaction of tris-poly(methylene) borane with dichloromethyl methyl ether in a basic solution followed by oxidation led to the formation of a 3-star poly(methylene) polymer with tunable  $\alpha$ -group and an alcohol at the core.<sup>75</sup> The use of bridged cyclooctane and adamantly boranes were utilized to grow a polymer which contained 2 and 3

poly(methylene) chains anchored to the same organic core.<sup>75, 76</sup> Cyclic poly(methylene) was created through post polymerization oxidation of poly(methylene) grown using a hexyl bridged thexylborocane catalyst.<sup>77</sup>

Another use of end group functionalization has been in the synthesis of block copolymers. This has been achieved both by using poly(methylene) as a macroinitiator as well as growing poly(methylene) from macroinitiators. Poly(styrene), poly(ethylene glycol), and poly(dimethyl siloxane) have all been utilized as macroinitiators for polyhomologation, with the polymers first being outfitted with alkene endgroups which were subsequently transformed into boranes through hydroboration.<sup>78, 79</sup> This led to the formation of di-block copolymers which were subsequently shown to have unique properties as compatibilizers. Triblock copolymers were also made from a poly(dimethyl siloxane) containing thexyl borane initiator, which was oxidized after polyhomologation to produce the final triblock.<sup>80</sup> These triblock copolymers were found to form nanodisks in room temperature solutions due to the insolubility of the poly(methylene) blocks. On the other hand, poly(methylene) was utilized as a macroinitiator for ATRP by esterification of the polymer's alcohol endgroup with bromoacetate. This macroinitiator was subsequently used in the ATRP of styrene to produce block copolymers with low PDI's, however conversion of styrene was below 70%.<sup>81</sup>

Polyhomologation provides access to poly(methylene) with controlled molecular weights and extremely low PDIs. In addition to this, vast control over endgroup functionalization and topology of the final polymer is possible through the appropriate choice of organoborane catalyst and work up method. This has allowed for the synthesis of poly(methylene) containing endgroups which can potentially be used in a number of fields. Additionally, end group functionalization allows the facile creation of copolymers. The primary setback to polyhomologation is that to date, only dimethyloxosulfonium methylide has successfully been homopolymerized. A number of copolymers with ethyl and cyclopropyl ylides have been reported, but due to steric crowding around the boron center, every other group in the polymer chain must be an unsubstituted methylene group.<sup>82, 83</sup> If a workaround could be found for polymerizing substituted ylides in a controlled manner similar to methyl ylides, polyhomologation could prove to be one of the most important modern polymerization techniques.

## 1.4 Stoichiometric C1 Polymerizations

To date, the only C1 polymerization to utilize a carbene precursor and a group I or II metal was reported by Inoue and coworkers in 2006.<sup>84</sup> Stoichiometric quantities of Mg in THF were used to

polymerize  $\alpha,\alpha$ -dibromotoluene (**70**) or  $\alpha,\alpha$ -dichlorotoluene (**71**) (see Figure 23). Relatively optimal results were obtained when a six-fold excess of Mg was used and the reaction temperature was slowly increased from 0 to 55 °C. Polymers were obtained in yields of up to 53% under these conditions and their molecular weights ranged from 0.7 to 1.1 kDa. Elemental analysis of the polymers revealed higher C : H ratios than expected, and indicated that loss of hydrogen may be occurring during the polymerization reaction. Indeed, olefins were detected in the polymer backbone via UV-Vis spectroscopy and confirmed through the addition of Br<sub>2</sub>.

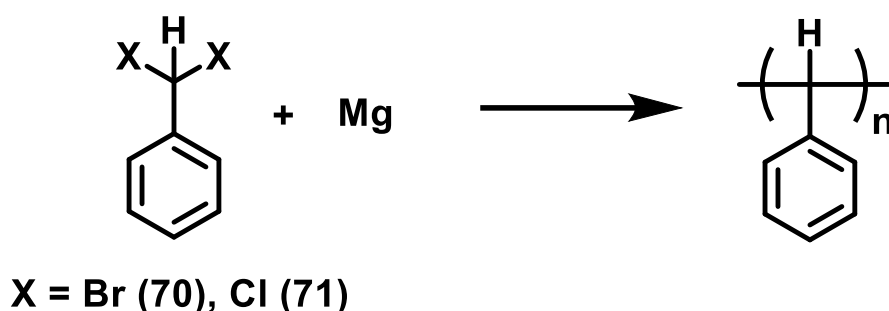


**Figure 15.** Generalized example of “Grignard-like” C1 polymerization of geminal dihalides.

The mechanism proposed for these polymerizations begins with a reaction between the Mg and the monomer (see Figure 24). The  $\alpha$ -carbon of the resulting Grignard-like reagent then acts as a nucleophile and attacks another monomer in a manner that results in the formation of a C–C bond while releasing MgX<sub>2</sub>. The two remaining halogens on the resulting dimer species are then available to form another nucleophilic species or may undergo attack by a Grignard-like species in solution, either of which effectively add monomer to the growing chain. A mechanism was also proposed for the observation of olefins in the resultant polymers. The high acidity of the benzylic groups on the monomers may result in elimination of vicinal hydrogen and halogen groups through reaction with a base.

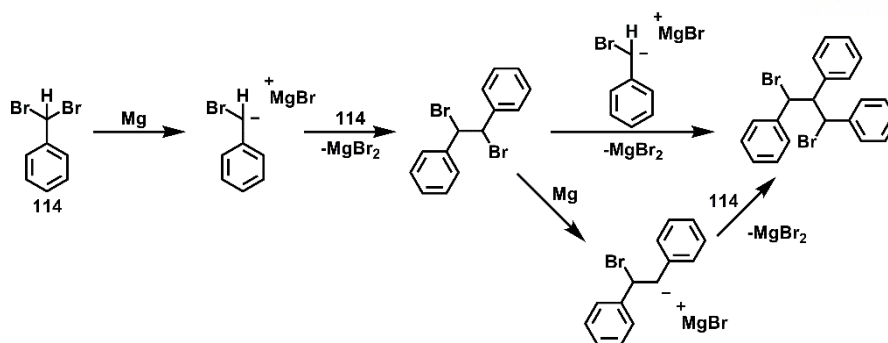


**Figure 16.** Proposed mechanism for Grignard-like C1 polymerizations of geminal dihalides

Geminal trihalides, which can be viewed as precursors to carbynes, species that formally contain a neutral carbon atom with three unpaired electrons, have also been used as monomers in several reductive C1 polymerizations. In general, the monomers are reduced in solution, leading to the conversion of C-X bonds to C-C bonds, with the additional production of small molecule byproducts, generally MX (Figure 25). Two of these new carbon-carbon bonds form the backbone of the polymer, with the third bond determining the polymer's structure. The final bond can either be a  $\sigma$  bond to a third monomer, creating a  $sp^3$  network polymer, or a  $\pi$  bond to one of the other adjacent monomers, forming a highly unsaturated backbone. While the potential variance in structure is unique and interesting, very few reports exist on these so called “poly(carbyne)s. These reports mostly focus on synthesis and use of these polymers in materials chemistry. An in depth summary of these reports will be given in the introductions of the next two chapters.

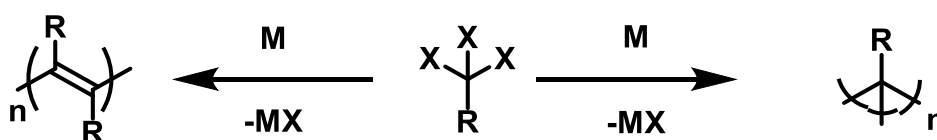


**Figure 17.** General reaction scheme for poly(carbyne) synthesis

## 1.5 Conclusions and Perspectives

Since the 1950s, a number of synthetic strategies have been developed for C1 polymerizations. Many of such reactions are promoted by metals and commonly utilize either diazo- or isocyanide-containing monomers. Initial work explored the polymerization of diazoalkanes using Cu and Au. While a number of different monomers were polymerized using these metals, fine control over the corresponding reactions was not achieved and the polymerization of monomers containing polar side

groups remains a challenge as does accessing high molecular weight polymers. More recent studies have focused on the use of Pd- and Rh-based catalysts, both of which have been shown to polymerize diazoacetates. Since the polymerization of a relatively large library of functionalized monomers using Pd has been established, current efforts appear to be focused on realizing catalysts that facilitate control over the polymerization chemistry and afford materials in high yields, high molecular weights, and with high stereoregularity. In comparison, Rh has been primarily used to polymerize ethyl diazoacetate and, more recently, copolymers with methylene. Such catalysts have also provided high molecular weight polymers and offer excellent control over stereochemistry. Finally, the polymerization of isocyanides has most frequently been conducted using relatively simple Ni salts, which may be because such complexes offer a relatively straightforward means to access polymers that adopt higher-order (i.e., helical) structures. However, isocyanides have been polymerized in a controlled fashion using a variety of Ni, Pd and Rh complexes. The relatively few reports on metal-promoted carbyne polymerizations have revealed that the polymer produced may be strongly dependent on the reaction conditions employed.

Compared to conventional C2 polymerizations, C1 polymerizations provide an alternative synthetic strategy to access a wide range of polymeric materials, including persubstituted derivatives. Polymers synthesized through C1 polymerizations can feature a high density of functional groups and, as such, often display chemical and physical properties not seen in C2 polymer analogs. Moreover, some polymers, such as those derived from isocyanides, can adopt helical structures and thus be used to control features that range from solid-state morphology to optoelectronics. The backbones of the poly(carbyne)s described above are apparently sufficiently rich in  $sp^3$ -hybridized carbons such that they can be converted into diamond-like carbons, and thus offer potential for accessing new classes of high-performance materials that display excellent mechanical and/or thermal properties.

While a foundation has been laid and an understanding of the scope and mechanistic pathways for some metal-promoted C1 polymerizations have been established, opportunity abounds. Early termination and chain transfer processes continue to challenge the polymerization of diazo compounds when catalyzed by metal complexes, and the realization of a catalyst that enables fine control could be transformative. The organometallic chemistry of Au and Cu has flourished recently and lessons learned from those studies may offer new classes of catalysts for polymerizing diazoalkanes and other monomers. Although controlled isocyanide polymerizations have been developed, the number of reports that have capitalized on such advances are relatively few. Indeed, homo- and copolymers derived from isocyanides and capable of adopting tunable conformations are now accessible and it may prove interesting to study the performance of such types of materials in various applications. Poly(carbyne)s represent the least studied class of C1 polymers as only a few examples exist in literature.

While such polymers have been used as precursors for carbon materials, a deeper understanding of the underlying polymerization mechanism(s) may enable control over the architecture and molecular weight of the polymers produced and/or facilitate their transformation into high-value materials. Currently, only four chemicals have been utilized as monomers in these reactions, yet a broad range of other germinal trifunctionalized compounds are known and theoretically should be amenable to polymerization. The development of a catalytic variant, potentially in conjunction with a sacrificial reductant, may also be worthy of investigation. It is because of this that further research into synthesis of poly(carbyne)s through reductive C1 polymerization was deemed worthy. Specifically, we sought to optimize synthetic strategies, probe the variety of monomers prone to these polymerizations, and mechanistically investigate their polymerization mechanism. We hope that these efforts will lay the groundwork for future work in seeking the controlled synthesis of persubstituted poly(carbyne)s, whose unique structures could provide utility in many fields.

## 1.6 References

1. Pearce, E. M., Principles of polymerization (third edition), by George Odian, Wiley-Interscience, New York, 1991, 768 pp. price: \$59.95. *J. Polym. Sci., Part A: Polym. Chem.* **1992**, 30 (7), 1508-1508.
2. Endo, K.; Kondo, Y., Polymerization of trans-2-Butene with ( $\alpha$ -Diimine)Ni(II) Complex in Combination with Et<sub>2</sub>AlCl. *Polym. J.* **2006**, 38, 1160.
3. Otsu, T.; Shimizu, A.; Imoto, M., Monomer-isomerization polymerization. V. Effects of transition metal compounds on monomer-isomerization polymerizations of butene-2 and pentene-2. *J. Polym. Sci. A-1* **1969**, 7 (11), 3111-3117.
4. Otsu, T.; Nagahama, H.; Endo, K., Monomer-isomerization polymerizations of heptene-2, heptene-3, and octene-2 with Ziegler-Natta catalyst. *J. Polym. Sci. B Polym.* **1972**, 10 (8), 601-604.
5. Otsu, T.; Nagahama, H.; Endo, K., Monomer-Isomerization Polymerization. XII. Monomer-Isomerization Polymerizations of 2-Heptene and 3-Heptene with Ziegler-Natta Catalyst. *J. Macromol. Sci. A* **1975**, 9 (7), 1245-1254.
6. Jellema, E.; Jongerius, A. L.; Reek, J. N. H.; de Bruin, B., C1 polymerisation and related C-C bond forming 'carbene insertion' reactions. *Chem. Soc. Rev.* **2010**, 39 (5), 1706-1723.
7. Suginome, M.; Ito, Y., Transition Metal-Mediated Polymerization of Isocyanides. In *Polymer Synthesis. Advances in Polymer Science*, Springer: Berlin, Heidelberg, 2004; Vol. 171, pp 77-136.
8. de Bruin, B.; Chikkali, S. H., Carbene or C1 Polymerization. In *Metal-Catalyzed Polymerization: Fundamentals to Applications*, Chikkali, S. H., Ed. CRC Press: 2018; pp 117-136.

9. Luo, J.; Shea, K. J., Polyhomologation. A Living C1 Polymerization. *Acc. Chem. Res.* **2010**, *43* (11), 1420-1433.
10. Luo, J.; Shea, K. J., Polyhomologation: The Living Polymerization of Ylides. In *Complex Macromolecular Architectures*, Hadjichristidis, N.; Hirao, A.; Tezuka, Y.; Prez, F. D., Eds. John Wiley & Sons: Asia, 2011; pp 349-376.
11. Buckley, G. D.; Cross, L. H.; Ray, N. H., The copper-catalysed decomposition of aliphatic diazo-compounds: the formation of paraffins of high molecular weight. *J. Chem. Soc.* **1950**, (0), 2714-2718.
12. Bawn, C. E. H.; Rhodes, T. B., High molecular weight polymethylene. Part 1.-The kinetics of the copper salt catalyzed decomposition of diazomethane. *Trans. Faraday Soc.* **1954**, *50* (0), 934-941.
13. Feltzin, J.; Restaino, A. J.; Mesrobian, R. B., The Kinetics of the Catalyzed Decomposition of Diazohydrocarbons1. *J. Am. Chem. Soc.* **1955**, *77* (1), 206-210.
14. Liu, L.; Song, Y.; Li, H., Carbene polymerization: characterization of poly(carballyloxycarbene). *Polym. Int.* **2002**, *51* (10), 1047-1049.
15. Cowell, G. W.; Ledwith, A., Developments in the chemistry of diazo-alkanes. *Q. Rev. Chem. Soc.* **1970**, *24* (1), 119-167.
16. Kantor, S. W.; Osthoff, R. C., High Molecular Weight Polymethylene. *J. Am. Chem. Soc.* **1953**, *75* (4), 931-932.
17. *Copper-Mediated Cross-Coupling Reactions*. John Wiley & Sons, Inc: 2013.
18. Allen, S. E.; Walvoord, R. R.; Padilla-Salinas, R.; Kozlowski, M. C., Aerobic Copper-Catalyzed Organic Reactions. *Chem. Rev.* **2013**, *113* (8), 6234-6458.
19. Amal Joseph, P. J.; Priyadarshini, S., Copper-Mediated C–X Functionalization of Aryl Halides. *Org. Process Res. Dev.* **2017**, *21* (12), 1889-1924.
20. Meerwein, H., *Angew. Chem.* **1948**, *60* (6), 78.
21. Buckley, G. D.; Ray, N. H., The decomposition of aliphatic diazo-compounds by trimethyl borate: the preparation of branched-chain paraffins of high molecular weight. *J. Chem. Soc.* **1952**, (0), 3701-3704.
22. Kubota, H.; Morawetz, H., Polymerization of gaseous diazomethane on silicone grease. *J. Polym. Sci. A-1* **1967**, *5* (3), 585-591.



23. Davies, A. G.; Hare, D. G.; Khan, O. R.; Sikora, J., Monomethylation and polymethylenation by diazomethane in the presence of boron compounds. *J. Chem. Soc.* **1963**, (0), 4461-4471.
24. Imoto, M.; Nakaya, T., Polymerization by Carbenoids, Carbenes, and Nitrenes. *Journal of Macromolecular Science, Part C* **1972**, 7 (1), 1-48.
25. Matthies et. al. used a different naming convention, calling it poly(ethylidene). I have chosen to use poly(methyl methylene) to keep things consistent.
26. H., B. C. E.; A., L.; P., M., The mechanism of the polymerization of diazoalkanes catalyzed by boron compounds. *Journal of Polymer Science* **1959**, 34 (127), 93-108.
27. Wada, N.; Morisaki, Y.; Chujo, Y., Polymethylenes Containing [2.2]Paracyclophane in the Side Chain. *Macromolecules* **2009**, 42 (5), 1439-1442.
28. Hooz, J.; Linke, S., Alkylation of diazoacetonitrile and ethyl diazoacetate by organoboranes. Synthesis of nitriles and esters. *J. Am. Chem. Soc.* **1968**, 90 (24), 6891-6892.
29. Hooz, J.; Gunn, D. M., The reaction of B-vinyl- and B-alkyl-9-borabicyclo[3.3.1]nonane derivatives with ethyl diazoacetate and diazoacetone. *Tetrahedron Lett.* **1969**, 10 (40), 3455-3458.
30. Hooz, J.; Morrison, G. F., Reaction of trialkylboranes with diazoacetaldehyde. A new synthesis of aldehydes. *Can. J. Chem.* **1970**, 48 (5), 868-870.
31. Hooz, J.; Linke, S., The reaction of trialkylboranes with diazoacetone. A new ketone synthesis. *J. Am. Chem. Soc.* **1968**, 90 (21), 5936-5937.
32. Pasto, D. J.; Wojtkowski, P. W., Transfer reactions involving boron. XXI intermediates formed in the alkylation of diazocompounds and dimethylsulfonium phenacylide via organoboranes. *Tetrahedron Lett.* **1970**, 11 (3), 215-218.
33. Bai, J.; Burke, L. D.; Shea, K. J., BH<sub>3</sub>-Catalyzed Oligomerization of Ethyl Diazoacetate: The Role of C-Boron Enolates. *J. Am. Chem. Soc.* **2007**, 129 (16), 4981-4991.
34. Ihara, E.; Kida, M.; Itoh, T.; Inoue, K., Organoaluminum-mediated polymerization of diazoketones. *J. Polym. Sci., Part A: Polym. Chem.* **2007**, 45 (22), 5209-5214.
35. Nasini, A. G.; Trossarelli, L.; Saini, G., Reactions of diazoalkanes upon metallic surfaces: Polymer formation and a stereoregulating action of gold. *Makromol. Chem.* **1961**, 44 (1), 550-569.
36. Krakovyak, M. G.; Skorokhodov, S. S., The polymerization of higher diazoalkanes. *Pol. Sci. U.S.S.R.* **1969**, 11 (4), 894-903.



37. Nasini, A. G.; Trossarelli, L., Recent progress in the mechanism of the formation of polyethylidene from diazoethane. *J. Polym. Sci., C Polym. symp.* **1963**, *4* (1), 167-171.
38. Seshadri, K.; Atre, S. V.; Tao, Y.-T.; Lee, M.-T.; Allara, D. L., Synthesis of Crystalline, Nanometer-Scale,  $-(CH_2)_x-$  Clusters and Films on Gold Surfaces. *J. Am. Chem. Soc.* **1997**, *119* (20), 4698-4711.
39. Guo, W.; Jennings, G. K., Use of Underpotentially Deposited Metals on Gold To Affect the Surface-Catalyzed Formation of Polymethylene Films. *Langmuir* **2002**, *18* (8), 3123-3126.
40. Bai, D.; Jennings, G. K., Surface-Catalyzed Growth of Polymethylene-Rich Copolymer Films on Gold. *J. Am. Chem. Soc.* **2005**, *127* (9), 3048-3056.
41. Bai, D.; Habersberger, B. M.; Jennings, G. K., pH-Responsive Copolymer Films by Surface-Catalyzed Growth. *J. Am. Chem. Soc.* **2005**, *127* (47), 16486-16493.
42. Bai, D.; Ibrahim, Z.; Jennings, G. K., pH-Responsive Random Copolymer Films with Amine Side Chains. *J. Phys. Chem. C* **2007**, *111* (1), 461-466.
43. Ihara, E.; Haida, N.; Iio, M.; Inoue, K., Palladium-Mediated Polymerization of Alkyl Diazoacetates To Afford Poly(alkoxycarbonylmethylene)s. First Synthesis of Polymethylenes Bearing Polar Substituents. *Macromolecules* **2003**, *36* (1), 36-41.
44. Ihara, E.; Fujioka, M.; Haida, N.; Itoh, T.; Inoue, K., First Synthesis of Poly(acylmethylene)s via Palladium-Mediated Polymerization of Diazoketones. *Macromolecules* **2005**, *38* (6), 2101-2108.
45. Ihara, E.; Hiraren, T.; Itoh, T.; Inoue, K., Palladium-mediated Polymerization of Diazoacetamides. *Polym. J.* **2008**, *40*, 1094.
46. Ihara, E.; Hiraren, T.; Itoh, T.; Inoue, K., Palladium-mediated polymerization of cyclic diazoketones. *J. Polym. Sci., Part A: Polym. Chem.* **2008**, *46* (5), 1638-1648.
47. Ihara, E.; Goto, Y.; Itoh, T.; Inoue, K., Palladium-Mediated Polymerization of Bifunctional Diazocarbonyl Compounds: Preparation of Crosslinked Polymers by Copolymerization of Bi- and Monofunctional Diazocarbonyl Compounds. *Polym. J.* **2009**, *41*, 1117.
48. Ihara, E.; Kida, M.; Fujioka, M.; Haida, N.; Itoh, T.; Inoue, K., Palladium-mediated copolymerization of diazocarbonyl compounds with phenyldiazomethane. *J. Polym. Sci., Part A: Polym. Chem.* **2007**, *45* (8), 1536-1545.
49. Ihara, E.; Ishiguro, Y.; Yoshida, N.; Hiraren, T.; Itoh, T.; Inoue, K., (N-Heterocyclic Carbene)Pd/Borate Initiating Systems for Polymerization of Ethyl Diazoacetate. *Macromolecules* **2009**, *42* (22), 8608-8610.
50. Ihara, E.; Takahashi, H.; Akazawa, M.; Itoh, T.; Inoue, K., Polymerization of Various Alkyl Diazoacetates Initiated with (N-Heterocyclic Carbene)Pd/Borate Systems. *Macromolecules* **2011**, *44* (9), 3287-3292.

51. Ihara, E.; Akazawa, M.; Itoh, T.; Fujii, M.; Yamashita, K.; Inoue, K.; Itoh, T.; Shimomoto, H.,  $\pi$ -AllylPdCl-Based Initiating Systems for Polymerization of Alkyl Diazoacetates: Initiation and Termination Mechanism Based on Analysis of Polymer Chain End Structures. *Macromolecules* **2012**, *45* (17), 6869-6877.
52. Shimomoto, H.; Asano, H.; Itoh, T.; Ihara, E., Pd-initiated controlled polymerization of diazoacetates with a bulky substituent: synthesis of well-defined homopolymers and block copolymers with narrow molecular weight distribution from cyclophosphazene-containing diazoacetates. *Polym. Chem.* **2015**, *6* (26), 4709-4714.
53. Ihara, E.; Okada, R.; Sogai, T.; Asano, T.; Kida, M.; Inoue, K.; Itoh, T.; Shimomoto, H.; Ishibashi, Y.; Asahi, T., Pd-mediated polymerization of diazoacetates with aromatic ester group: Synthesis and photophysical property of poly(1-pyrenylmethoxycarbonylmethylene). *J. Polym. Sci., Part A: Polym. Chem.* **2013**, *51* (5), 1020-1023.
54. Shimomoto, H.; Itoh, E.; Itoh, T.; Ihara, E.; Hoshikawa, N.; Hasegawa, N., Polymerization of Hydroxy-Containing Diazoacetates: Synthesis of Hydroxy-Containing "Poly(substituted methylene)s" by Palladium-Mediated Polymerization and Poly(ester-ether)s by Polycondensation through O-H Insertion Reaction. *Macromolecules* **2014**, *47* (13), 4169-4177.
55. Shimomoto, H.; Shimizu, K.; Takeda, C.; Kikuchi, M.; Kudo, T.; Mukai, H.; Itoh, T.; Ihara, E.; Hoshikawa, N.; Koiwai, A.; Hasegawa, N., Synthesis of polymers with densely-grafted oligo(ethylene glycol)s by Pd-initiated polymerization of oxyethylene-containing diazoacetates. *Polym. Chem.* **2015**, *6* (47), 8124-8131.
56. Shimomoto, H.; Kudo, T.; Tsunematsu, S.; Itoh, T.; Ihara, E., Fluorinated Poly(substituted methylene)s Prepared by Pd-Initiated Polymerization of Fluorine-Containing Alkyl and Phenyl Diazoacetates: Their Unique Solubility and Postpolymerization Modification. *Macromolecules* **2018**, *51* (2), 328-335.
57. Shimomoto, H.; Kawamata, J.; Murakami, H.; Yamashita, K.; Itoh, T.; Ihara, E., Polymerization of alkyl diazoacetates initiated by the amidinate/Pd system: efficient synthesis of high molecular weight poly(alkoxycarbonylmethylene)s with moderate stereoregularity. *Polym. Chem.* **2017**, *8* (27), 4030-4037.
58. Hetterscheid, D. G. H.; Hendriksen, C.; Dzik, W. I.; Smits, J. M. M.; van Eck, E. R. H.; Rowan, A. E.; Busico, V.; Vacatello, M.; Van Axel Castelli, V.; Segre, A.; Jellema, E.; Bloembergen, T. G.; de Bruin, B., Rhodium-Mediated Stereoselective Polymerization of "Carbenes". *J. Am. Chem. Soc.* **2006**, *128* (30), 9746-9752.
59. Jellema, E.; Budzelaar, P. H. M.; Reek, J. N. H.; de Bruin, B., Rh-Mediated Polymerization of Carbenes: Mechanism and Stereoregulation. *J. Am. Chem. Soc.* **2007**, *129* (37), 11631-11641.
60. Yoshioka, M.; Matsumoto, A.; Otsu, T.; Ando, I., <sup>13</sup>C nuclear magnetic resonance study of stereoregularity in poly(dialkyl fumarate)s bearing t-butyl ester groups. *Polymer* **1991**, *32* (15), 2741-2746.

61. Jellema, E.; Jongerius, A. L.; van Ekenstein, G. A.; Mookhoek, S. D.; Dingemans, T. J.; Reingruber, E. M.; Chojnacka, A.; Schoenmakers, P. J.; Sprenkels, R.; van Eck, E. R. H.; Reek, J. N. H.; de Bruin, B., Rhodium-Mediated Stereospecific Carbene Polymerization: From Homopolymers to Random and Block Copolymers. *Macromolecules* **2010**, *43* (21), 8892-8903.
62. Franssen, N. M. G.; Ensing, B.; Hegde, M.; Dingemans, T. J.; Norder, B.; Picken, S. J.; Ekenstein, G. O. R. A. v.; Eck, E. R. H. v.; Elemans, J. A. A. W.; Vis, M.; Reek, J. N. H.; Bruin, B. d., On the "Tertiary Structure" of Poly-Carbenes; Self-Assembly of sp<sup>3</sup>-Carbon-Based Polymers into Liquid-Crystalline Aggregates. *Chem. Eur. J.* **2013**, *19* (35), 11577-11589.
63. Jellema, E.; Jongerius, A. L.; Walters, A. J. C.; Smits, J. M. M.; Reek, J. N. H.; de Bruin, B., Ligand Design in Rh(diene)-Mediated "Carbene" Polymerization; Efficient Synthesis of High-Mass, Highly Stereoregular, and Fully Functionalized Carbon-Chain Polymers. *Organometallics* **2010**, *29* (12), 2823-2826.
64. Walters, A. J. C.; Troeppner, O.; Ivanović-Burmazović, I.; Tejel, C.; Río, M. P. d.; Reek, J. N. H.; deBruin, B., Stereospecific Carbene Polymerization with Oxygenated Rh(diene) Species. *Angew. Chem. Int. Ed.* **2012**, *51* (21), 5157-5161.
65. Walters, A. J. C.; Reek, J. N. H.; de Bruin, B., Computed Propagation and Termination Steps in [(Cycloocta-2,6-dien-1-yl)RhIII(polymeryl)]<sup>+</sup> Catalyzed Carbene Polymerization Reactions. *ACS Catal.* **2014**, *4* (5), 1376-1389.
66. Finger, M.; Reek, J. N. H.; de Bruin, B., Role of  $\beta$ -H Elimination in Rhodium-Mediated Carbene Insertion Polymerization. *Organometallics* **2011**, *30* (5), 1094-1101.
67. Walters, A. J. C.; Jellema, E.; Finger, M.; Aarnoutse, P.; Smits, J. M. M.; Reek, J. N. H.; de Bruin, B., Rh-Mediated Carbene Polymerization: from Multistep Catalyst Activation to Alcohol-Mediated Chain-Transfer. *ACS Catal.* **2012**, *2* (2), 246-260.
68. Franssen, N. M. G.; Remerie, K.; Macko, T.; Reek, J. N. H.; de Bruin, B., Controlled Synthesis of Functional Copolymers with Blocky Architectures via Carbene Polymerization. *Macromolecules* **2012**, *45* (9), 3711-3721.
69. Suarez, A. I. O.; del Río, M. P.; Remerie, K.; Reek, J. N. H.; de Bruin, B., Rh-Mediated C1-Polymerization: Copolymers from Diazoesters and Sulfoxonium Ylides. *ACS Catal.* **2012**, *2* (9), 2046-2059.
70. Tufariello, J. J.; Lee, L. T. C., The Reaction of Trialkylboranes with Dimethyloxosulfonium Methylide. *J. Am. Chem. Soc.* **1966**, *88* (20), 4757-4759.
71. Shea, K. J.; Walker, J. W.; Zhu, H.; Paz, M.; Greaves, J., Polyhomologation. A Living Polymethylene Synthesis. *J. Am. Chem. Soc.* **1997**, *119* (38), 9049-9050.
72. It is important to note that because each alkyl borane can grow 3 polymer chains, the expected D.P. is 1/3 the monomer to catalyst ratio.

73. Busch, B. B.; Staiger, C. L.; Stoddard, J. M.; Shea, K. J., Living Polymerization of Sulfur Ylides. Synthesis of Terminally Functionalized and Telechelic Polymethylene. *Macromolecules* **2002**, *35* (22), 8330-8337.
74. Wagner, C. E.; Rodriguez, A. A.; Shea, K. J., Synthesis of Linear  $\alpha$ -Olefins via Polyhomologation. *Macromolecules* **2005**, *38* (17), 7286-7291.
75. Shea, K. J.; Busch, B. B.; Paz, M. M., Polyhomologation: Synthesis of Novel Polymethylene Architectures by a Living Polymerization of Dimethylsulfoxonium Methylide. *Angew. Chem. Int. Ed.* **1998**, *37* (10), 1391-1393.
76. Wagner, C. E.; Kim, J.-S.; Shea, K. J., The Polyhomologation of 1-Boraadamantane: Mapping the Migration Pathways of a Propagating Macrotricyclic Trialkylborane. *J. Am. Chem. Soc.* **2003**, *125* (40), 12179-12195.
77. Shea, K. J.; Lee, S. Y.; Busch, B. B., A New Strategy for the Synthesis of Macrocycles. The Polyhomologation of Boracyclanes. *The Journal of Organic Chemistry* **1998**, *63* (17), 5746-5747.
78. Zhou, X.-Z.; Shea, K. J., Synthesis of Poly(methylene-b-styrene) by Sequential Living Polymerization. *Macromolecules* **2001**, *34* (9), 3111-3114.
79. Shea, K. J.; Staiger, C. L.; Lee, S. Y., Synthesis of Polymethylene Block Copolymers by the Polyhomologation of Organoboranes. *Macromolecules* **1999**, *32* (9), 3157-3158.
80. Wang, J.; Horton, J. H.; Liu, G.; Lee, S.-Y.; Shea, K. J., Polymethylene-block-poly(dimethyl siloxane)-block-polymethylene nanoaggregates in toluene at room temperature. *Polymer* **2007**, *48* (14), 4123-4129.
81. Chen, J.-Z.; Cui, K.; Zhang, S.-Y.; Xie, P.; Zhao, Q.-L.; Huang, J.; Shi, L.-P.; Li, G.-Y.; Ma, Z., New Strategy Targeting Well-Defined Polymethylene-block-Polystyrene Copolymers: The Combination of Living Polymerization of Ylides and Atom Transfer Radical Polymerization. *Macromol. Rapid Commun.* **2009**, *30* (7), 532-538.
82. Zhou, X.-Z.; Shea, K. J., Ersatz Ethylene-Propylene Copolymers: The Synthesis of Linear Carbon Backbone Copolymers One Carbon Atom at a Time. *J. Am. Chem. Soc.* **2000**, *122* (46), 11515-11516.
83. Sulc, R.; Zhou, X.-Z.; Shea, K. J., Repetitive  $sp^3$ - $sp^3$  Carbon-Carbon Bond-Forming Copolymerizations of Primary and Tertiary Ylides. Synthesis of Substituted Carbon Backbone Polymers: Poly(cyclopropylidene-co-methylidene). *Macromolecules* **2006**, *39* (15), 4948-4952.
84. Ihara, E.; Wake, T.; Mokume, N.; Itoh, T.; Inoue, K.,  $\alpha,\alpha$ -Dibromotoluene as a monomer for poly (substituted methylene) synthesis: Magnesium-mediated polycondensation of  $\alpha,\alpha$ -dibromotoluene and magnesium/copper-mediated copolycondensation of  $\alpha,\alpha$ -dibromotoluene with 1,6-dibromohexane. *J. Polym. Sci., Part A: Polym. Chem.* **2006**, *44* (19), 5661-5671.

# Chapter 2: Optimization of Poly(phenyl carbyne) Synthesis and Characterization

## 2.1 Introduction

While a number of poly(carbyne)s exist in the literature, poly(phenyl carbyne) was the first to be synthesized and has received the most attention. Additionally, it was previous reports on poly(phenyl carbyne) that sparked interest in this project. To date, a number of reductants and techniques have been used in the synthesis of aryl poly(carbyne)s. This work has been performed primarily by two groups, initially by Kryazhev and Brodskaya,<sup>1, 2</sup> and more recently by Visscher and Bianconi<sup>3-5</sup>. While both groups produced unique poly(carbynes) using parallel synthetic techniques, both produced poly(phenyl carbyne) from  $\alpha,\alpha,\alpha$ -trichlorotoluene (TCT). Interestingly, the two groups came up with differing structures for poly(phenyl carbyne) with Brodskaya reporting a linear polymer with an unsaturated backbone and Bianconi reporting a network polymer with a branching  $sp^3$  backbone. While synthetic details are given in both cases, no extensive attempt at optimization of the polymerization was reported.

The first reports of poly(carbynes), which were at the time referred to as poly(methine)s, were by Kryazhev and Brodskaya.<sup>1</sup> Initially, the polymers were prepared by adding excess Li (3.16 equivalents) to a 1 M solution of TCT in THF. The reactions were conducted at room temperature and produced a dechlorinated material, termed poly(phenyl methine), in 85% yield after 5 hours. The molecular weight of the polymer was determined to be 8 kDa by vapor phase osmometry (VPO). Lower temperatures ( $-7^\circ\text{C}$ ) and shorter reaction times were seen to produce lower molecular weights and yields, as well as polymer with higher contents of unreacted chlorine, though no other experimental conditions were reported. Characterization of the polymer structure was primarily done through IR (infra-red) spectroscopy. In addition to the expected bands from benzene rings at  $1445$  and  $1495\text{ cm}^{-1}$ , additional signals were reported at  $1000$ - $1300$ ,  $1680$  and  $1720$ , and  $2800$ - $3000\text{ cm}^{-1}$ , which were attributed to C-O-C, C=O, and C-H vibrations, respectively, occurring from addition of THF into the polymer. Proof of an unsaturated backbone came from a comparison of UV-Vis spectra of the polymer to that of thermally polymerized poly(diphenyl acetylene)<sup>6</sup>, where the poly(phenyl methine) displayed some absorption at higher wavelengths ( $\sim 500\text{ nm}$ ) than the poly(diphenyl acetylene) ( $< 500\text{ nm}$ ). From this comparison, it was concluded that larger conjugated chains must exist in the poly(phenyl methine) than the poly(diphenyl acetylene) for such a bathochromic shift to exist. Electron paramagnetic resonance

spectroscopy of the poly(phenyl methine) showed a narrow singlet corresponding to a concentration of  $10^{17}$  -  $10^{18}$  spins/g.

A subsequent report by Kryazhev investigated the polymerization of TCT using Mg and Zn as reducing agents.<sup>2</sup> These reactions were performed by adding the TCT dropwise to an already refluxing mixture of THF and reductant. Reduction of TCT by Mg yielded polymers with molecular weights and yields that were comparable to those generated from the reduction of TCT by Li, while reduction with Zn gave substantially lower molecular weights (0.85 kDa) at a yield of 70%. IR spectra of the poly(phenyl methine) synthesized using Mg was identical to that made using Li, while polymer formed using Zn contained several new peaks. A broad background peak between 700 and 1800  $\text{cm}^{-1}$  in the polymer prepared with Zn was attributed to a branched, polyconjugated backbone, with additional peaks at 1600 and 1620  $\text{cm}^{-1}$  confirming the presence of C=C in the backbone. Kryazhev remarks that these vibrations are inactive in polymers generated using Li or Mg due to high symmetry across the double bond. EPR and Uv-Vis spectra from the poly(phenyl methine) generated using Mg and Zn both appeared identical to the previously reported spectra for the polymer synthesized using Li. Additionally, newly reported H-NMR (proton nuclear magnetic resonance) spectra of the polymer were reported to show a single broad signal between 6.5 – 7.5 ppm, indicative of the phenyl pendant groups. The signal observed was the same regardless of the choice of reductant, and also identical to spectra of poly(diphenyl acetylene).

The first use of the term “poly(phenyl carbyne)” came from Bianconi in 1993 when they prepared the polymer from TCT using NaK amalgam as a reductant.<sup>3</sup> Using an adapted procedure originally developed to produce network alkyl silane polymers, the TCT was reduced with assistance of an ultrasonicator in an inert atmosphere.<sup>7</sup> 3 equivalents of a NaK (1 : 1 molar ratio) amalgam were suspended in THF using an ultrasonic immersion horn. To the sonicated suspension, a solution of TCT in pentane was slowly added over 20 minutes. After an additional 20 minutes, quenching with water and subsequent reprecipitation from THF into methanol and ethanol gave a 25% yield of poly(phenyl carbyne) with a molecular weight of 3 kDa, as determined by gel permeation chromatography (GPC) using a poly(styrene) standard. Despite NaK amalgam having a lower reduction potential than Li, the reaction proceeds much faster with NaK amalgam as it is dispersed in THF which greatly increases the surface area of reactive material. IR spectra of poly(phenyl carbyne) show peaks attributed to phenyl ring stretches similar to those reported by Kryazhev, as well as aliphatic C-H stretches (2930  $\text{cm}^{-1}$ ) attributed to THF incorporation. IR spectra lack any signal indicative of either C=C stretching (1640-1650  $\text{cm}^{-1}$ ) or phenylene structures (730 – 830  $\text{cm}^{-1}$ ) demonstrating the lack of both unsaturation in the backbone as well as crosslinking between rings. Further proof that the poly(phenyl carbyne) contains a branched  $\text{sp}^3$  backbone rather than an unsaturated backbone, as reported by Kryazhev, comes from the



$^{13}\text{C}$  CP-MAS NMR ( $^{13}\text{C}$  Cross Polarization Magic Angle Spin Nuclear Magnetic Resonance) spectra of the polymer. In addition to two broad peaks at 140 and 125 ppm arising from the phenyl rings, an additional broad peak is seen centered at 51 ppm indicative of a quaternary  $\text{sp}^3$  carbon. This peak was attributed to the backbone of the polymer, and was consistent with a branched network polymer. When the polymer was prepared using TCT with an enrichment of  $^{13}\text{C}$  in the alpha position, which should increase the signal amplitude of the polymer backbone, only the signal at 51 ppm was seen to increase, further supporting the lack of  $\text{C}=\text{C}$  in the backbone. It was seen, however, that slower additions of TCT to the NaK/ THF suspension did lead to some double bond formation according to IR spectroscopy.

Since poly(phenyl carbyne) generated from TCT has been reported from several different sources, it was deemed a good place to start further investigation into poly(carbyne)s in general. This is due both to the discrepancies in reported structure, as well as the lack of a rigorous optimization. We felt that the synthetic strategies employed by Kryazhev, with polymerization occurring by the reduction of TCT in THF by solid metals, were the optimal starting point. This procedure is both simpler and safer, not requiring the use of a probe sonicator in an inert atmosphere or the handling of highly pyrophoric NaK amalgam, making both optimization of poly(phenyl carbyne) synthesis as well as any other future poly(carbyne) synthesis easier to perform. Additionally, we thought further structural investigation of the polymers synthesized by the methods of Kryazhev using modern techniques (C-NMR, GPC) were worthwhile, to determine whether choice of reductant actually leads to structural differences or if the polymers were mischaracterized. Work in this chapter focuses on first optimization of the synthesis of poly(phenyl carbyne), and secondly an in depth structural and chemical analysis of the polymer.

## 2.2 Results and Discussion

The first step in the investigation was to prepare poly(phenyl carbyne) using the initial experimental conditions given by Brodskaya<sup>1</sup>, with a 3.16 eq. of Li being added slowly to a 1 M solution of TCT in THF under an Ar atmosphere. Immediately upon addition, the solution began to turn black, and Li addition had to be spread out over the course of about 30 minutes to prevent excessive heating. Once all Li was added, the reaction was allowed to react for 24 hours at room temperature. Methanol was then added slowly to quench the remaining lithium. Once no metallic lithium remained, the solution was dried under vacuum, redissolved in minimal amounts of THF, and reprecipitated in methanol twice followed by hexane twice. The final mixture was centrifuged and the solvent decanted, then the remaining reddish-brown solid was dried under vacuum at 70 °C. These initial conditions led to formation of a 0.77 kDa polymer in 58% yield, as determined by GPC using a conventional calibration

versus a poly(styrene) standard (table 1). The reaction was repeated using the same equivalence of Na, which yielded a slightly larger polymer (0.97 kDa) in a lower yield of 47.3%. Poly(phenyl carbyne) was also synthesized using Mg and Zn according to the procedures of Kryazhev.<sup>2</sup> In these experiments, TCT was added dropwise to a refluxing solution of THF with 2.3 eq. of the reducing metal. After 24 hr., the solution was quenched with MeOH and worked up in the manner mentioned above. Use of Zn lead to isolation of a polymer with a molecular weight of 1.07 kDa in a 22% yield while Mg produced a polymer in 60% yield with a low molecular weight of 0.24 kDa.

**Table 1.** Effect of Monomer Concentration on Synthesis of Poly(phenyl carbyne)<sup>a</sup>

Concentration (M)	Yield	M <sub>n</sub> (kDa)	PDI
2	39%	1.28	2.26
1	78%	0.77	2.53
.5	30%	0.91	1.74
.25	27%	0.29	1.78

<sup>a</sup>Conditions: 5 mmol trichlorotoluene, 17.5 mmol Li, 24 Hrs. @ R.T.

Since Li provided the highest polymer yields of the 4 reductants, it was chosen for further optimization. Optimization began by first varying the concentration of TCT from the previously reported 1M value (Table 1). While higher molecular weights could be obtained using a 2M monomer concentration, substantially higher yields were obtained when reactions were performed using a 1M initial monomer concentration. Likewise, reactions with monomer concentrations of 0.5 M or lower provide substantially lower yields than those run at 1 M. Further improvements in yield and molecular weight were seen when the reaction was run at 70 °C (Table 2). Additionally, reactions reached completion three times faster than when run at room temperature.



**Table 2.** Effect of Temperature and Time on Synthesis of Poly(phenyl carbyne)<sup>a</sup>

Reaction Temperature (°C)	Reaction Time (hours)	Yield	M <sub>n</sub> (kDa)
25	12	52%	1.09
	24	38%	1.06
	36	54%	0.81
70	1	42%	1.27
	3	55%	1.12
	6	61%	2.16
	12	58%	2.48
	12 <sup>b</sup>	85%	4.10
	24	50%	2.39
	36	57%	2.22

<sup>a</sup>Conditions: 5 mmol trichlorotoluene, 17.5 mmol Li, 5 mL THF <sup>b</sup> Conditions: 5 mmol trichlorotoluene, 30 mmol Li, 5 mL THF

Since higher yields and molecular weights were seen at elevated temperatures, it was hypothesized that even higher reaction temperature would further improve these values. Unfortunately, further increases above 70 °C would lead to high pressure reactions if THF was used. In order to test the effects of temperatures above the boiling point of THF, two higher-boiling ethers were employed as solvents (Table 3). Reactions were carried out in dioxane and dibutyl ether near their boiling points at 100 and 140 °C, respectively. Even at higher temperatures, these solvents proved less effective than THF, giving lower yields and molecular weights. In the case of dibutyl ether, no precipitate was seen, with the only isolated product being a brown oil. These results highlight the importance of solvent choice in these polymerizations. This fact was further solidified by the lack of a reaction observed when lithium was added directly to TCT without solvent.

**Table 3.** Effect of Solvent on Synthesis of Poly(phenyl carbyne)<sup>a</sup>

Solvent System	Temperature (C°)	Yield	M <sub>n</sub> (kDa)
THF	70	58%	2.48
Dioxane	100	43%	0.62
Dibutyl Ether	140	Oligomeric	
Neat	25	N.R.	

<sup>a</sup> 5 mmol trichlorotoluene, 17.5 mmol Li, 5 mL Solvent, 12 hrs. @ 70 °C

Throughout the course of the reaction, it was observed that a large amount of metallic Li remained in the reaction until quenching. Additionally, this Li was coated in a black film, presumably made of the poly(carbyne) and precipitated LiCl. In order to increase the amount of Li that is able to react before film formation, 6 equivalents were added instead of 3.5. The additional Li led to an increase in yield and M<sub>n</sub> from 58% to 85% and 2.48 to 4.10 kDa, respectively. Thusly, the optimized procedure for the polymerization of trichlorotoluene was found to be the addition of 6 eq. of Li to a 1 M solution of trichlorotoluene in THF which is subsequently heated to 70 °C for 12 hours.

The <sup>1</sup>H-NMR spectra of poly(phenyl carbyne) synthesized using the aforementioned procedure displays a characteristic broad peak between 6.5 and 7.5 ppm as seen in spectra of poly(phenyl carbyne) synthesized using other methods (Figure 1).<sup>2-4</sup> Additionally, however, several peaks are seen between 0.5 and 2.5 ppm, even after extensive purification and drying. These are likely due to the incorporation of THF into the polymer, which is reported previously for poly(phenyl carbyne).<sup>4</sup> The <sup>13</sup>C-NMR spectra shows the two reported broad aromatic peaks at 140 and 128 ppm (Figure S1).<sup>4</sup> Additionally, narrow peaks are seen at 67, 32, 23, and 14 ppm, which corresponds to the incorporation of THF and alkyl groups into the polymer, potentially as end groups added during quenching. No peak from the backbone carbon can be observed in solution state NMR. This is consistent with previous reports, and is likely do the quaternary nature of backbone carbon, as well as the presence of paramagnetic centers in the polymer, as observed by EPR. The polymer exhibited a 10 G wide EPR peak at g=2.002 characteristic of a carbon centered radical (Figure S2).

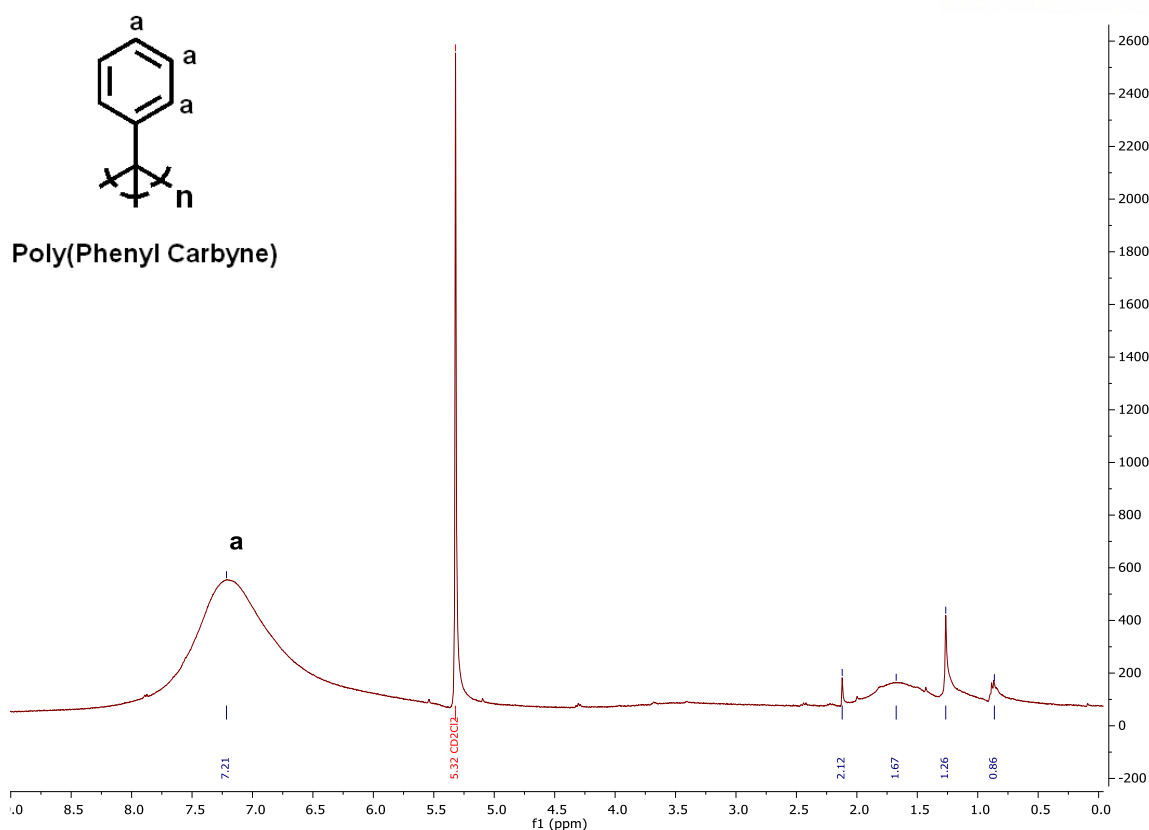


**Figure 1.**  $^1\text{H}$ -NMR of poly(phenyl carbyne) synthesized using Li in THF taken in  $\text{CD}_2\text{Cl}_2$

An additional broad peak centered at 50 ppm can be observed in the solid state CPMAS NMR spectrum of poly(phenyl carbyne) (Figure 2). This is consistent with the presence of  $\text{sp}^3$  backbone carbons in a network polymer as reported by Bianconi, et al.<sup>4</sup> No  $^{13}\text{C}$  peaks were reported by Kryazhev for the poly(phenyl carbyne) with a linear, unsaturated backbone, however poly(diphenyl acetylene), a structurally identical polymer, shows an additional  $^{13}\text{C}$ -NMR peak at 144 ppm due to the alkenes in the backbone.<sup>3</sup> Kryazhev also reports a shoulder at  $1620\text{ cm}^{-1}$  on the FTIR spectra of poly(phenyl carbyne) which is attributed to unsaturation in the backbone of the polymer.<sup>2</sup> Both of these peaks attributed to poly(phenyl carbyne) with an unsaturated backbone are absent in samples of poly(phenyl carbyne) as synthesized here, leading to the conclusion that a branched  $\text{sp}^3$  backbone is present in our samples.

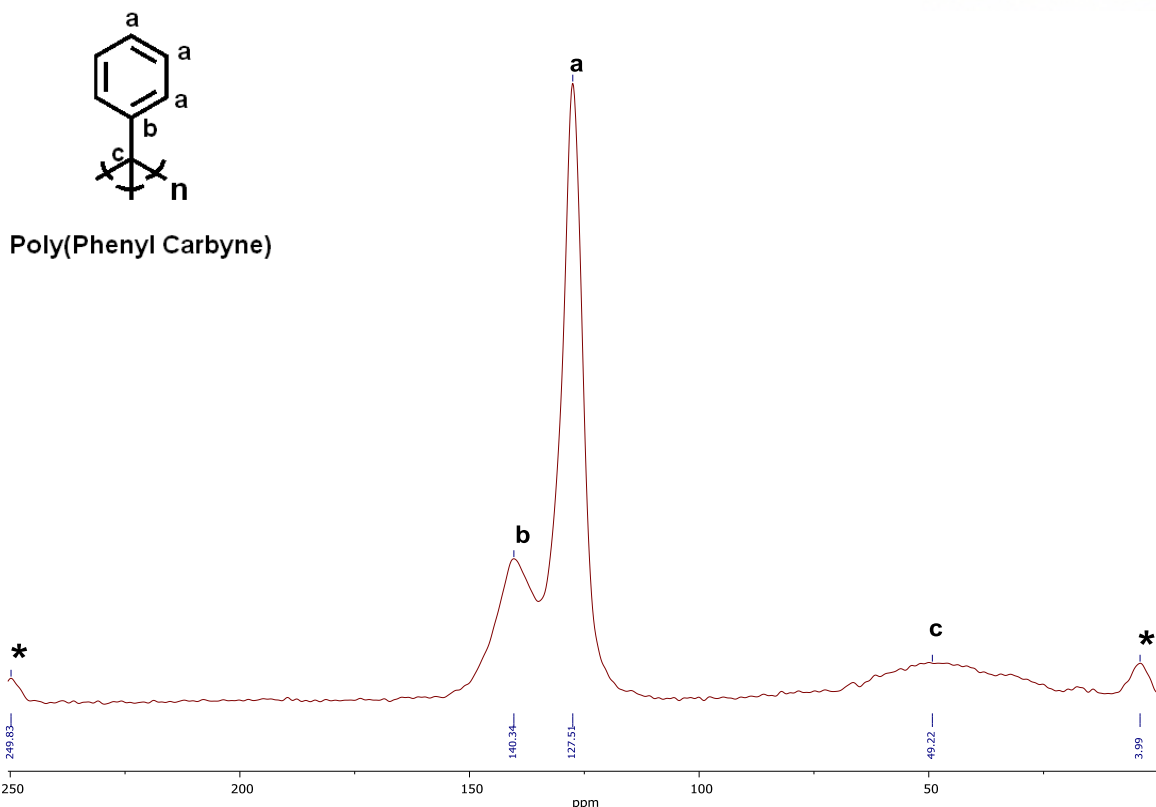


**Figure 2.** Solid state  $^{13}\text{C}$  CPMAS NMR of poly(phenyl carbyne)

The C : H : O weight ratio of the polymer was 90.6 : 5.8 : 2.3%, with a remainder of 1.3%, compared to the expected ratio of 94.3 : 5.7 : 0%. The presence of oxygen in the polymer is consistent with the incorporation of some THF into the polymer. The 1.3% that is unaccounted for is due to residual chlorine in the polymer, which is supported through the presence of 0.29 atomic percent chlorine as determined by X-ray photoelectron spectroscopy. The near complete dechlorination of the monomer was further confirmed by a 95% recovery of  $\text{Cl}^-$  ions from the reaction mixture, as determined by gravimetric analysis.

## 2.3 Conclusions

Structurally, the polymer synthesized here is almost certainly a network polymer, possessing a backbone with no unsaturation. The  $^{13}\text{C}$ -CPMAS NMR, which was not given in Kryazev's report, provides conclusive evidence of a quaternary  $\text{sp}^3$  carbon in the polymer. Peaks from this spectra, specifically the peak at 50 ppm, are also reported by Bianconi and others for poly(carbyne)s which possess branched structures.<sup>3, 4, 8-10</sup> Additionally, no evidence of alkenes exist in NMR or IR spectra for the poly(phenyl carbyne) synthesized here.

The concentrations used in Kryazhev's work (1 M) were found to be optimal, though higher temperatures (70 °C) and equivalences of Li (6 eq.) were beneficial to the polymerization. The optimized polymerization conditions for TCT produced a 4.1 kDa polymer in an 85% yield. The yield is substantially higher than that reported by Bianconi and on par with the maximum yields reported by Kryazhev. The molecular weights of poly(phenyl carbyne) synthesized here are approximately 1/3 larger than the polymer isolated from reduction by NaK but only half as large as what was previously reported by Kryazhev. This discrepancy could possibly stem from the use of different characterization techniques. While Kryazhev used VPO, which can give an absolute number average molecular weight, poly(phenyl carbyne) synthesized here was analyzed using GPC, and molecular weights are relative to poly(styrene) standard. It is well known in the literature that branched polymers appear smaller when compared to linear polymers by GPC, so molecular weights of poly(phenyl carbyne) reported here might be smaller than actual values.<sup>11</sup> Overall, the reduction of trifunctionalized monomers by Li is a relatively easy method to obtain C1 poly(carbyne)s, and is worthy of further study. Particularly, further investigation into the scope of potential monomers and study into the details of the polymerization mechanism.

## 2.4 Experimental

*General Considerations.* All solvents were dried using a Vac Atmospheres solvent purification system. Monomer syntheses were performed under an atmosphere of nitrogen using standard Schlenk techniques unless otherwise noted. Since lithium nitride can form when lithium is exposed to nitrogen, the polymerization reactions were set up under an atmosphere of argon and run in sealed vials. All reagents were purchased from commercial sources and used as received unless otherwise noted.  $\alpha,\alpha,\alpha$ -trichlorotoluene was purchased from Alfa Aesar. Solution-state  $^1\text{H}$  and  $^{13}\text{C}$  NMR spectra were recorded at room temperature on a Bruker Avance III HD spectrometer operating at 400 MHz for  $^1\text{H}$ , in  $\text{CDCl}_3$  (internal standard: 7.26 ppm,  $^1\text{H}$ ; 77.16 ppm,  $^{13}\text{C}$ ),  $\text{CD}_2\text{Cl}_2$  (internal standard: 5.32 ppm,  $^1\text{H}$ ; 53.84 ppm,  $^{13}\text{C}$ ) or  $\text{THF}-d_8$  (internal standard: 3.58 ppm,  $^1\text{H}$ ; 67.21 ppm,  $^{13}\text{C}$ ). Splitting patterns are denoted as follows: br, broad; s, singlet; d, doublet; t, triplet; q, quartet; m, multiplet. Solid-state  $^1\text{H}$ - $^{13}\text{C}$  CP MAS NMR spectra were recorded at room temperature using a Bruker Avance III HD 11.7 T wide-bore spectrometer operating at a  $^1\text{H}$  NMR frequency of 500.31 MHz and a  $^{13}\text{C}$  NMR frequency of 125.81 MHz. For all measurements, a Bruker triple-resonance MAS NMR probe (MASDVT500W2 BL3.2) was used with 3.2 mm diameter rotors consisting of  $\text{ZrO}_2$  barrels and Vespel® end caps. The magic angle was set using the  $^{79}\text{Br}$  resonance of KBr. The  $^{13}\text{C}$  chemical shifts were externally referenced to the  $-\text{COOH}$  signal of  $\alpha$ -glycine ( $\delta = 176.03$  ppm relative to tetramethylsilane). The CP MAS measurements started with a 2.25 ms,  $90^\circ$   $^1\text{H}$  pulse. During the contact time, the  $^{13}\text{C}$  spin lock field

strength was held constant while the  $^1\text{H}$  spin lock field was ramped linearly (ramped-amplitude CP) down to 50% of the initial value.<sup>11</sup>  $^1\text{H}$  decoupling was carried out with a SPINAL-64 sequence.<sup>12</sup> Samples were run at various spin rates using a 2 ms cross polarization time and a relaxation delay of 10 s. Size exclusion chromatography was performed on a Malvern Viscotek 305 TDA system equipped with a refractive index detector using THF as an eluent at  $0.8\text{ mL min}^{-1}$ . Infrared spectra were collected either by attenuated total reflectance (ATR) on an Agilent Cary-630 spectrometer using a germanium crystal for liquid samples or via transmission through a KBr pellet on a Perkin-Elmer Frontier spectrometer for solid samples. EPR spectra were collected at 295 K with an X-band microwave frequency of 9.393 GHz, a modulation frequency of 100 kHz, a modulation amplitude of 10 G, a microwave power of 0.633 mW, a time constant of 5.12 ms, and a sweep time of 30 s.

*Poly(phenyl carbyne)s.* Under an atmosphere of argon, a 20 mL glass vial equipped with a glass-coated stir bar was charged with 5 mmol of monomer and 5 mL of anhydrous THF. While stirring the solution, Li granules were added to the vial over the course of 30 min. The vial was then sealed, immersed in a heating bath that was pre-heated to a predetermined temperature, and stirred overnight. To quench the reaction, methanol was added until solid lithium was no longer observed. The mixture was then added dropwise to 500 mL of methanol to precipitate the polymer and filtered through a medium pore size frit. The precipitate was collected, dissolved in a minimal volume of THF, and added dropwise to 500 mL of methanol again. The precipitated solids were collected, dissolved in a minimal volume of THF, and added dropwise to 500 mL of *n*-hexane. The precipitated solids were collected by filtration, dried under vacuum at  $70\text{ }^\circ\text{C}$ . In order to obtain the degree of dechlorination, reaction mixtures were dried after quenching, dissolved in DCM and rinsed twice with 100 mL of water. The water layer was heated to  $70\text{ }^\circ\text{C}$  and an excess of  $0.1\text{ M AgNO}_3$  was added. The reaction was allowed to mix for 5 minutes before the solidified AgCl was collected by filtration onto a dry piece of filter paper with a known weight. Subsequent drying under vacuum and weighing allowed quantification of the amount of Cl present. Note: similar to data reported for other poly(carbyne)s,<sup>1, 4</sup> signals consistent with the incorporation of THF into the polymer were observed in some cases as minor side-products.  $^1\text{H}$  NMR (400 MHz, THF- $d_8$ ):  $\delta$  7.21 (br), 2.12 (s), 2.67 (br), 1.26 (s), 0.86 (m).  $^{13}\text{C}$  NMR (100 MHz, THF- $d_8$ ):  $\delta$  140.6, 128.52, 67.10, 31.68, 27.01, 22.76, 14.03.  $^{13}\text{C}$  CP MAS NMR (15.5 kHz):  $\delta$  140.34, 127.51, 49.22. FT-IR (KBr): 3432, 3055, 3024, 2929, 2870, 1598, 1492, 1444, 1179, 1157, 1073, 1029 913, 863, 757,  $697\text{ cm}^{-1}$ .

## 2.5 Additional Data

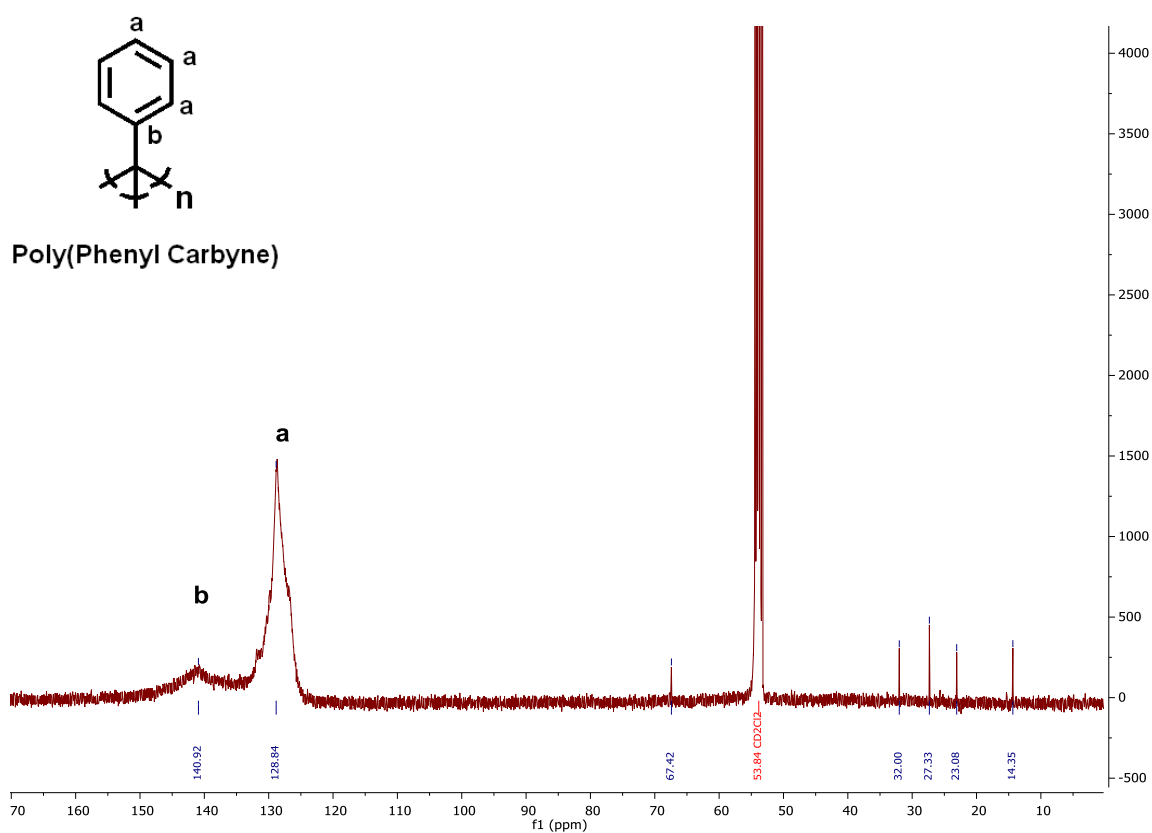


**Figure S1.**  $^{13}\text{C}$ -NMR of poly(phenyl carbyne) synthesized using Li in THF taken in  $\text{CD}_2\text{Cl}_2$

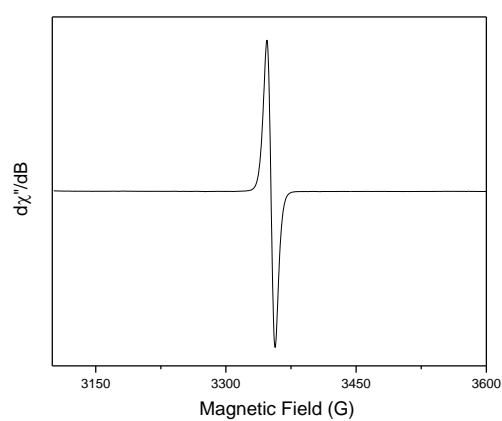


**Figure S2.** EPR signal of poly(phenyl carbyne) showing the presence of a carbon centered radical.

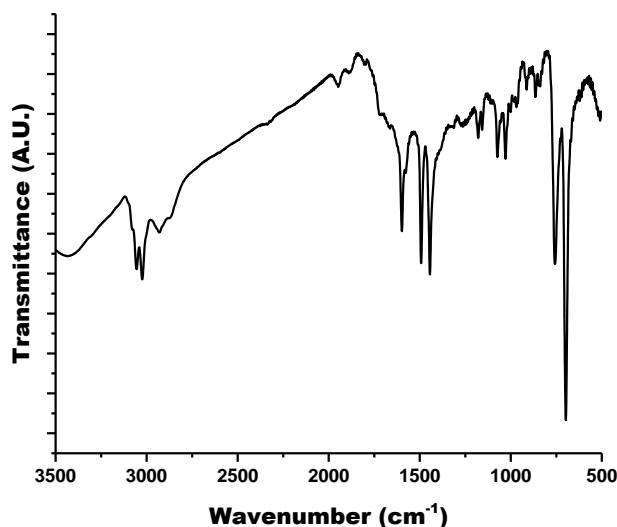


**Figure S3.** FT-IR spectrum (KBr) recorded from poly(phenyl carbyne)

## 2.6 References

1. Kryazhev, Y. G.; Petrinska, V. B.; Brodskaya, E. I., Synthesis of polyphenylmethine by dechlorination of benzene trichloride. *Pol. Sci. U.S.S.R.* **1969**, *11* (12), 2964-2970.
2. Klimov, V. I.; Raida, V. S.; Kryazhev, Y. G., Synthesis of polyenes from trichloromethyl derivatives. *Pol. Sci. U.S.S.R.* **1979**, *21* (1), 184-190.
3. Visscher, G. T.; Nesting, D. C.; Badding, J. V.; Bianconi, P. A., Poly(phenylcarbyne): A Polymer Precursor to Diamond-Like Carbon. *Science* **1993**, *260* (5113), 1496-1499.
4. Visscher, G. T.; Bianconi, P. A., Synthesis and characterization of polycarbynes, a new class of carbon-based network polymers. *J. Am. Chem. Soc.* **1994**, *116* (5), 1805-1811.
5. Bianconi, P. A.; Joray, S. J.; Aldrich, B. L.; Sumranjit, J.; Duffy, D. J.; Long, D. P.; Lazorcik, J. L.; Raboin, L.; Kearns, J. K.; Smulligan, S. L.; Babyak, J. M., Diamond and Diamond-Like Carbon from a Preceramic Polymer. *J. Am. Chem. Soc.* **2004**, *126* (10), 3191-3202.
6. Drabkin, I. A.; Tsaryuk, V. I.; Cherkashin, M. I.; Kisilitsa, P. P.; Chauser, M. G.; Chigir, A. N.; Berlin, A. A., Electronic spectra of polymers with conjugated bonds. *Pol. Sci. U.S.S.R.* **1968**, *10* (8), 1998-2007.
7. Bianconi, P. A.; Weidman, T. W., Poly(n-hexylsilylene): synthesis and properties of the first alkyl silicon [RSi]<sub>n</sub> network polymer. *J. Am. Chem. Soc.* **1988**, *110* (7), 2342-2344.



8. Kavan, L., Electrochemical preparation of hydrogen free carbyne-like materials. *Carbon* **1998**, *36* (5), 801-808.
9. Cataldo, F.; Capitani, D., Preparation and characterization of carbonaceous matter rich in diamond-like carbon and carbyne moieties. *Mater. Chem. Phys.* **1999**, *59* (3), 225-231.
10. Nur, Y.; Pitcher, M. W.; Seyyidoğlu, S.; Toppare, L., Facile Synthesis of Poly(hydridocarbyne): A Precursor to Diamond and Diamond-like Ceramics. *J. Macromol. Sci. A* **2008**, *45* (5), 358-363.
11. Podzimek, S., Light Scattering, Size Exclusion Chromatography, and Asymmetric Flow Field Flow Fractionation. Hokoken, : Wilkey, 2011
12. Metz, G.; Wu, X. L.; Smith, S. O., Ramped-Amplitude Cross Polarization in Magic-Angle-Spinning NMR. *Journal of Magnetic Resonance, Series A* **1994**, *110* (2), 219-227.
13. Fung, B. M.; Khitrin, A. K.; Ermolaev, K., An Improved Broadband Decoupling Sequence for Liquid Crystals and Solids. *Journal of Magnetic Resonance* **2000**, *142* (1), 97-101.

# Chapter 3: Synthesis and Characterization of New Poly(carbyne)s

## 3.1 Introduction

Theoretically, a large number of monomers should be viable for use in the synthesis of poly(carbyne)s. Considering just poly(carbyne)s produced through a reductive polymerization, the primary requirement for an acceptable monomer should be a carbon atom in a +3 oxidation state with leaving groups that can be replaced with new C-C bonds through some number of reductive processes (Figure 1). Theoretically, as long as the polarized bonds can be replaced with C-C bonds, there is no reason the carbon couldn't be attached to three, two, or even one electron withdrawing groups, though the latter two have not been seen experimentally. A large number of functional groups exist with a carbon atom in this state, and these could be attached to a near limitless number of side chains. Interestingly, however, very little work has been reported on varying either the leaving group or side chains in monomers for poly(carbyne)s. Other than poly(phenyl carbyne), the only other examples of poly(carbyne)s in the literature are poly(hydrido carbyne) and poly(methyl carbyne).

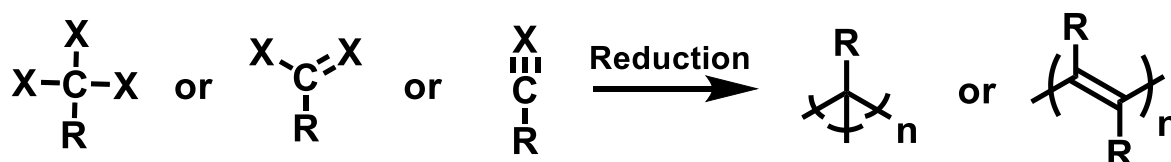


**Figure 1.** Theoretically, poly(carbyne)s could be made from any molecule with a carbon atom in the +3 oxidation state if the bonds to the electron withdrawing groups could be replaced with new C-C bonds through reduction. X = electron withdrawing leaving group

Poly(methyl carbyne) was first synthesized by Bianconi using the same procedure used to make poly(phenyl carbyne), with 1,1,1-trichloroethane being added to a sonicated emulsion of NaK amalgam in THF (Figure 2, a).<sup>1</sup> Poly(methyl carbyne) was isolated in a 3.5% yield via precipitation and was found to have a number average molecular weight,  $M_n$ , of 4.4 kDa ( $\bar{D} = 1.85$ ), slightly higher than that of poly(phenyl carbyne) synthesized using the same synthetic method. Poly(methyl carbyne) was also synthesized through electrochemical reduction (-6.0 V, reference not given) of 1,1,1-trichloroethane in acetonitrile followed by chemical reduction using  $\text{LiAlH}_4$ .<sup>2</sup> This produced 6-10% of soluble poly(methyl carbyne) ( $M_n = 9.3$  kDa,  $\bar{D} = 1.80$ ) as well as a presumably higher molecular weight

insoluble fraction. In addition to the expected aliphatic peaks,  $^1\text{H}$ -NMR of the polymer after electrolysis showed a strong peak at 2.1 ppm due to remaining chlorine in the backbone. After the reaction with  $\text{LiAlH}_4$ , the signal at 2.1 ppm was replaced with a more up-field peak at 1.4 ppm consistent with reduction of the C-Cl bonds to C-H. IR (Infra-red) and NMR (nuclear magnetic resonance) analysis of poly(methyl carbyne) were consistent with a branched network structure and showed no significant signs of side products.

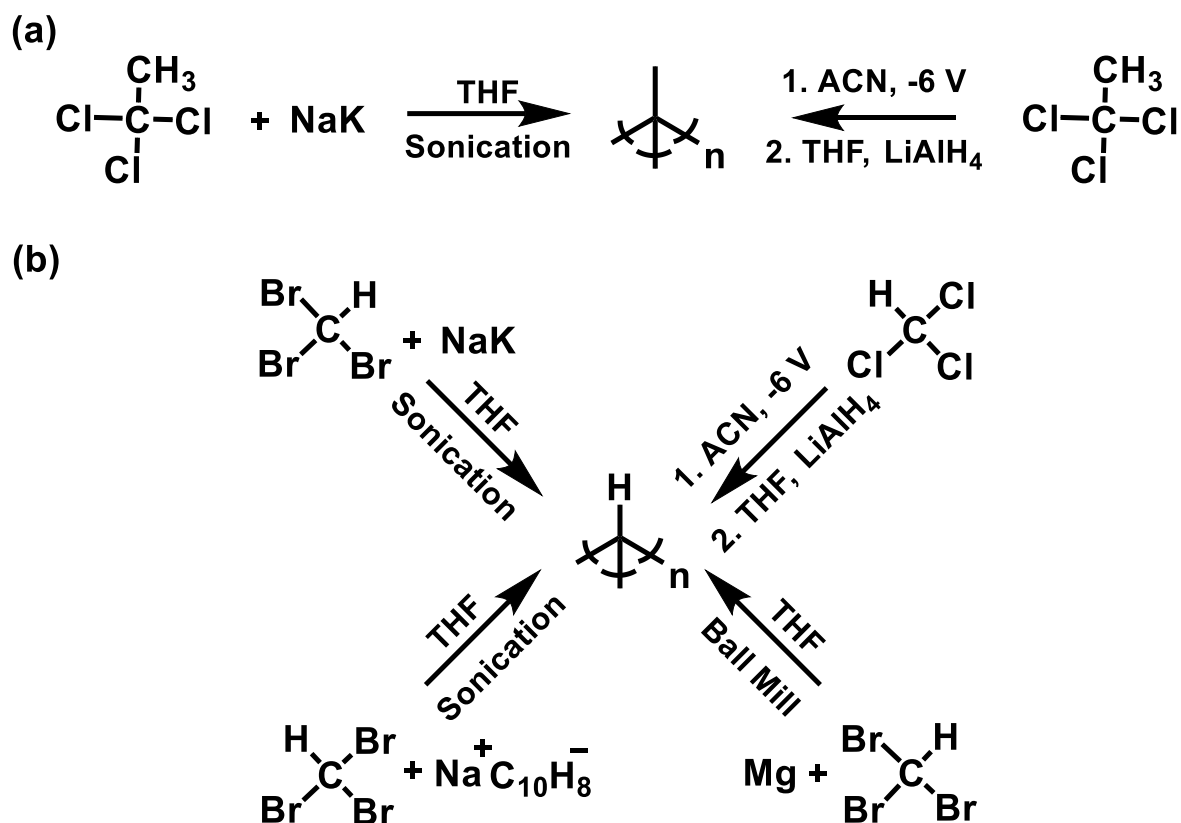


**Figure 2.** Reported synthetic strategies for poly(methyl carbyne) (a) and poly(hydrido carbyne) (b).

Bianconi was also the first to prepare poly(hydrido carbyne) by ultrasonic irradiation of a mixture of bromoform and NaK amalgam in THF which led to the formation of poly(hydrido carbyne) in yields between 45 – 86% (Figure 2, b).<sup>3</sup> While the product of this reaction was shown to be a macromolecule by light scattering, no exact molecular weight data was given. Similar to samples of poly(phenyl carbyne), poly(hydrido carbyne) has a strong electron paramagnetic resonance (EPR) signal indicative of a carbon centered radical.<sup>1, 3, 4</sup> IR and CP-MAS (cross polarized magic angle spin)  $^{13}\text{C}$ -NMR spectra indicated the polymer primarily contained a branching  $\text{sp}^3$  backbone, however  $^{13}\text{C}$ -NMR signals from residual C-Br sites were seen, as well as peaks assigned to cis- and trans-polyacetylene. Interestingly, some double bonds in the backbone of poly(carbyne)s were also seen previously when trichlorotoluene was added slowly to the NaK/ THF emulsion.<sup>1</sup> In the case of poly(hydrido carbyne), these double bond peaks were seen in all cases when NaK amalgam was used,

regardless of reaction conditions. A more pure polymer was obtained when poly(hydrido carbyne) was prepared through electrolysis of chloroform.<sup>5</sup> Using a method identical to the electrochemical synthesis of poly(methyl carbyne) (save for the use of chloroform instead of trichloroethane), poly(hydrido carbyne) with a  $M_n$  of 5.6 kDa ( $\bar{D} = 1.1$ ) could be isolated in 30 – 40% yields. After reduction with  $\text{LiAlH}_4$ ,  $^1\text{H}$ -NMR and IR spectra showed no indication of any impurities, though direct comparison to the poly(hydrido carbyne) from Bianconi's work is difficult as no CP-MAS data is given. Poly(hydrido carbyne) was also synthesized from bromoform by reduction using sodium naphthalenide in THF.<sup>6</sup> This process was reported to produce a polymer with one unit of naphthalene in the polymer for every 30 monomer units based on integration of  $^1\text{H}$ -NMR spectra, though the method or location of this incorporation was not discussed. The final method of synthesis utilized for poly(hydrido carbyne) was through mechanochemical synthesis.<sup>7, 8</sup> Bromoform was spun in a centrifugal ball mill with Mg and THF for 15 minutes, which after several extractions led to the isolation of the expected polymer in 40 – 60 % yield. The molecular weight of these samples was found to be slightly lower ( $M_n = 1.6$  kDa,  $\bar{D} = 2.1$ ) than poly(hydrido carbyne) synthesized by other methods, but the polymer appeared spectroscopically identical according to FT-IR,  $^1\text{H}$ -NMR, and EPR.

The aforementioned methods (both in chapters 2 and 3) fully cover the reported syntheses of poly(carbynes). While various reduction methods have been used, only germinal trichlorides and bromides have been utilized as monomers. The use of C-Cl and C-Br bonds is an excellent starting point for reductive poly(carbyne) synthesis due to their frequent use in the formation of nucleophilic organometallic compounds, C-C bond forming substitution reactions, and alkali metal couplings such as the Wurtz reaction.<sup>9, 10</sup> As mentioned before, however, many strongly oxidized carbon atoms could potentially form poly(carbyne)s under reducing conditions. Other carbon centers possessing 3 bonds to more electronegative atoms such as oxygen or nitrogen could also be amenable to reductive polymerizations to form poly(carbyne)s. In contrast to halide-based carbyne precursors, O and N based precursors could potentially have 1 or 2 heteroatoms attached to a carbon with an oxidation state of +3 (*e.g.* esters or nitriles). In addition to increasing our fundamental understanding of what oxidized carbons can be converted in poly(carbynes), exploration into new potential leaving groups in reductive polymerizations can greatly expand the range of potential monomers unitized in poly(carbyne) synthesis.

In addition to varying the leaving groups attached to the reactive carbon center, the unreactive “side chain” substituent can also be varied. To date, only phenyl, methyl, and hydrogen side chains have been used in poly(carbyne) synthesis. Variation of polymer side chains can have drastic effects on a range of polymer properties such as crystallinity, solubility, thermal properties, and more.<sup>11, 12</sup> The use of ester side chains, like those seen in poly(acrylate)s, can be particularly useful as a wide range of functionalities can easily be attached without strongly altering the polymerizable portion of the

monomer. This technique has been utilized extensively in the polymerization of diazoacetates<sup>13-16</sup>, and has led to the formation of several C1 polymers that show enhanced properties like increased thermal stability<sup>14</sup> or fluorescence<sup>17</sup>, or unique properties such as lower critical solution temperatures<sup>18</sup>. Because of the utility of ester functionalities as side chains, synthesis of ester containing poly(carbyne)s is particularly appealing.

Herein, we have investigated a number of new poly(carbyne)s synthesized through reductive polymerizations using Li. In order to greatly expand the scope of potential monomers for these polymerizations, we have varied both the leaving groups as well as the side chains. Reaction conditions were first optimized, including the addition of an electron transfer catalyst. Subsequently, new poly(carbyne)s were synthesized and characterized, doubling the number of carbyne precursors known to polymerize under reductive conditions.

## 3.2 Results and Discussion

A library of monomers that were envisioned to afford poly(carbyne)s via a reductive C1 polymerization is shown in Figure 3. The monomers were selected because they feature electron deficient carbon atoms in the +3-oxidation state and could potentially form new C-C bonds under reduction. Germinal trichlorides **1** – **4** were chosen to test the effects varying the side chain would have on the polymer structure. Monomers **1** – **3** were chosen to see if poly(ester carbyne)s could be synthesized and determine the effect of alkyl chain length on the polymer. Monomer **4** was tested to see if other polar ketone containing functionalities could be polymerized as well. Molecules **5** – **8** all contain phenyl side chains and were designed to test the viability of using new leaving groups in the reductive polymerization. Monomers **5** and **6** were selected to test the effects of relatively less (OMe) and more (F) electronegative leaving groups than Cl or Br, and **7** and **8** were chosen to see if sp<sup>2</sup> and sp carbons in the +3 oxidation state could be used in poly(carbyne) synthesis.

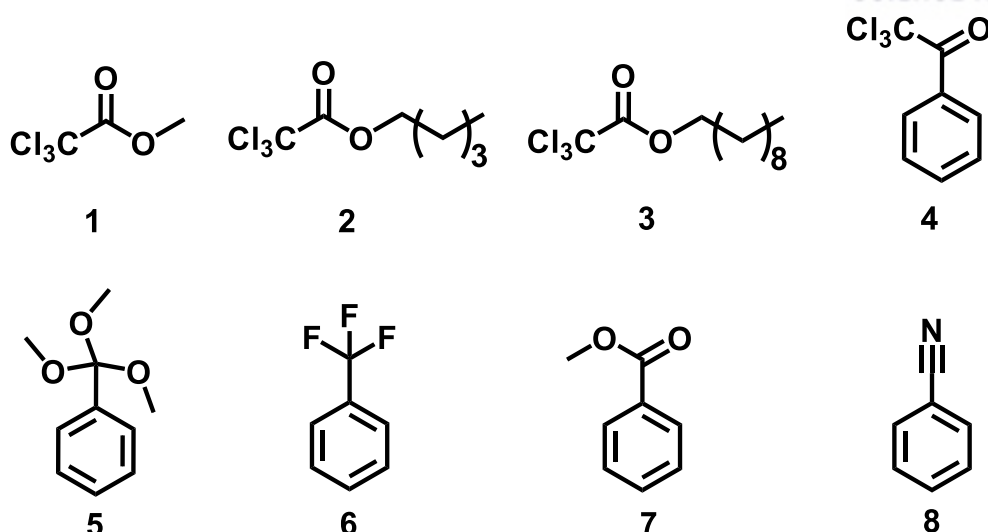


**Figure 3.** Structures of potential poly(carbyne) monomers tested.

A preliminary set of polymerization reactions was performed with *n*-pentyl 2,2,2-trichloroacetate (**2**), starting with the original procedure from Brodskya.<sup>19</sup> A 1.0 M THF solution of the monomer was charged with 3.2 equivalents of Li at room temperature. After 24 hours, the reaction mixture was quenched with methanol, extracted, and then added dropwise into *n*-hexane to induce precipitation. Collection of the precipitated solids afforded the corresponding polymer in 21% yield. Variation of monomer concentration to higher and lower values was not seen to improve yields or molecular weights of the isolated polymer (Table S1). Increasing reaction temperature while maintaining all other reaction conditions was seen to lead to incremental increases in yields and molecular weights up to 70 °C, where a yield of 31% was obtained (Table S2). Since the use of other non-THF solvents produced undesirable effects in the synthesis of poly(phenyl carbyne), higher boiling ethers were tested. Similar to poly(phenyl carbyne) synthesis, maximum yields (39%) and molecular weights (909 Da,  $\bar{D} = 1.1$ ) were obtained by performing the reaction at 70 °C with 6 equivalents of Li after only 12 hours (Table S3).

Electron transfer agents have been reported to facilitate the activation of carbon–halogen bonds by alkali metals.<sup>20, 21</sup> As such, it was reasoned that the addition of an electron transfer agent to the reaction may improve the performance of the polymerization. Naphthalene was selected because it readily forms lithium naphthalenide, a radical anion, upon exposure to lithium. The addition of naphthalene (0.25 equiv. with respect to monomer) to the optimized reaction parameters described above ( $[2]_0 = 1.0$  M,  $[Li]_0/[2]_0 = 6$ , THF, 70 °C, 12 h) increased the yield of polymer to 50%. The use of relatively more or less naphthalene was observed to have detrimental effects (Table S4). As such, the conditions were deemed optimal and applied toward the polymerization of the other monomers shown in Figure 3; see Table 1 for a summary.

**Table 1.** Polymerization of various monomers<sup>a</sup>

Monomer	M <sub>n</sub> (kDa) <sup>b</sup>	PDI	Yield (%)
<i>n</i> -Pentyl Trichloroacetate ( <b>2</b> )	1.64	4.5	50
Methyl Trichloroacetate ( <b>1</b> )	0.72	2.9	78
<i>n</i> -Decyl Trichloroacetate ( <b>3</b> )	1.92	6.1	34
2,2,2-Trichloroacetophenone ( <b>4</b> )	2.28	5.7	48
Trimethyl Orthobenzoate ( <b>5</b> )	1.21	2.0	30
$\alpha,\alpha,\alpha$ -Trifluorotoluene ( <b>6</b> )	2.31	2.7	29
Methyl Benzoate( <b>7</b> )	N.R.	N.R.	N.R.
Benzonitrile( <b>8</b> )	N.R.	N.R.	N.R.
$\alpha,\alpha,\alpha$ -Trichlorotoluene	2.45	2.7	37
$\alpha,\alpha,\alpha$ -Trichlorotoluene <sup>c</sup>	4.10	2.8	86

a Conditions: [monomer]<sub>0</sub> = 1.0 M, [Li]<sub>0</sub>/[monomer]<sub>0</sub> = 6, [naphthalene]<sub>0</sub> = 0.25 M, THF, 70 °C, 12 h. b Determined by SEC versus a polystyrene standard in THF. c

Conditions: [monomer]<sub>0</sub> = 1.0 M, [Li]<sub>0</sub>/[monomer]<sub>0</sub> = 6, THF, 70 °C, 12 h (no added naphthalene).

The majority of monomers tested successfully formed polymers under the optimized reaction conditions. All three ester containing monomers, **1** – **3**, as well as the ketone-containing monomer, **4**, were amenable to polymerization using the optimized reaction conditions. These collectively represent the first reported poly(carbyne)s to contain carbonyl groups as well as any sort of polar side chains. Yields for the poly(ester carbyne)s appear to be inversely related to the length of the alkyl side chain, while PDI values seem to increase with increasing chain length. These trends could be attributed to the relatively lower steric bulk of small alkyl chains leading to more favorable couplings. While molecular weights increase with increasing chain length, average D.P. (degree of polymerization) is relatively consistent with **1**, **2**, and **3** having 10, 13, and 10 repeat units, respectively. Gravimetric analysis of chloride produced in the polymerization of **1** – **4** confirmed that between 90 – 100% of the C-Cl bonds were removed in the polymerization, showing very high conversion. The two new germinal trifunctionalized monomers (**5** and **6**) were smoothly polymerized into poly(phenyl carbyne), making them the first reported poly(carbyne)s precursors to be utilized using fluorine or non-halogen leaving groups. Use of **5** and **6** as monomers led to lower molecular weights and yields in comparison to PPC prepared from trichlorotoluene (TCT) without naphthalene. Interestingly, PPC prepared from TCT in



the presence of naphthalene also produced lower yields and molecular weights than when naphthalene was not present, possibly due to the formation of more hexane soluble oligomers. Neither **7** nor **8** polymerized under any reductive conditions tried, suggesting that perhaps germinal trifunctionalized monomers are required for the reductive synthesis of poly(carbyne)s. This is understandable as reductions through Li (as well as Li naphthalenide) occur through single-electron transfers. In the case of trifunctionalized monomers, a reactive carbon center primed for C-C bond formation can be created through a single electron transfer from the reductant to the leaving group followed by hemolytic bond cleavage. In the case of C=O and C $\equiv$ N bonds, this route is not viable as multiple single electron transfers to the same atom would be required to fully remove the bond.

In addition to GPC results, a series of spectroscopic measurements indicated that monomers **1** - **6** were converted into polymeric derivatives. For example, the infrared spectrum recorded for the polymer obtained from **2** exhibited relatively broad signals when compared to that of its monomer (Figure 4). Moreover, the characteristic  $\nu_{\text{C-H}}$ ,  $\nu_{\text{C=O}}$ , and  $\nu_{\text{C-O}}$  signals of **2** were retained while the  $\nu_{\text{C-Cl}}$  signals present at 880, 824, and 680  $\text{cm}^{-1}$  were absent. A new signal at 1619  $\text{cm}^{-1}$ , consistent with an alkene stretching frequency and indicative of an unsaturated polymer backbone, was also observed. Similar signals (1628 – 1598  $\text{cm}^{-1}$ ) were observed in infrared spectra recorded for the polymers derived from **1**, **3**, and **4** (see Figures S28 – S30). The IR spectra for the polymers obtained from **5** and **6** (see Figures S31 – S32) were very similar to that of poly(phenyl carbyne), both as reported<sup>1</sup> and as synthesized here, and thus their structures were assigned as branched.

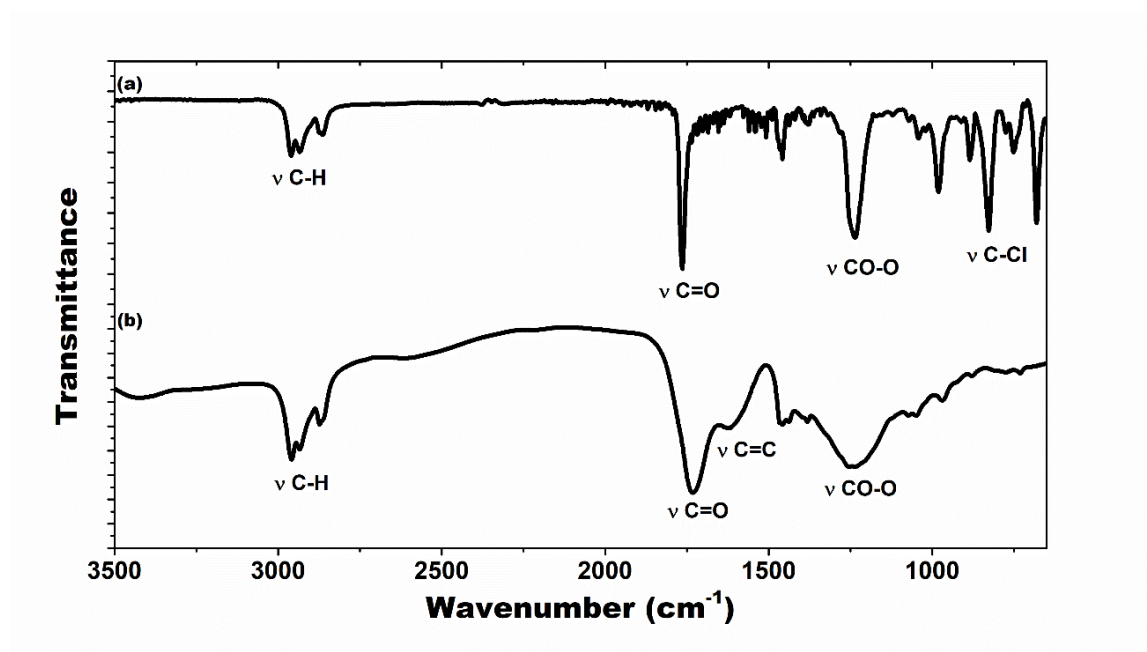


**Figure 4.** Infrared spectra recorded for (a) monomer **2** and (b) its polymeric derivative.



NMR spectroscopy was utilized to further elucidate the structures of the poly(carbyne)s. While the solution-state  $^1\text{H}$  and  $^{13}\text{C}$  NMR spectra recorded for the polymers synthesized from **1** – **6** were consistent with their structures, the signals were found to be broad which challenged refinement. For example, the  $^{13}\text{C}$  NMR signal assigned to the carbonyl group in **4** can be observed at 162 ppm; however, the corresponding signal was suppressed upon analysis of the polymer (Figure 5). Additionally, the signal for the germinal trichloride is seen at 90 ppm in the monomer, but no peak is visible for the backbone, appearing in either the vinyl or alkyl region, in the polymer product. The “quaternary”<sup>22</sup> nature of these carbons could partially explain why they do not appear, as carbons not attached to a proton often show weak signals due to long relaxation times, however, non-quaternary carbons were also suppressed. In both  $^1\text{H}$  (Figure S9) and  $^{13}\text{C}$  NMR (Figure 5b) spectra of poly(**4**), the peaks from the methylene adjacent to the ester (4.03 and 62 ppm, respectively) show substantially lower intensity relative to the other alkyl peaks, showing that even carbons bonded to protons show decreased NMR signals based on their proximity to the backbone.

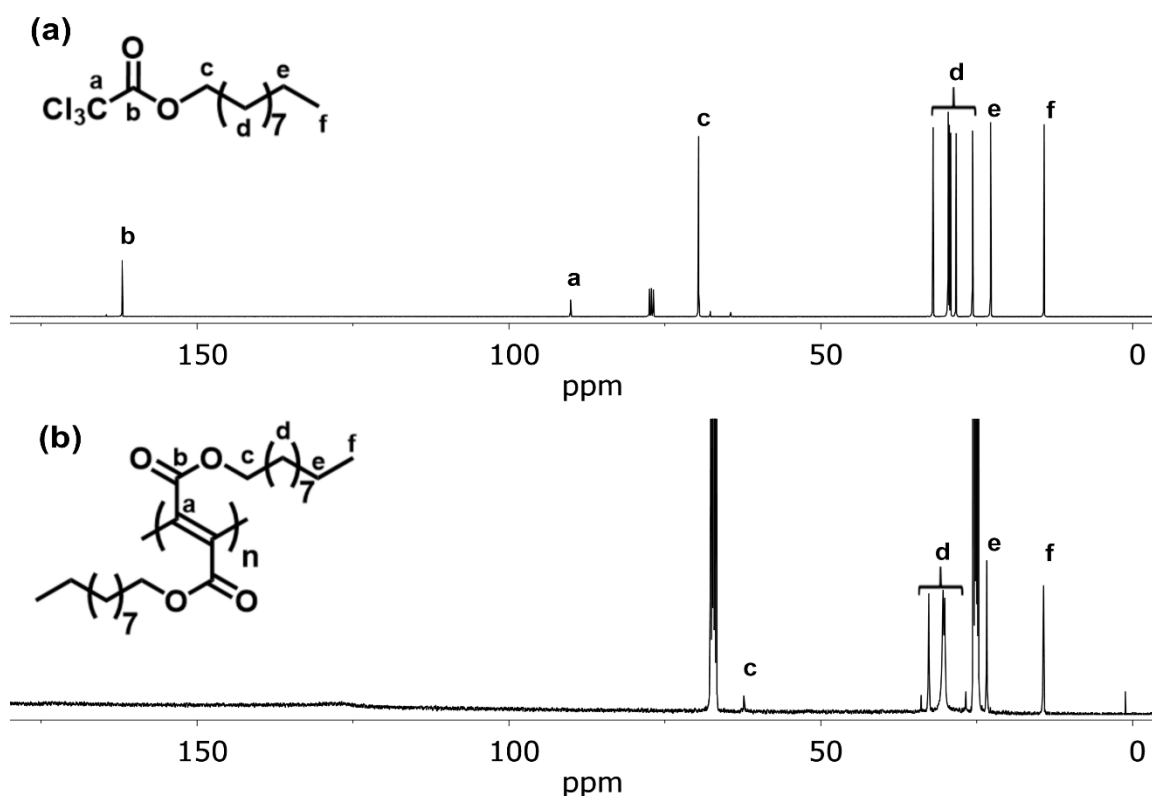


**Figure 5.**  $^{13}\text{C}$  NMR spectra recorded for **4** before (a,  $\text{CDCl}_3$ ) and after (b,  $\text{THF-}d_8$ ) polymerization.

It was reasoned that the NMR signal suppression effects may be due to the presence of polymer-based radicals. It is known in the literature that atoms spatially near to paramagnetic centers are often rendered invisible on NMR spectra due to hyperfine coupling or paramagnetic relaxation enhancement.<sup>23</sup> Poly(carbyne)s have been previously reported to contain unpaired electrons along their backbones, so their presence in the new polymers is reasonable.<sup>4, 7, 8, 19, 24</sup> Electron paramagnetic

resonance (EPR) spectroscopy revealed that the polymers described above exhibited sharp signals at  $g = 2.002 - 2.003$  with a separation of  $8 - 10$  G, consistent with carbon-centered radicals. The corresponding spin densities were calculated to be on the order of  $10^{17} - 10^{18}$  spins/g, with poly(**4**) exhibiting ten times higher unpaired electron concentrations than poly(phenyl carbyne) (Table 2).

**Table 2.** Spin Densities Measured for Various Poly(carbyne)s<sup>a</sup>

Entry	Polymer	Spins/g
1	Poly(phenyl carbyne)	$9.81 \times 10^{16}$
2	Poly(n-pentyl ester carbyne)	$1.85 \times 10^{17}$
3	Poly(methyl ester carbyne)	$1.99 \times 10^{17}$
4	Poly(n-decyl ester carbyne)	$6.23 \times 10^{17}$
5	Poly(benzoyl carbyne)	$9.99 \times 10^{17}$

<sup>a</sup> Synthesized using General Procedure B

The NMR peak suppression was effectively managed using  $^1\text{H}$ – $^{13}\text{C}$  cross-polarization magic-angle spinning (CP MAS) NMR spectroscopy, where the  $^{13}\text{C}$  NMR signal of the carbonyl group in the poly(**3**) was observed at 173 ppm (Figure 6). A  $^{13}\text{C}$  NMR signal was also recorded at 126 ppm and attributed to alkene groups present in an unsaturated linear backbone, consistent with the FT-IR data. Similar data were recorded for the polymers that were synthesized from **1**, **2**, **4** (see Figures S19 – S22). The  $^1\text{H}$ – $^{13}\text{C}$  CP MAS NMR spectra of the polymers obtained from **5** and **6** (see Figures S23, S24) exhibited broad signals at 51 ppm, which has been attributed to the quaternary carbons of a branched network, further reinforcing their structural assignment.<sup>1</sup>

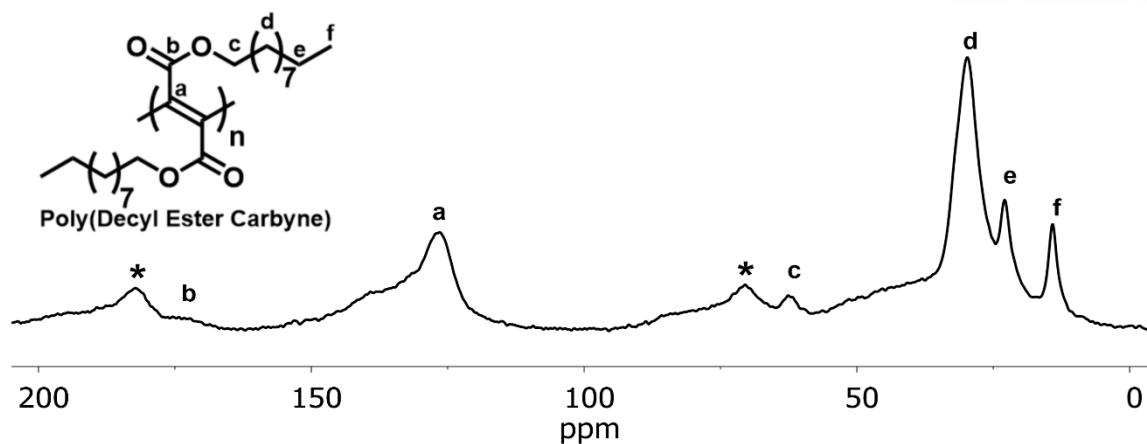


**Figure 6.**  $^1\text{H}$ - $^{13}\text{C}$  CP MAS NMR spectrum recorded for the polymer obtained from **3**. Conditions: MAS = 7 kHz,  $t_{\text{CP}}$  = 2 ms, relaxation delay = 10 s; \* denotes spinning sidebands.

### 3.3 Conclusion

In conclusion, we have demonstrated that a wide range of molecules could potentially be used as monomers in the polymerization of poly(carbynes). It was successfully demonstrated that a number of new geminally functionalized molecules could be utilized as poly(carbyne) precursors, including those containing C-F and C-O bonds. Unfortunately, all monomers tried that contained less than 3 leaving groups (**7**, **8**) were not polymerizable under the conditions tried. Additionally, the first poly(carbyne)s containing polar side chains, including versatile ester groups were successfully synthesized. Further variation of the side chains on poly(ester carbyne)s could lead to per-substituted polymers with dense functionalization which could potentially show unique or enhanced physicochemical properties over conventional polymers. The polymerization was successfully optimized, significantly increasing yields of the poly(carbyne)s through the addition of an electron transfer catalyst. Characterization of the new poly(carbyne)s led to an interesting dichotomy, with the carbonyl-containing polymers possessing an unsaturated backbone in contrast to previously reported poly(carbyne)s, which contain branched  $\text{sp}^3$  backbones.

### 3.4 Experimental

*General Considerations.* All solvents were dried using a Vac Atmospheres solvent purification system. Monomer syntheses were performed under an atmosphere of nitrogen using standard Schlenk techniques unless otherwise noted. Since lithium nitride can form when lithium is exposed to nitrogen, the polymerization reactions were set up under an atmosphere of argon and run in sealed vials. All reagents were purchased from commercial sources and used as received unless otherwise noted.  $\alpha,\alpha,\alpha$ -trichlorotoluene and 2,2,2-trichloroacetophenone were purchased from Alfa Aesar. Methyl 2,2,2-

trichloroacetate and  $\alpha,\alpha,\alpha$ -trifluorotoluene were purchased from TCI Chemicals. Methyl orthobenzoate was purchased from Sigma Aldrich. Solution-state  $^1\text{H}$  and  $^{13}\text{C}$  NMR spectra were recorded at room temperature on a Bruker Avance III HD spectrometer operating at 400 MHz for  $^1\text{H}$ , in  $\text{CDCl}_3$  (internal standard: 7.26 ppm,  $^1\text{H}$ ; 77.16 ppm,  $^{13}\text{C}$ ),  $\text{CD}_2\text{Cl}_2$  (internal standard: 5.32 ppm,  $^1\text{H}$ ; 53.84 ppm,  $^{13}\text{C}$ ) or  $\text{THF}-d_8$  (internal standard: 3.58 ppm,  $^1\text{H}$ ; 67.21 ppm,  $^{13}\text{C}$ ). Splitting patterns are denoted as follows: br, broad; s, singlet; d, doublet; t, triplet; q, quartet; m, multiplet. Solid-state  $^1\text{H}$ - $^{13}\text{C}$  CP MAS NMR spectra were recorded at room temperature using a Bruker Avance III HD 11.7 T wide-bore spectrometer operating at a  $^1\text{H}$  NMR frequency of 500.31 MHz and a  $^{13}\text{C}$  NMR frequency of 125.81 MHz. For all measurements, a Bruker triple-resonance MAS NMR probe (MASDVT500W2 BL3.2) was used with 3.2 mm diameter rotors consisting of  $\text{ZrO}_2$  barrels and Vespel® end caps. The magic angle was set using the  $^{79}\text{Br}$  resonance of KBr. The  $^{13}\text{C}$  chemical shifts were externally referenced to the  $-\text{COOH}$  signal of  $\alpha$ -glycine ( $\delta = 176.03$  ppm relative to tetramethylsilane). The CP MAS measurements started with a 2.25 ms,  $90^\circ$   $^1\text{H}$  pulse. During the contact time, the  $^{13}\text{C}$  spin lock field strength was held constant while the  $^1\text{H}$  spin lock field was ramped linearly (ramped-amplitude CP) down to 50% of the initial value.<sup>25</sup>  $^1\text{H}$  decoupling was carried out with a SPINAL-64 sequence.<sup>26</sup> Samples were run at various spin rates using a 2 ms cross polarization time and a relaxation delay of 10 s. Size exclusion chromatography was performed on a Malvern Viscotek 305 TDA system equipped with a refractive index detector using THF as an eluent at  $0.8\text{ mL min}^{-1}$ . Infrared spectra were collected either by attenuated total reflectance (ATR) on an Agilent Cary-630 spectrometer using a germanium crystal for liquid samples or via transmission through a KBr pellet on a Perkin-Elmer Frontier spectrometer for solid samples. EPR spectra were collected at 295 K with an X-band microwave frequency of 9.393 GHz, a modulation frequency of 100 kHz, a modulation amplitude of 10 G, a microwave power of 0.633 mW, a time constant of 5.12 ms, and a sweep time of 30 s.

*n*-Pentyl Trichloroacetate (**2**). A dry 250 mL flask was charged with 100 mL of anhydrous  $\text{CH}_2\text{Cl}_2$  and 4.176 g (47.4 mmol) of 1-pentanol. The flask was cooled to  $0^\circ\text{C}$  and then charged with 10.306 g (54.7 mmol) of trichloroacetyl chloride. After adding 4 mL of pyridine in a dropwise manner to the flask, the resulting mixture was slowly warmed to room temperature and stirred overnight. The mixture was then washed with 100 mL of an aqueous solution of HCl (10%) followed by 100 mL of brine before being dried over  $\text{MgSO}_4$ . After filtration, the solvent was evaporated to afford 10.096 g (91% yield) of the desired compound as a straw-colored liquid.  $^1\text{H}$  NMR (400 MHz,  $\text{CDCl}_3$ ):  $\delta$  4.32 (t, 2H), 1.73 (m, 2H), 1.34 (m, 4H), 0.88 (t, 3H).  $^{13}\text{C}$  NMR (100 MHz,  $\text{CDCl}_3$ ):  $\delta$  161.86, 90.00, 69.43, 27.84, 27.67, 22.10, 13.80. FT-IR (Ge-ATR): 2960, 2932, 2863, 1763, 1457, 1379, 1236, 1042, 980, 885, 827, 751,  $680\text{ cm}^{-1}$ .

*n*-Decyl Trichloroacetate (**4**). A dry 250 mL flask was charged with 100 mL of anhydrous  $\text{CH}_2\text{Cl}_2$  and 7.622 g (48.15 mmol) of 1-decanol. The flask was cooled to  $0^\circ\text{C}$  and then charged with 10.129 g (55.7

mmol) of trichloroacetyl chloride. After adding 4 mL of pyridine in a dropwise manner to the flask, the resulting mixture was slowly warmed to room temperature and stirred overnight. The mixture was then washed with 100 mL of an aqueous solution of HCl (10%) followed by 100 mL of brine before being dried over MgSO<sub>4</sub>. After filtration, the solvent was evaporated to afford 14.216 g (97% yield) of the desired compound as a straw-colored liquid. <sup>1</sup>H NMR (400 MHz, CDCl<sub>3</sub>): δ 4.34 (t, 2H), 1.74 (m, 2H), 1.25 (m, 14H), 0.86 (t, 3H). <sup>13</sup>C NMR (100 MHz, CDCl<sub>3</sub>): δ 162.14, 90.16, 69.68, 32.01, 29.60, 29.55, 29.40, 29.19, 28.33, 25.70, 22.80, 14.22. FT-IR (Ge-ATR): 2956, 2924, 2854, 1765, 1457, 1379, 1239, 1042, 984, 878, 827, 751, 680 cm<sup>-1</sup>.

*General Procedure A: Synthesis of Poly(carbyne)s.* Under an atmosphere of argon, a 20 mL glass vial equipped with a glass-coated stir bar was charged with 5 mmol of monomer and 5 mL of anhydrous THF. While stirring the solution, Li granules were added to the vial over the course of 30 min. The vial was then sealed, immersed in a heating bath that was pre-heated to a predetermined temperature, and stirred overnight. To quench the reaction, methanol was added until solid lithium was no longer observed. The mixture was then added dropwise to 500 mL of methanol to precipitate the polymer and filtered through a medium pore size frit. The precipitate was collected, dissolved in a minimal volume of THF, and added dropwise to 500 mL of toluene. The precipitated solids were collected, dissolved in a minimal volume of THF, and added dropwise to 500 mL of *n*-hexane. The precipitated solids were collected by filtration, dried under vacuum at 70 °C. Note: similar to data reported for other poly(carbyne)s,<sup>1, 19</sup> signals consistent with the incorporation of THF into the polymer were observed in some cases as minor side-products.

*General Procedure B: Synthesis of Poly(carbyne)s in the Presence of Naphthalene.* Under an atmosphere of argon, 5 mL of anhydrous THF, 160.2 mg (1.25 mmol) of naphthalene, and 208.2 mg (30 mmol) of lithium were added to a 30 mL vial equipped with a glass-coated stir bar. The vial was sealed and then charged with 5 mmol of monomer in a dropwise manner via syringe before heating the mixture to 70 °C overnight. The reaction mixture was then cooled to room temperature. To quench the reaction, methanol was added until solid lithium was no longer observed. The solvent was then evaporated and the solid residue was washed with 50 mL of an aqueous solution of HCl (10%) and then dissolved in 100 mL of ethyl acetate. The organic phase was washed with 50 mL of an aqueous solution of HCl (10%) followed by 100 mL of brine. The organic phase was then dried over MgSO<sub>4</sub>, filtered, and the solvent was removed under vacuum. The product was dissolved in a minimal volume of THF, added dropwise to an excess of *n*-hexane, collected via filtration, and dried under vacuum at 70 °C. In order to obtain the degree of dechlorination, reaction mixtures were dried after quenching, dissolved in DCM and rinsed twice with 100 mL of water. The water layer was heated to 70 °C and an excess of 0.1 M AgNO<sub>3</sub> was added. The reaction was allowed to mix for 5 minutes before the solidified AgCl was collected by filtration onto a dry piece of filter paper with a known weight. Subsequent drying under

vacuum and weighing allowed quantification of the amount of Cl present. Note: similar to data reported for other poly(carbyne)s,<sup>1, 19</sup> signals consistent with the incorporation of THF into the polymer were observed in some cases as minor side-products.

*Poly(Phenyl Carbyne)*. Using General Procedure B, monomer **1**, **6**, and **7** afforded 165 mg (37% yield), 133 mg (30% yield), and 129 mg (29% yield), respectively, of poly(phenylcarbyne) as a brown powder. Poly(phenyl carbyne) samples prepared using **1**, **6**, and **7** are spectroscopically identical. <sup>1</sup>H NMR (400 MHz, THF-*d*<sub>8</sub>): δ 7.21 (br), 2.12 (s), 2.67 (br), 1.26 (s), 0.86 (m). <sup>13</sup>C NMR (100 MHz, THF-*d*<sub>8</sub>): δ 140.6, 128.52, 67.10, 31.68, 27.01, 22.76, 14.03. <sup>13</sup>C CP MAS NMR (15.5 kHz): δ 140.34, 127.51, 49.22. FT-IR (KBr): 3432, 3055, 3024, 2929, 2870, 1598, 1492, 1444, 1179, 1157, 1073, 1029 913, 863, 757, 697 cm<sup>-1</sup>.

*Poly(Pentyl Ester Carbyne)*. Using General Procedure B and monomer **2** afforded 317.9 mg (50 % yield) of a dark brown polymer. <sup>1</sup>H NMR (400 MHz, THF-*d*<sub>8</sub>): δ 4.17 (br), 1.36 (br), 0.94 (br). <sup>13</sup>C NMR (100 MHz, THF-*d*<sub>8</sub>): δ 28.08, 22.20, 13.36. <sup>13</sup>C CP MAS NMR (18 kHz): δ 172.36, 126.48, 62.43, 30.76, 22.82, 13.94. FT-IR (KBr): 3422, 2959, 2933, 2871, 1733, 1619, 1462, 1233 cm<sup>-1</sup>.

*Poly(Methyl Ester Carbyne)*. Using General Procedure B and monomer **3** afforded 252.3 mg (78% yield) of a dark brown polymer. <sup>1</sup>H NMR (400 MHz, THF-*d*<sub>8</sub>): δ 3.80 (br), 3.66 (m), 1.82 (m), 1.33 (m), 0.93 (t). <sup>13</sup>C NMR (100 MHz, THF-*d*<sub>8</sub>): δ 31.54, 22.53, 13.4. <sup>13</sup>C CP MAS NMR (18 kHz): δ 173.22, 125.05, 62.22, 31.79, 22.84, 14.12. FT-IR (KBr): 3376, 2955, 1738, 1628, 1444, 1222 cm<sup>-1</sup>.

*Poly(Decyl Ester Carbyne)*. Using General Procedure B and monomer **4** afforded 355.4 mg (34% yield) of a dark brown polymer. <sup>1</sup>H NMR (400 MHz, THF-*d*<sub>8</sub>): δ 2.08 (m), 1.33 (br), 0.91 (br). <sup>13</sup>C NMR (100 MHz, THF-*d*<sub>8</sub>): δ 62.34, 33.90, 32.68, 30.39, 30.12, 26.75, 23.39 14.29, 1.17. <sup>13</sup>C CP MAS NMR (7 kHz): δ 173.32, 130.16, 126.48, 61.89, 29.76, 22.91, 14.13. FT-IR (KBr): 3394, 2955, 2931, 2870, 1714, 1615, 1455, 1374, 1242, 1182, 1036, 757 cm<sup>-1</sup>.

*Poly(Benzoyl Carbyne)*. Using General Procedure B and monomer **5** afforded 281.1 mg (48% yield) of a dark brown polymer. <sup>1</sup>H NMR (400 MHz, THF-*d*<sub>8</sub>): δ 7.16 (br), 2.52 (s), 1.33 (s), 0.93 (t), 0.14 (s). <sup>13</sup>C NMR (100 MHz, THF-*d*<sub>8</sub>): δ 128.81. <sup>13</sup>C CP MAS NMR (10 kHz): δ 170.5, 138.18, 67.48, 31.53, 22.50, 22.50, 22.77, 14.12. FT-IR (KBr): 3443, 3058, 3028, 2931, 2874, 1718, 1598, 1494, 1447, 1247, 1076, 1030, 759, 700 cm<sup>-1</sup>.

### 3.5 Additional Data

#### Additional Synthetic Data

**Table S1.** Variation of Monomer Concentration Used in the Polymerization of **2**<sup>a</sup>

Entry	[ <b>2</b> ] <sub>0</sub> (M)	Yield (%)	<i>M</i> <sub>n</sub> (Da)
1	0.1	0	--
2	0.5	15	566
3	1.0	21	555
4	2.0	18	561

<sup>a</sup> Conditions: [*Li*]<sub>0</sub>/[monomer]<sub>0</sub> = 3.2, THF, R.T., 24 h.

**Table S2.** Variation of the Temperature Used in the Polymerization of **2**<sup>a</sup>

Entry	Temperature (°C)	Yield (%)	<i>M</i> <sub>n</sub> (Da)
1	40	28	677
2	55	30	700
3	70	31	788

<sup>a</sup> Conditions: [**2**]<sub>0</sub> = 1.0 M, [*Li*]<sub>0</sub>/[**2**]<sub>0</sub> = 3.2, THF, 24 h.

**Table S3.** Variation of Number of Equivalents of Li Used in the Polymerization of **2**<sup>a</sup>

Entry	Equiv.	Yield (%)	$M_n$ (Da)
1	4.5	31	807
2	6	39	909
3	8	36	897

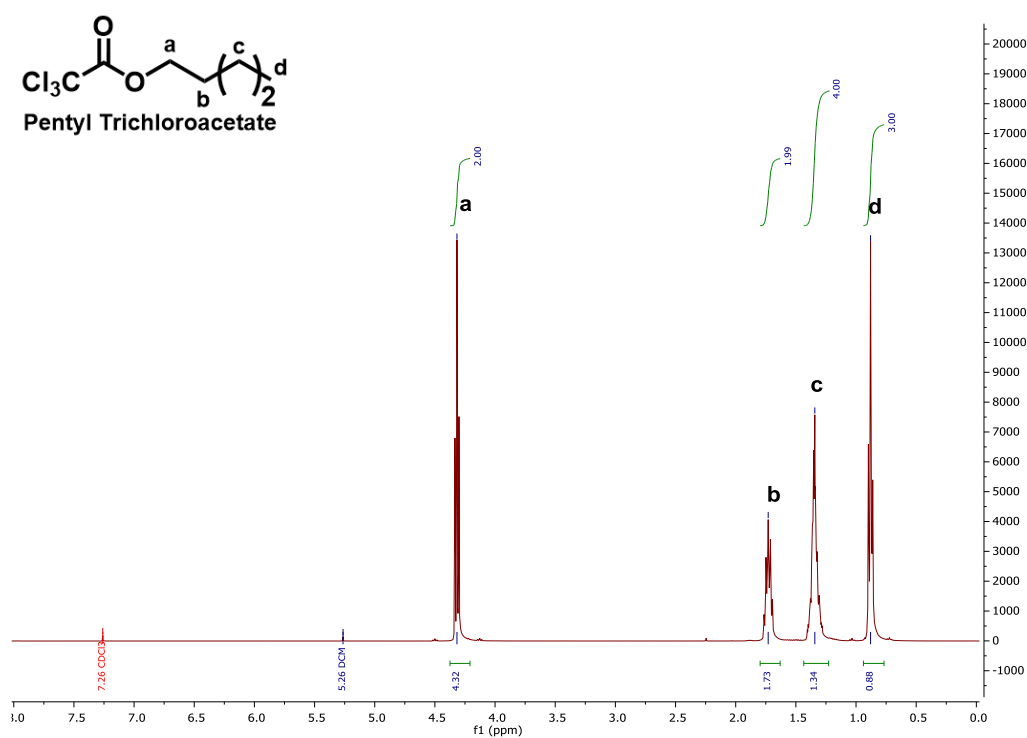
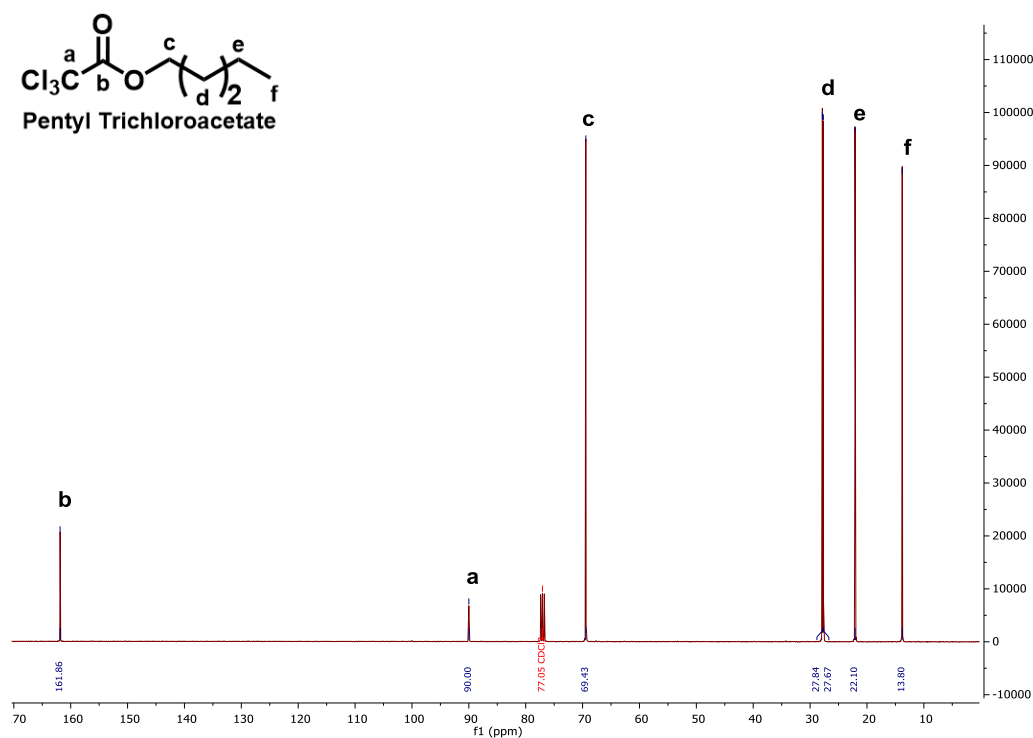
<sup>a</sup> Conditions:  $[2]_0 = 1\text{ M}$ ,  $[Li]_0/[2]_0 = 3.2$ , THF, 24 h.

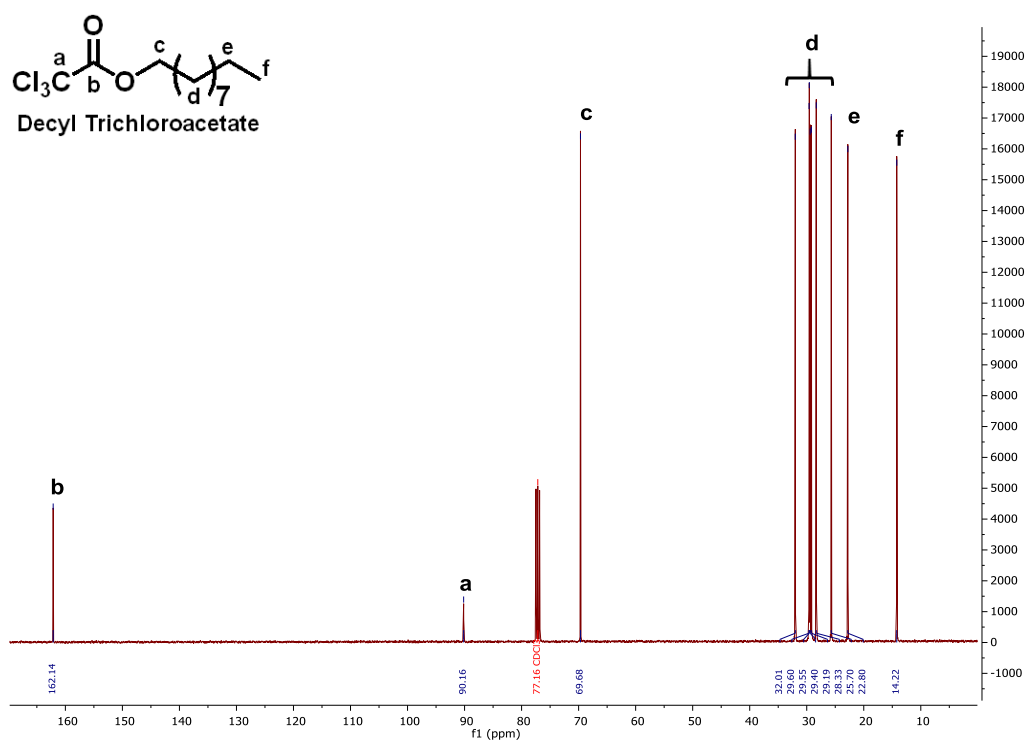
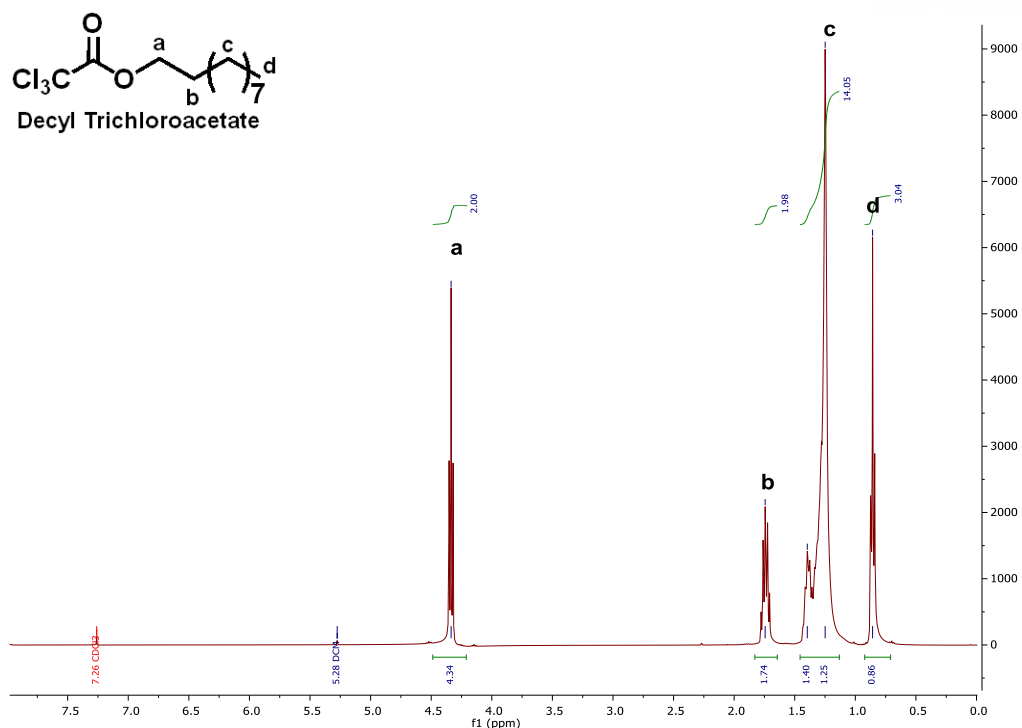
**Table S4.** Variation of the Naphthalene Concentration Used in the Polymerization of **2**<sup>a</sup>

Entry	[Naphthalene] <sub>0</sub> (M)	Yield (%)	$M_n$ (Da)
1	0.05	35	1020
2	0.15	51	1640
3	1.0	46	1330
4	6.0	44	1280

<sup>a</sup> Conditions:  $[2]_0 = 1.0\text{ M}$ ,  $[Li]_0/[2]_0 = 6.0$ , THF, 70 °C, 12 h.



**NMR Spectra** (Note: samples were prepared using General Procedure B)**Figure S1.** <sup>1</sup>H NMR spectrum of **2** (400 MHz, 298 K, CDCl<sub>3</sub>).**Figure S2.** <sup>13</sup>C NMR spectrum of **2** (100 MHz, 298 K, CDCl<sub>3</sub>).



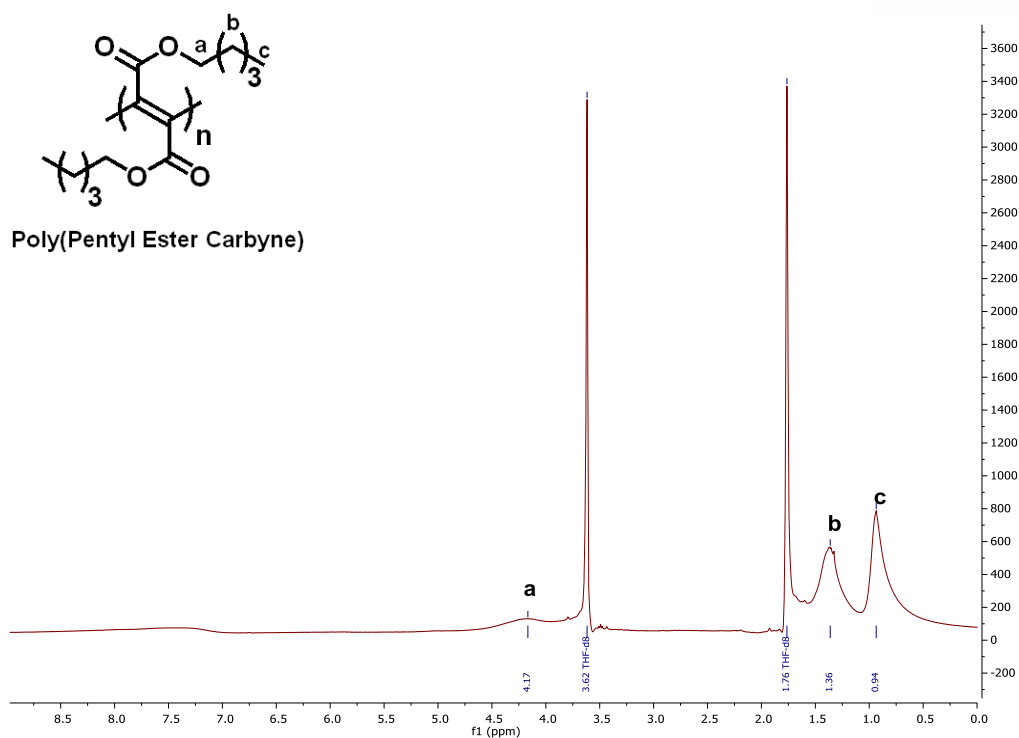


**Figure S5.**  $^1\text{H}$  NMR spectrum of the polymer obtained from **2** (400 MHz, 298 K,  $\text{THF-}d_8$ ).

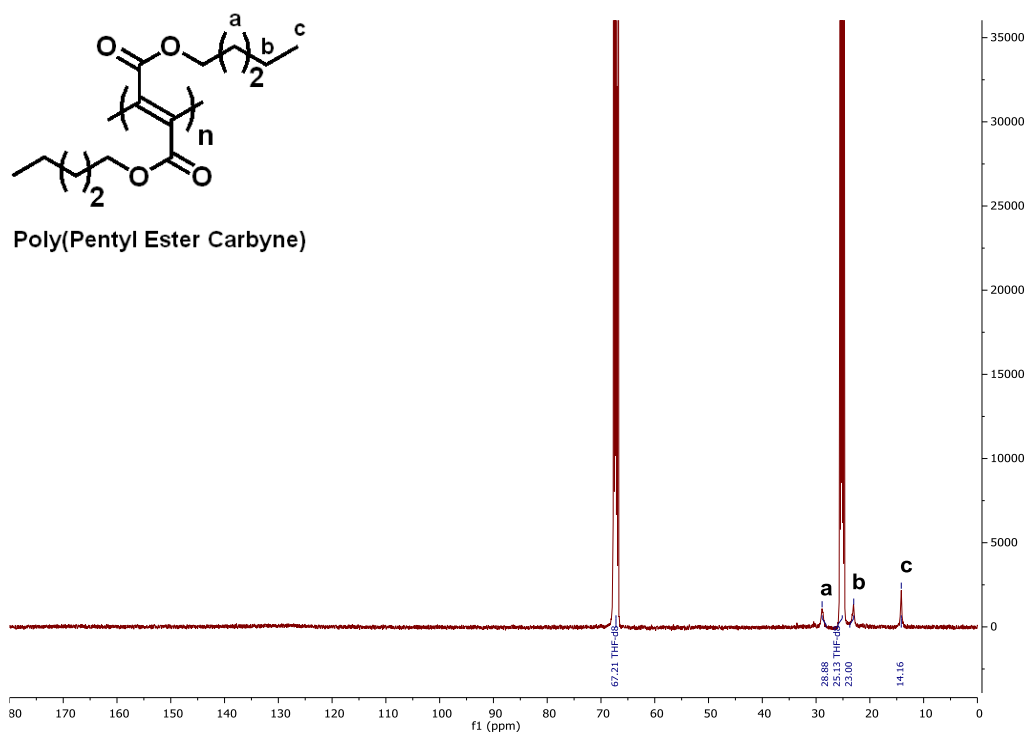


**Figure S6.**  $^{13}\text{C}$  NMR spectrum of the polymer obtained from **2** (100 MHz, 298 K,  $\text{THF-}d_8$ ).

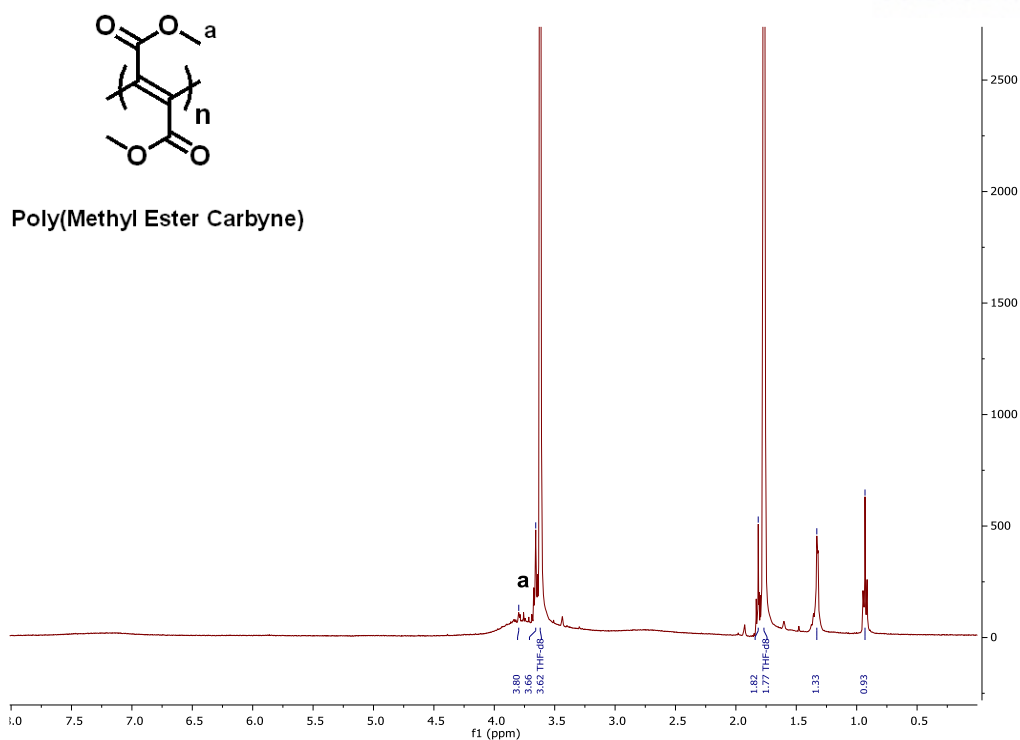


**Figure S7.**  $^1\text{H}$  NMR spectrum of the polymer obtained from **1** (400 MHz, 298 K, THF- $d_8$ ).

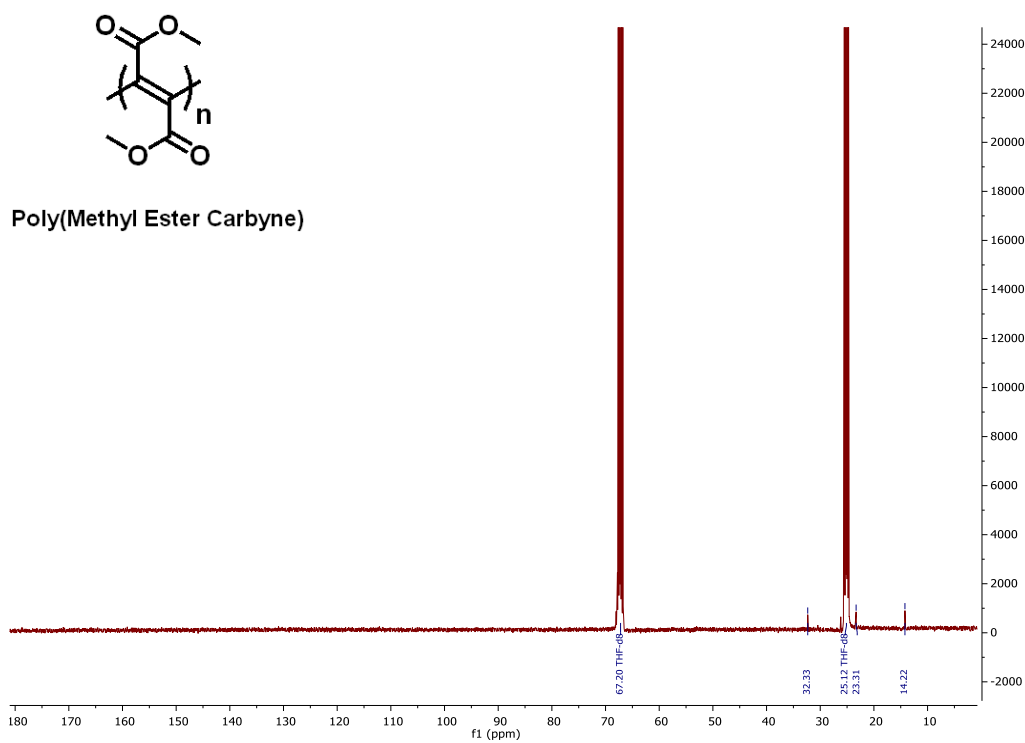


**Figure S8.**  $^{13}\text{C}$  NMR spectrum of the polymer obtained from **1** (100 MHz, 298 K, THF- $d_8$ ).

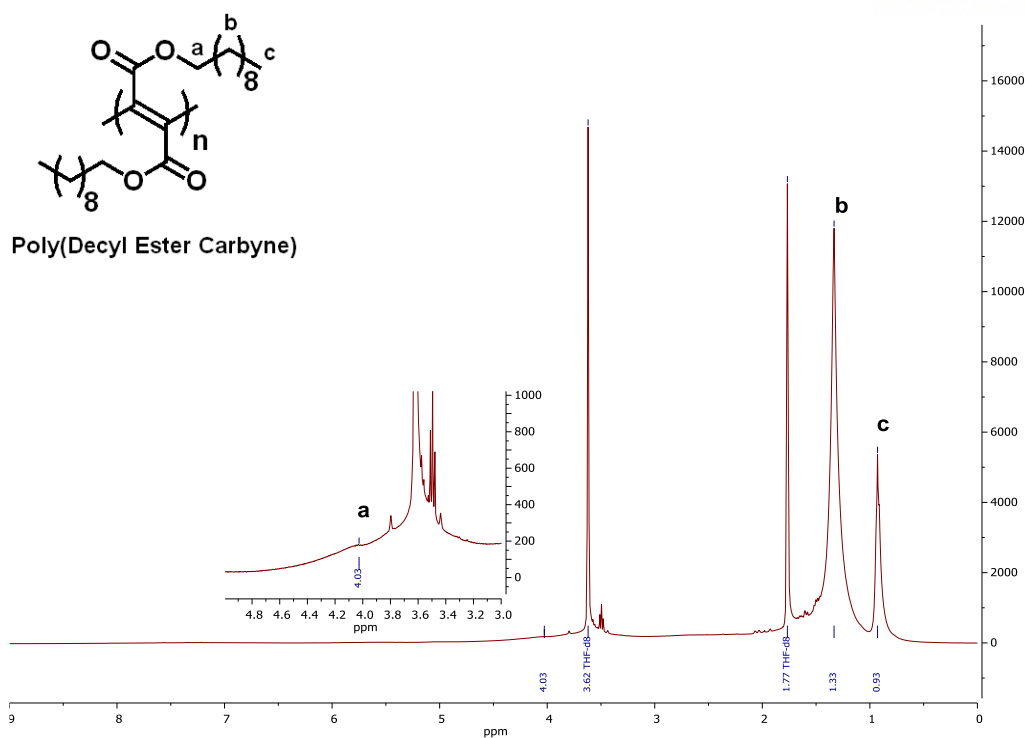


**Figure S9.**  $^1\text{H}$  NMR spectrum of the polymer obtained from **3** (400 MHz, 298 K, THF- $d_8$ ).

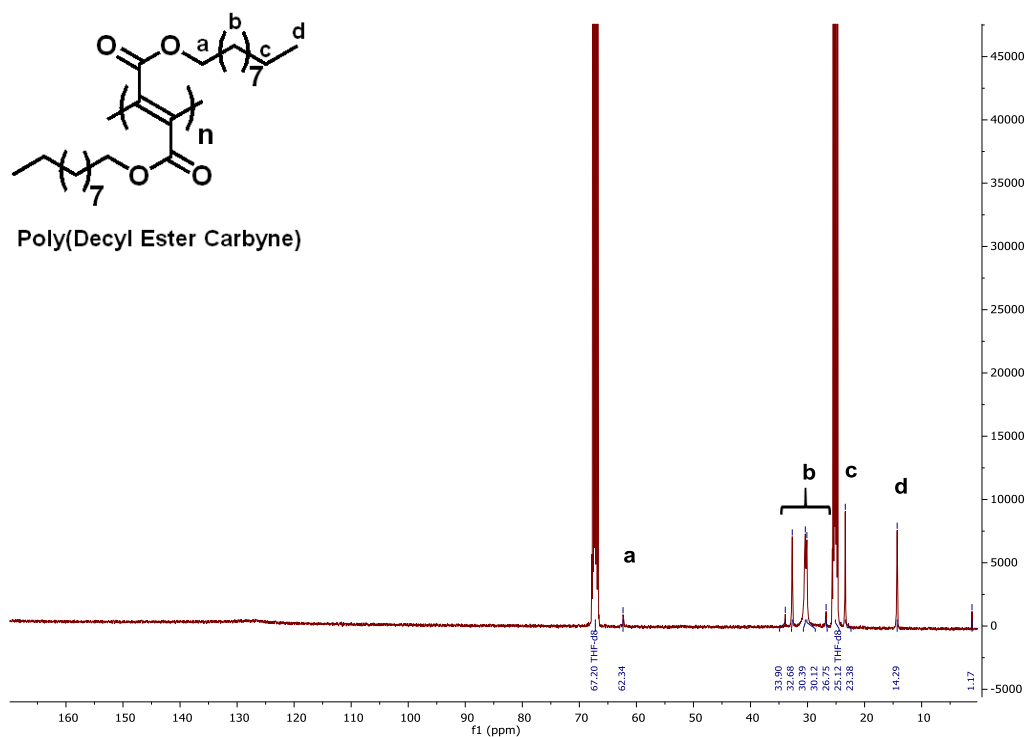


**Figure S10.**  $^{13}\text{C}$  NMR spectrum of the polymer obtained from **3** (100 MHz, 298 K, THF- $d_8$ ).

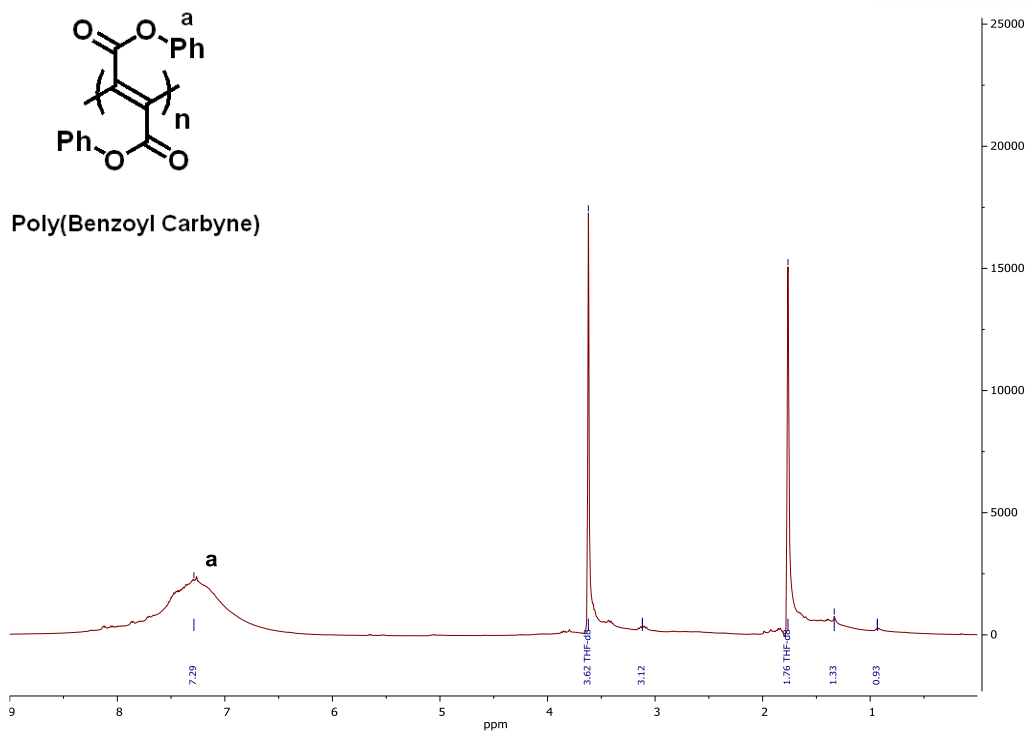


**Figure S11.**  $^1\text{H}$  NMR spectrum of the polymer obtained from **4** (400 MHz, 298 K,  $\text{THF-}d_8$ ).

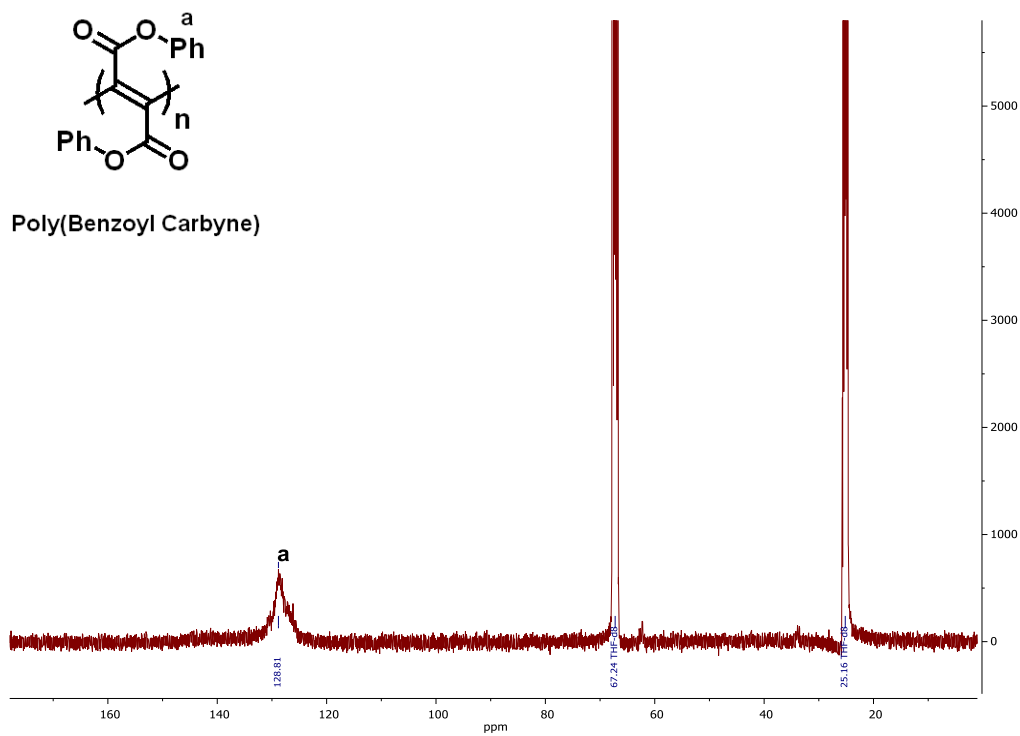


**Figure S12.**  $^{13}\text{C}$  NMR spectrum of the polymer obtained from **4** (100 MHz, 298 K,  $\text{THF-}d_8$ ).

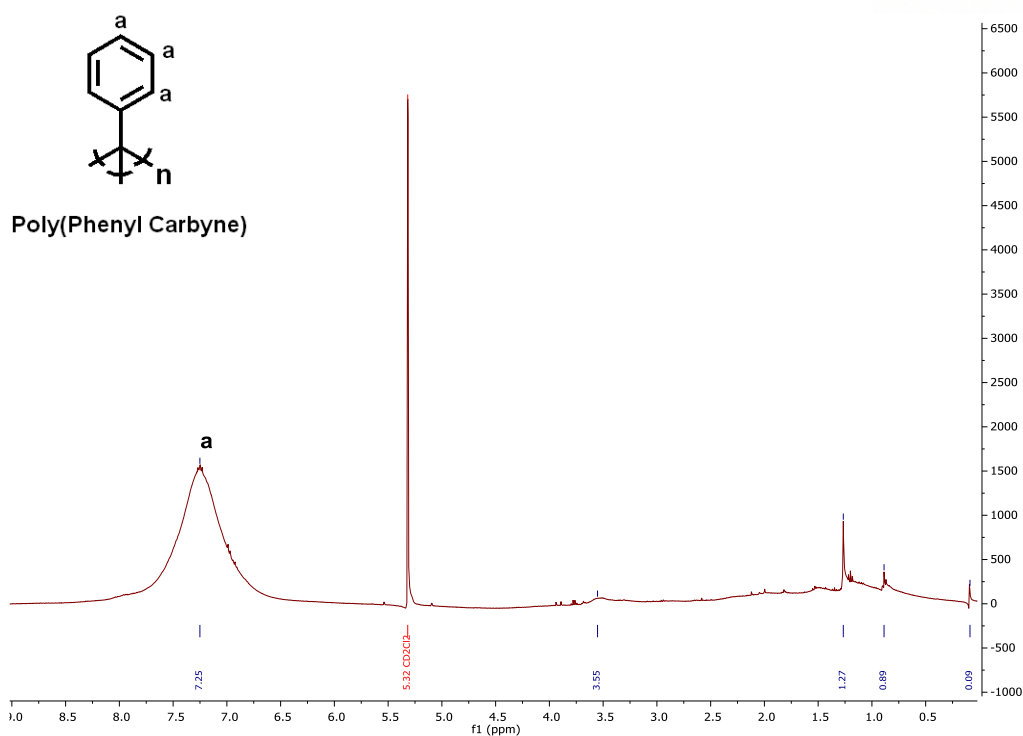


**Figure S13.**  $^1\text{H}$  NMR spectrum of the polymer obtained from **5** (400 MHz, 298 K,  $\text{CD}_2\text{Cl}_2$ ).

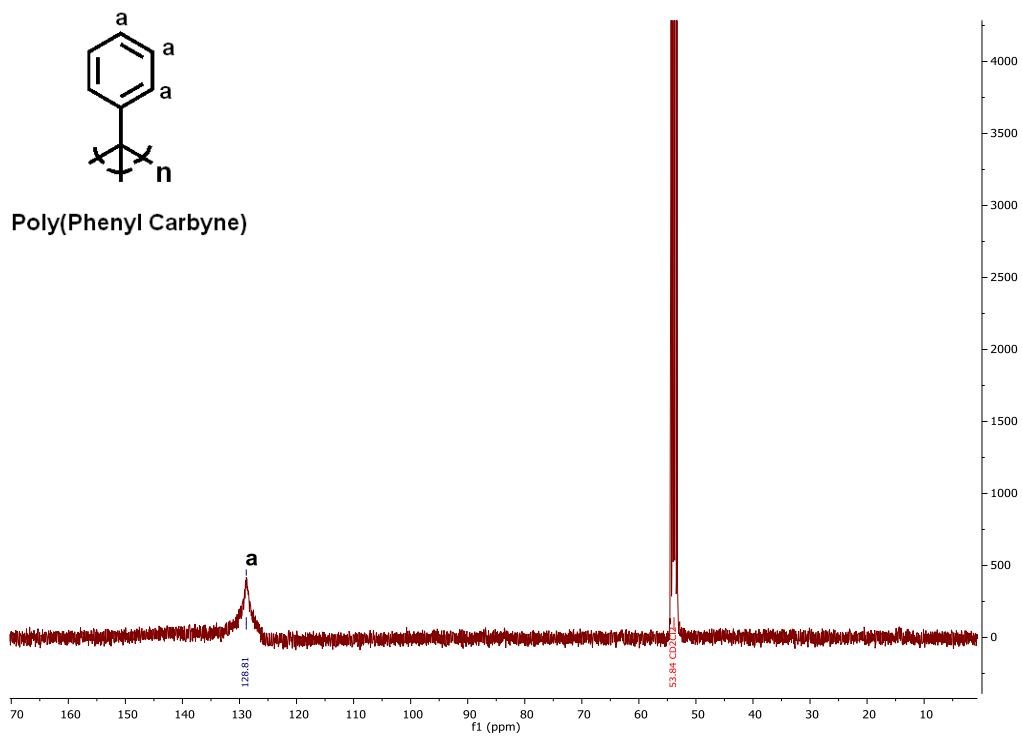


**Figure S14.**  $^{13}\text{C}$  NMR spectrum of the polymer obtained from **5** (100 MHz, 298 K,  $\text{CD}_2\text{Cl}_2$ ).

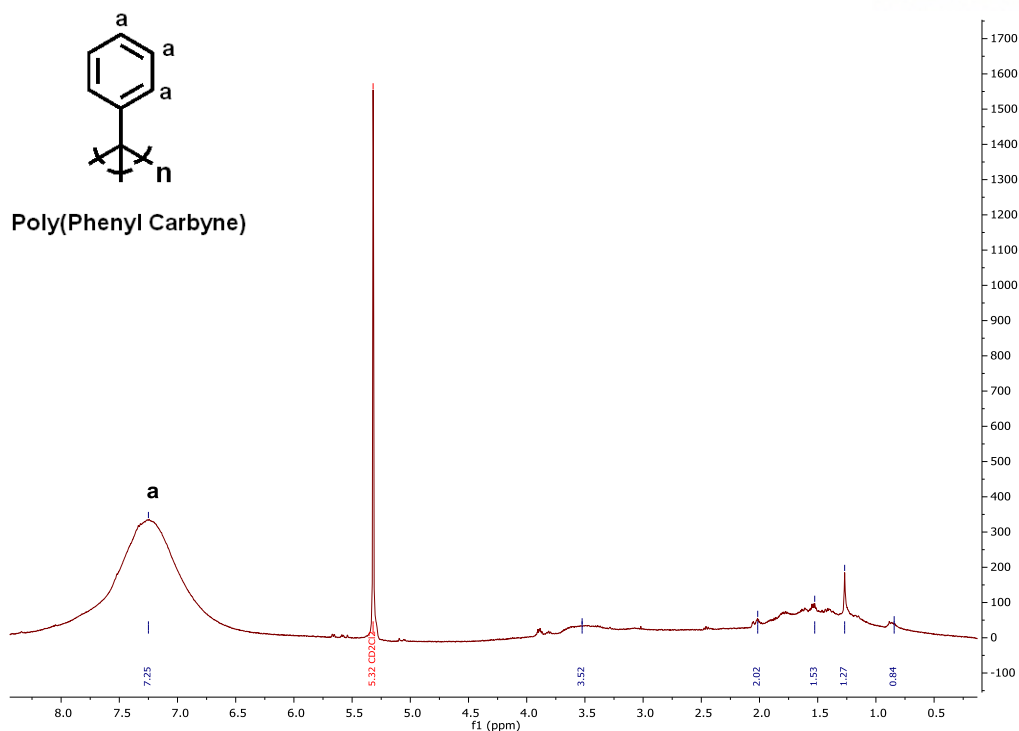


**Figure S15.**  $^1\text{H}$  NMR spectrum of the polymer obtained from **6** (400 MHz, 298 K,  $\text{CD}_2\text{Cl}_2$ ).

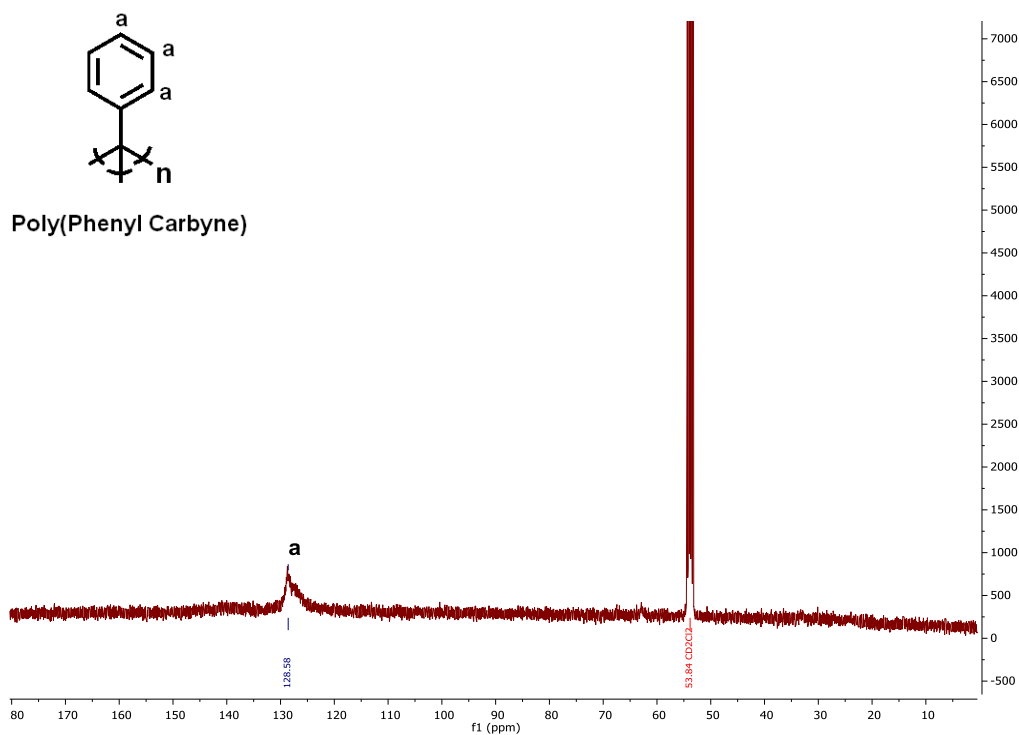


**Figure S16.**  $^{13}\text{C}$  NMR spectrum of the polymer obtained from **6** (100 MHz, 298 K,  $\text{CD}_2\text{Cl}_2$ ).



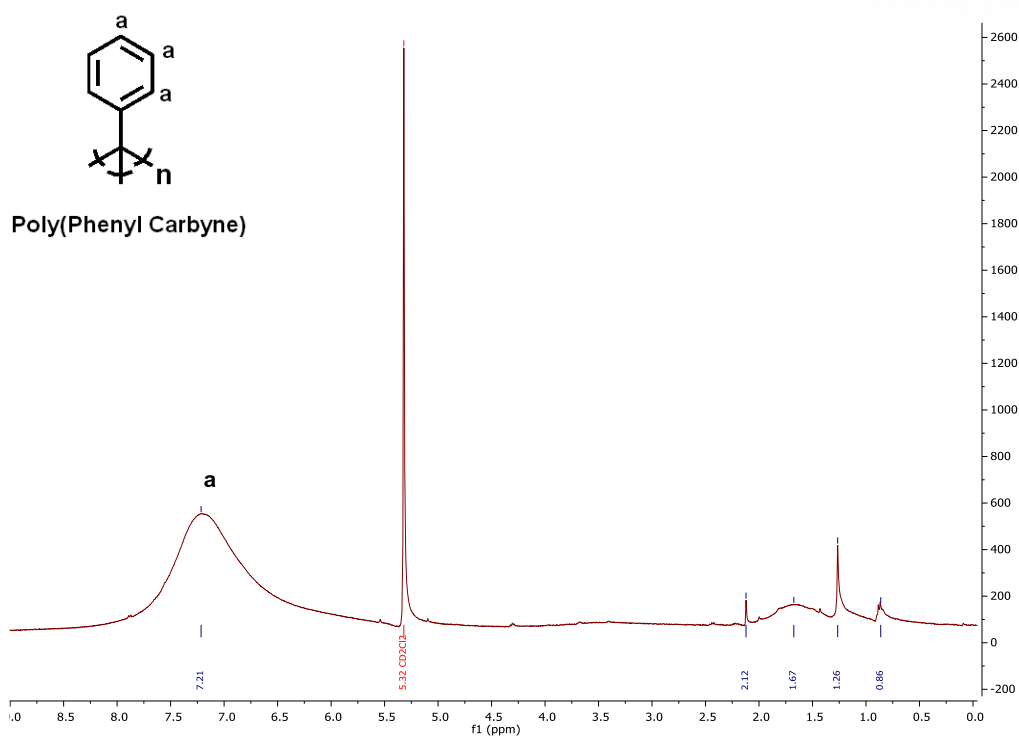


**Figure S17.**  $^1\text{H}$  NMR spectrum of the polymer obtained from **1** (400 MHz, 298 K,  $\text{CD}_2\text{Cl}_2$ ).

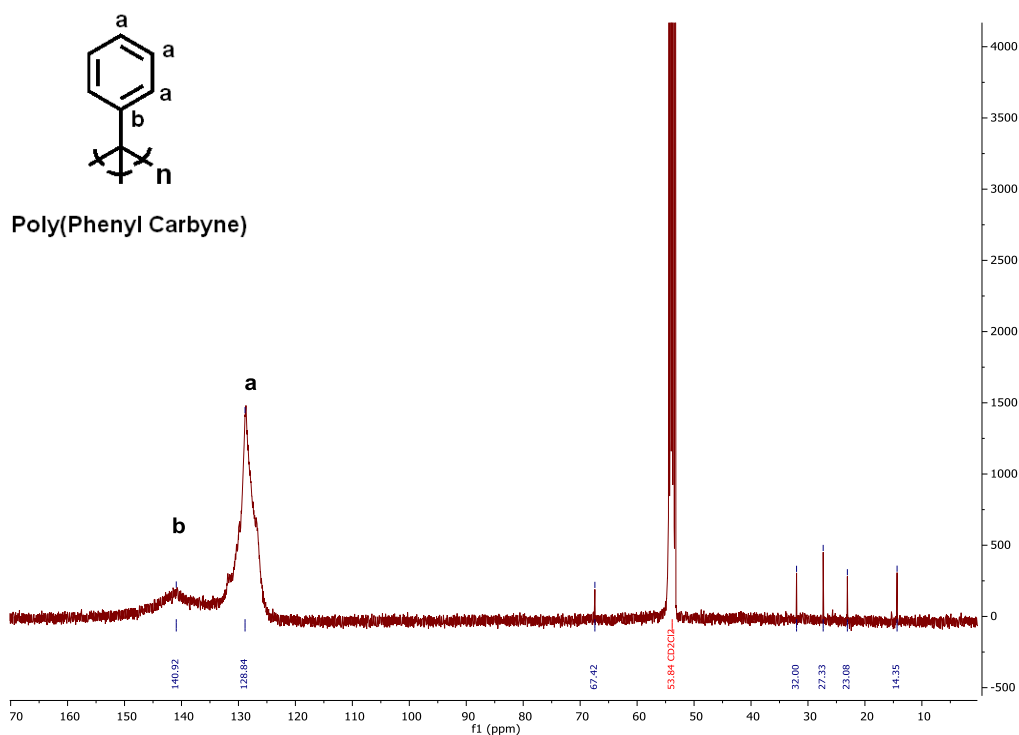


**Figure S18.**  $^{13}\text{C}$  NMR spectrum of the polymer obtained from **1** (100 MHz, 298 K,  $\text{CD}_2\text{Cl}_2$ ).

**CPMAS NMR Spectra** (Note: samples were prepared using General Procedure B)

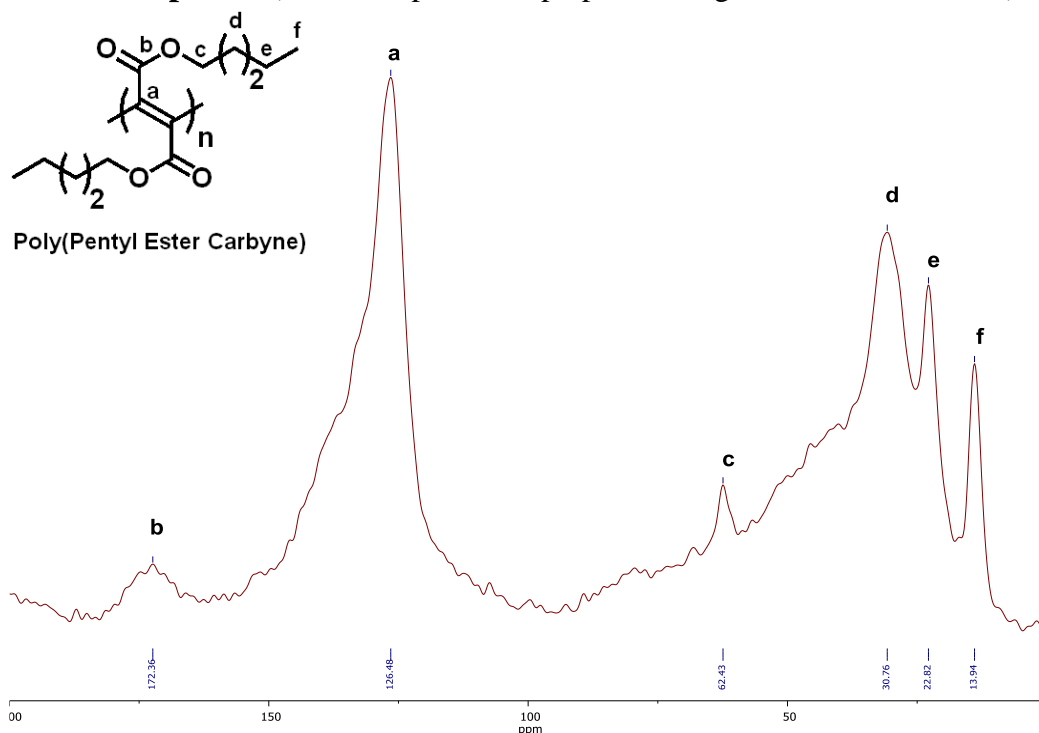


**Figure S19.**  $^{13}\text{C}$  CPMAS NMR spectrum of the polymer obtained from **2** (18 kHz MAS).

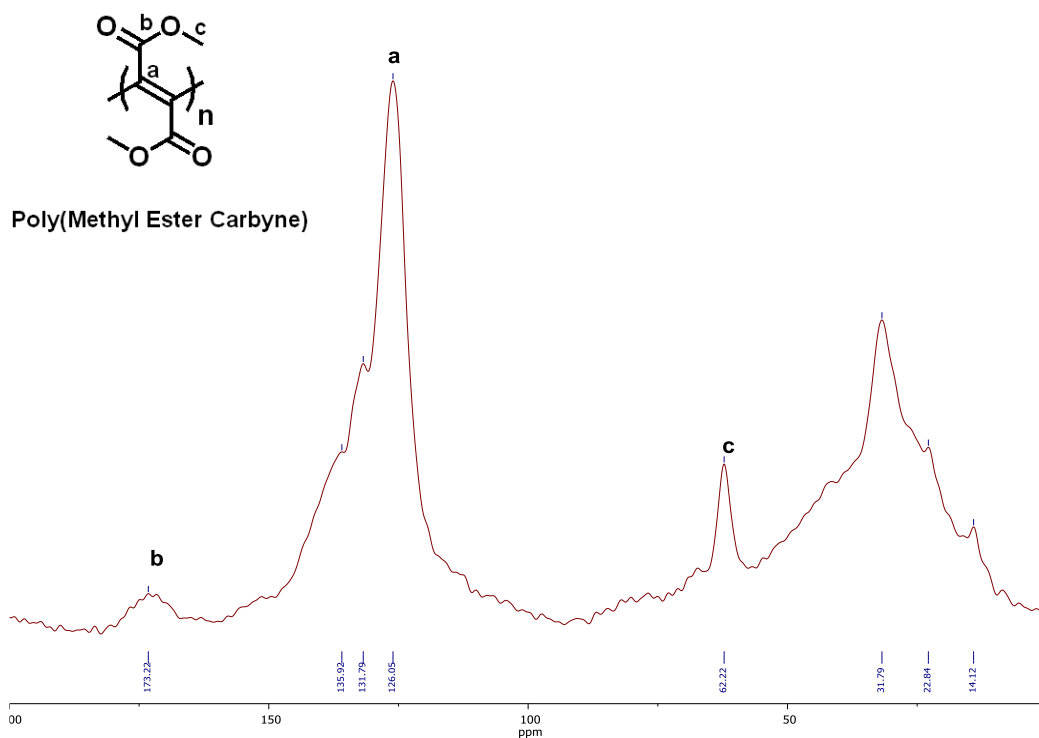


**Figure S20.**  $^{13}\text{C}$  CPMAS NMR spectrum of the polymer obtained from **1** (18 kHz MAS).

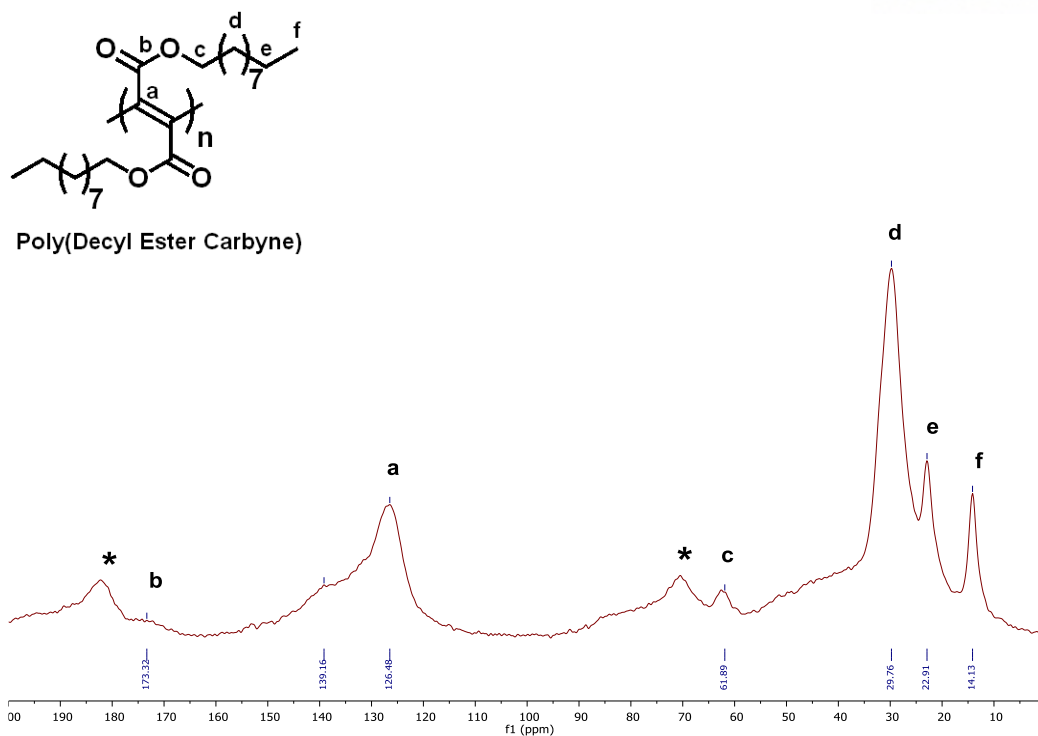


**Figure S21.**  $^{13}\text{C}$  CPMAS NMR spectrum of the polymer obtained from **3** (7 kHz MAS), \* denotes spinning sidebands.

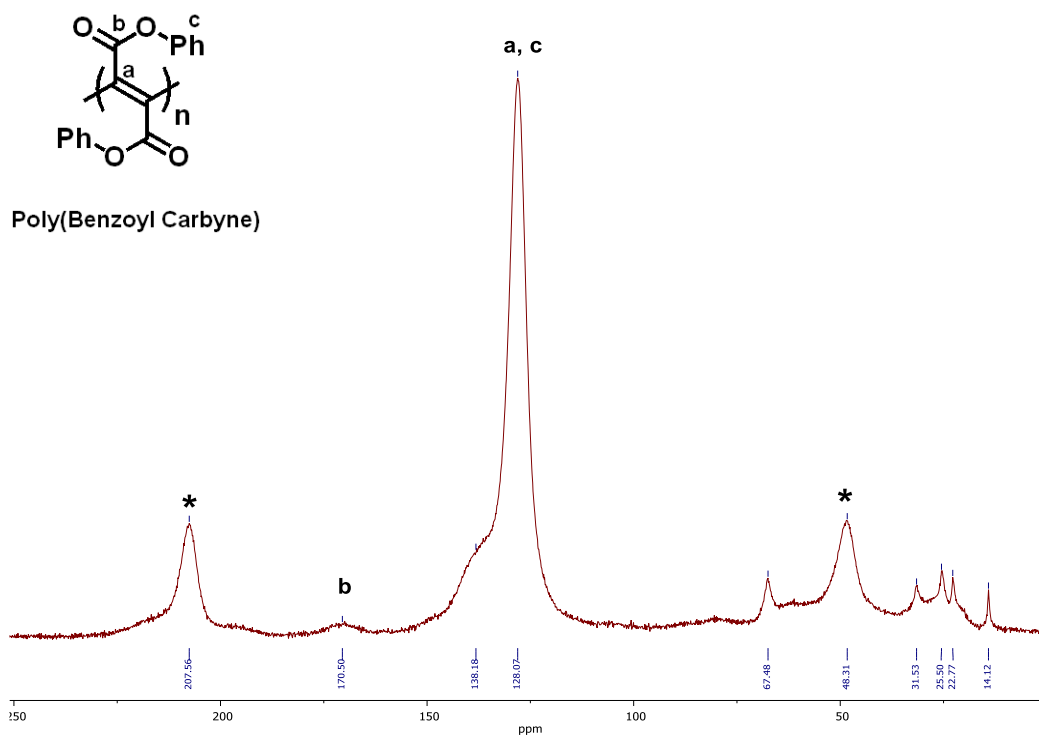


**Figure S22.**  $^{13}\text{C}$  CPMAS NMR spectrum of the polymer obtained from **4** (10 kHz MAS), \* denotes spinning sidebands.

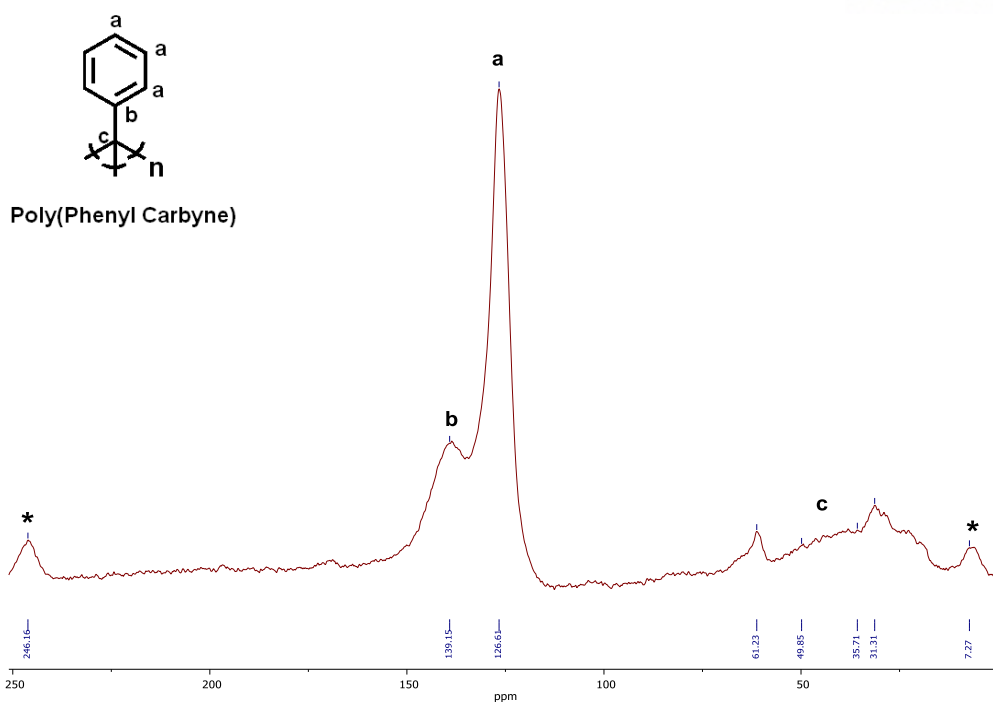


**Figure S23.**  $^{13}\text{C}$  CPMAS NMR spectrum of the polymer obtained from **5** (15 kHz MAS), \* denotes spinning sidebands.

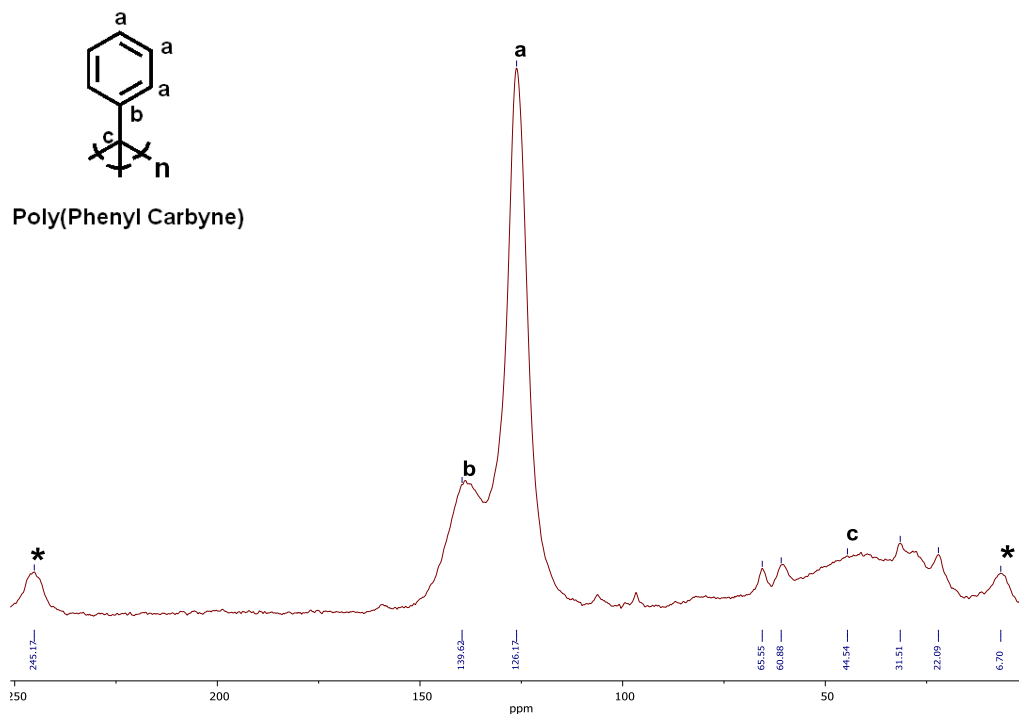


**Figure S24.**  $^{13}\text{C}$  CPMAS NMR spectrum of the polymer obtained from **6** (15 kHz MAS), \* denotes spinning sidebands.

**Infrared Spectra** (Note: polymer samples were prepared using General Procedure B)

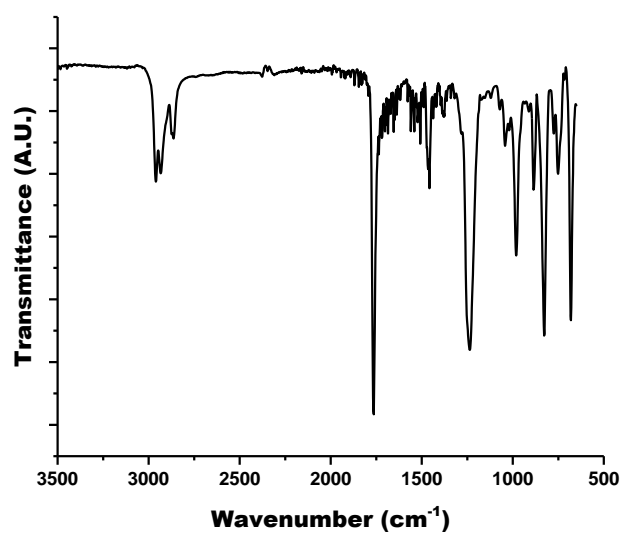


**Figure S25.** ATR FT-IR spectrum recorded for **2**.

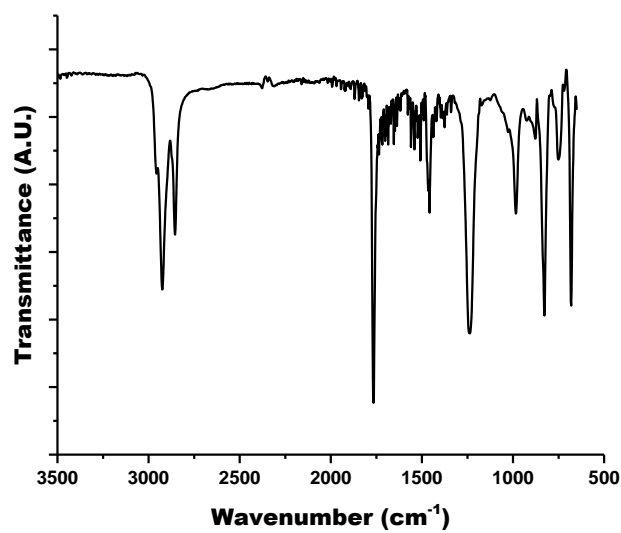


**Figure S26.** ATR FT-IR spectrum recorded for **3**.

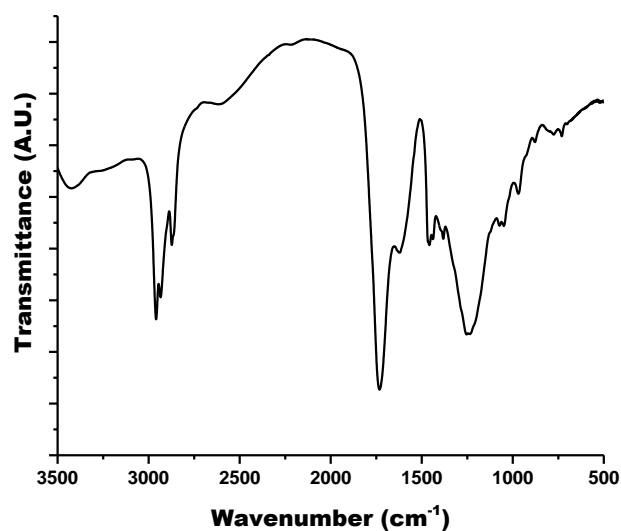


**Figure S27.** FT-IR spectrum (KBr) recorded for the polymer obtained from **2**.

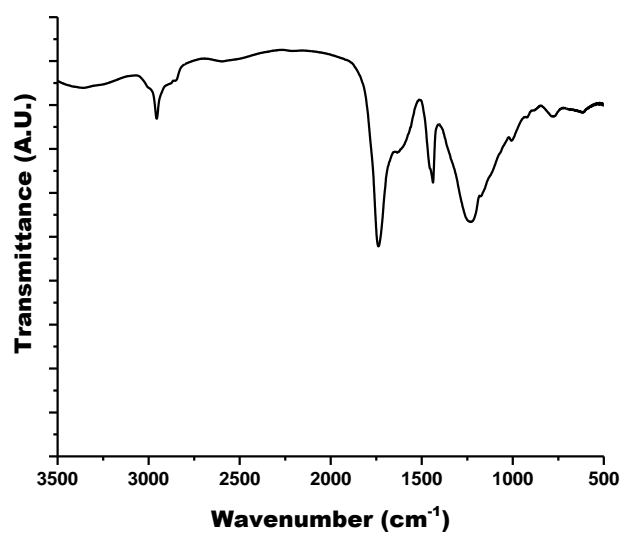


**Figure S28.** FT-IR spectrum (KBr) recorded for the polymer obtained from **1**.

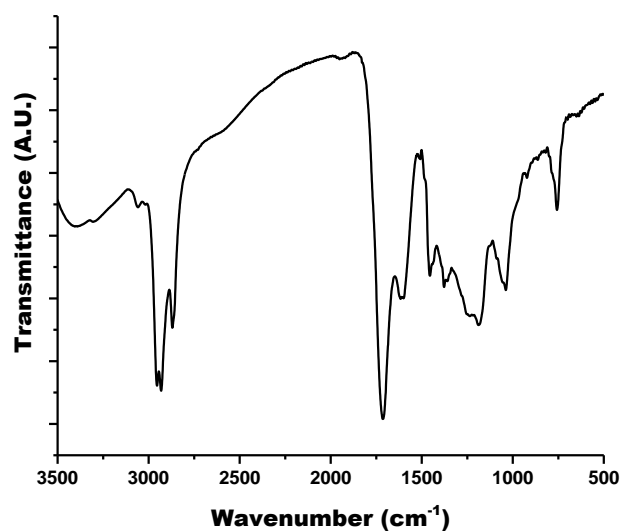


**Figure S29.** FT-IR spectrum (KBr) recorded for the polymer obtained from **3**.

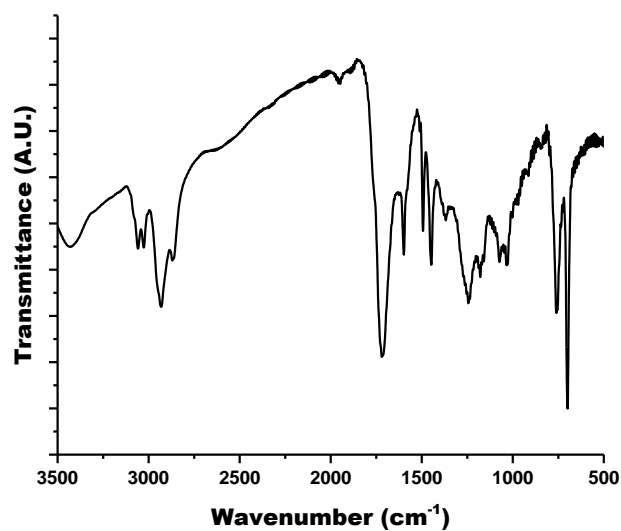


**Figure S30.** FT-IR spectrum (KBr) recorded for the polymer obtained from **4**.

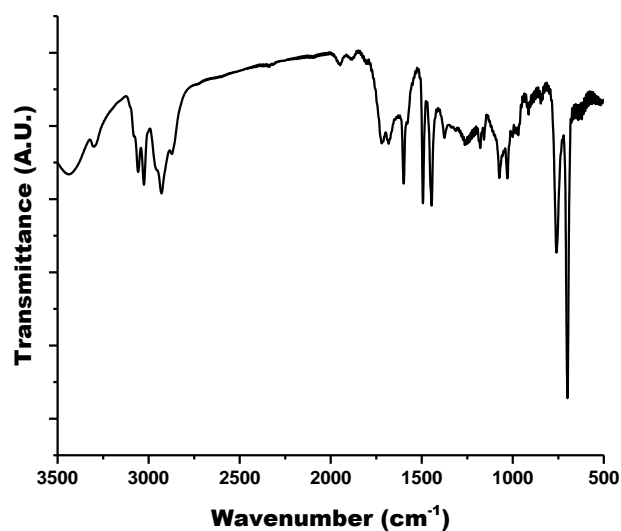


**Figure S31.** FT-IR spectrum (KBr) recorded for the polymer obtained from **5**.

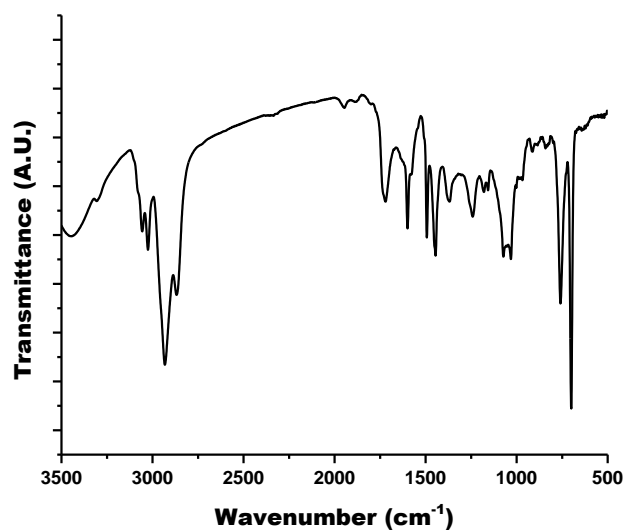


**Figure S32.** FT-IR spectrum (KBr) recorded for the polymer obtained from **6**.



**Size Exclusion Chromatograms** (Note: samples were prepared using General Procedure B unless stated otherwise)

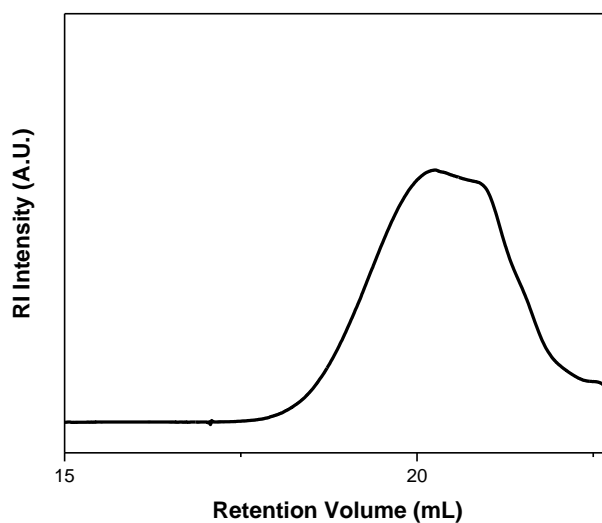


**Figure S33.** SEC data recorded for the polymer obtained from **2**.

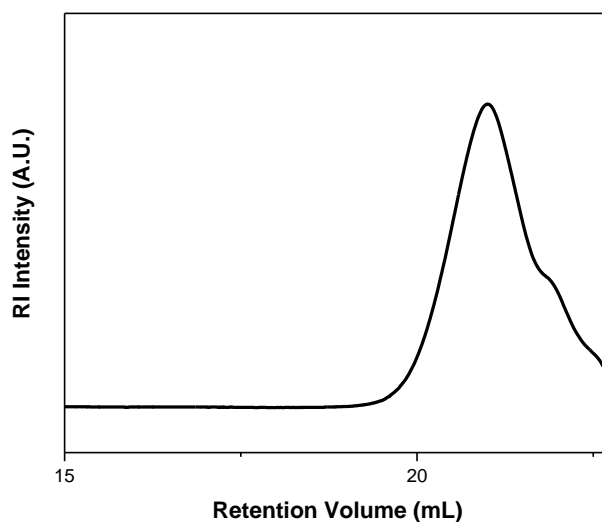


**Figure S34.** SEC data recorded for the polymer obtained from **1**.

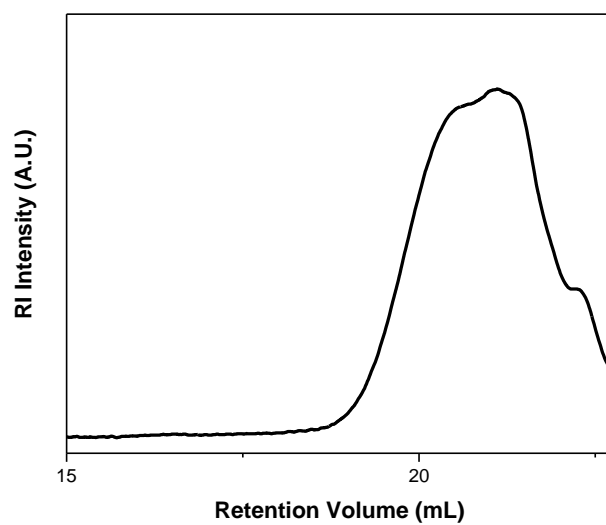


**Figure S35.** SEC data recorded for the polymer obtained from **3**.

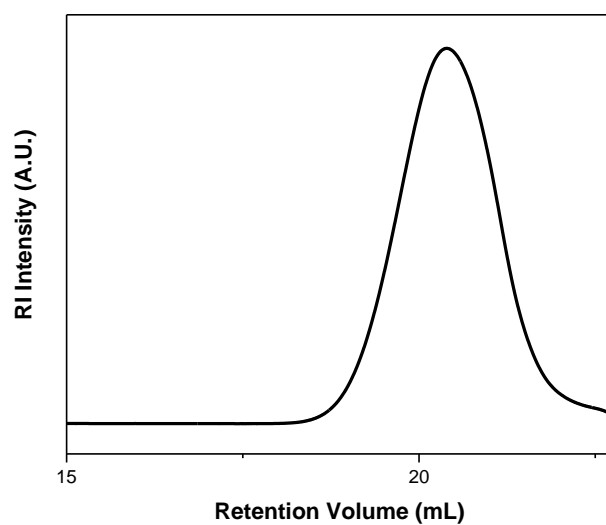


**Figure S36.** SEC data recorded for the polymer obtained from **4**.

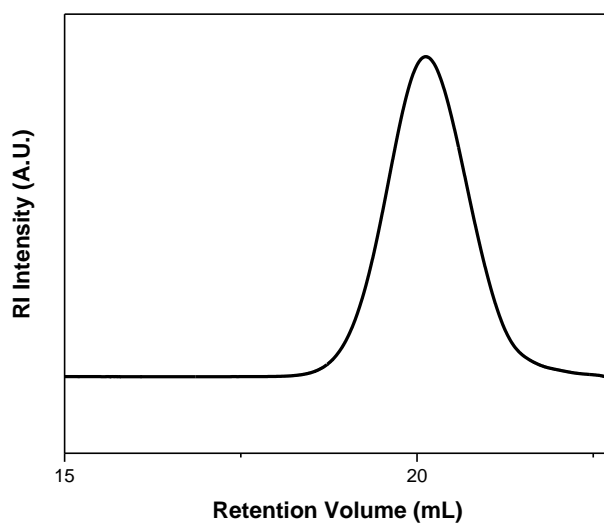


**Figure S37.** SEC data recorded for the polymer obtained from **5**.

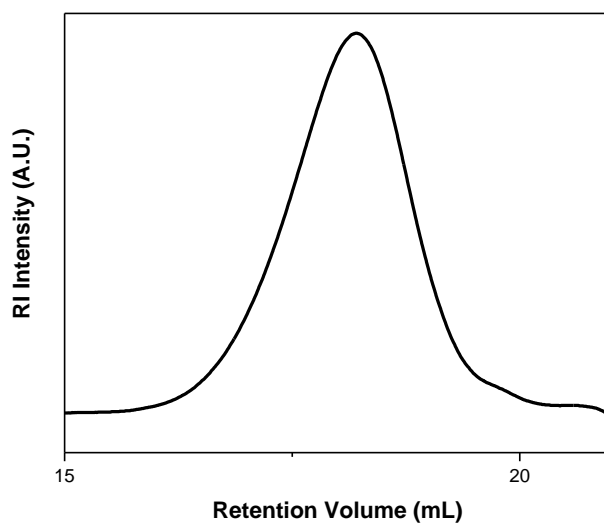


**Figure S38.** SEC data recorded for the polymer obtained from **6**.

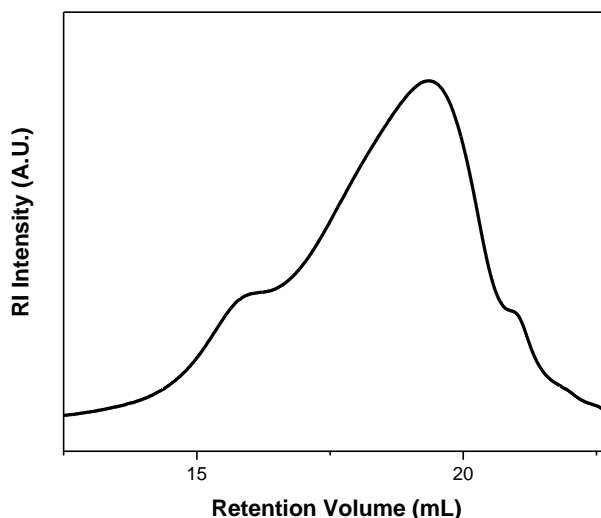


**Figure S39.** SEC data recorded for the polymer obtained from trichlorotoluene w/ naphthalene.

### 3.6 References

1. Visscher, G. T.; Bianconi, P. A., Synthesis and characterization of polycarbynes, a new class of carbon-based network polymers. *J. Am. Chem. Soc.* **1994**, *116* (5), 1805-1811.
2. Nur, Y.; Duygulu, Ş.; Pitcher, M. W.; Toppare, L., The electrochemical synthesis of poly(methylcarbyne) for diamond film coatings. *J. Appl. Polym. Sci.* **2012**, *124* (5), 3626-3632.
3. Bianconi, P. A.; Joray, S. J.; Aldrich, B. L.; Sumranjit, J.; Duffy, D. J.; Long, D. P.; Lazorcik, J. L.; Raboin, L.; Kearns, J. K.; Smulligan, S. L.; Babyak, J. M., Diamond and Diamond-Like Carbon from a Preceramic Polymer. *J. Am. Chem. Soc.* **2004**, *126* (10), 3191-3202.
4. Visscher, G. T.; Nesting, D. C.; Badding, J. V.; Bianconi, P. A., Poly(phenylcarbyne): A Polymer Precursor to Diamond-Like Carbon. *Science* **1993**, *260* (5113), 1496-1499.
5. Nur, Y.; Pitcher, M. W.; Seyyidoğlu, S.; Toppare, L., Facile Synthesis of Poly(hydridocarbyne): A Precursor to Diamond and Diamond-like Ceramics. *J. Macromol. Sci. A* **2008**, *45* (5), 358-363.
6. Bulychiev, B.; Zvukova, T.; Sizov, A. I.; Aleksandrov, A.; Korobov, Y.; Kanzyuba, M.; Khomich, A. V., Poly(naphthalenehydrocarbyne): Synthesis, characterization, and application to preparation of thin diamond films. *Russ. Chem. Bull.* **2010**, *59*, 1724-1728.
7. Sedov, V. S.; Ralchenko, V. G.; Zvukova, T. M.; Sizov, A. I., Polycarbynes: A new synthetic approach and application to the nucleation of CVD diamond. *Diamond Relat. Mater.* **2017**, *74*, 65-69.

8. Zvukova, T. M.; Sizov, A. I.; Bulychev, B. M., Improved synthesis of polycarbynes. *Mendeleev Commun.* **2016**, 26 (2), 127-128.
9. Brown, W. H., *Organic chemistry / William H. Brown, Beloit College, Brent L. Iverson, University of Texas, Austin, Eric V. Anslyn, University of Texas, Austin, Christopher S. Foote, University of California, Los Angeles*. Eighth edition. ed.; Cengage Learning: Australia ;, 2018.
10. Jones, R. G.; Holder, S. J., High-yield controlled syntheses of polysilanes by the Wurtz-type reductive coupling reaction. *Polym. Int.* **2005**, 55 (7), 711-718.
11. Odian, G. G., *Principles of polymerization : George Odian*. 4th ed. ed.; Wiley-Interscience: Hoboken, N.J, 2004.
12. Stevens, M. P., *Polymer chemistry : an introduction / Malcolm P. Stevens*. 3rd ed. ed.; Oxford University Press: New York, 1999.
13. Ihara, E.; Fujioka, M.; Haida, N.; Itoh, T.; Inoue, K., First Synthesis of Poly(acylmethylene)s via Palladium-Mediated Polymerization of Diazoketones. *Macromolecules* **2005**, 38 (6), 2101-2108.
14. Shimomoto, H.; Asano, H.; Itoh, T.; Ihara, E., Pd-initiated controlled polymerization of diazoacetates with a bulky substituent: synthesis of well-defined homopolymers and block copolymers with narrow molecular weight distribution from cyclophosphazene-containing diazoacetates. *Polym. Chem.* **2015**, 6 (26), 4709-4714.
15. Shimomoto, H.; Kikuchi, M.; Aoyama, J.; Sakayoshi, D.; Itoh, T.; Ihara, E., Cyclopolymerization of Bis(diazocarbonyl) Compounds Leading to Well-Defined Polymers Essentially Consisting of Cyclic Constitutional Units. *Macromolecules* **2016**, 49 (22), 8459-8465.
16. Shimomoto, H.; Kudo, T.; Tsunematsu, S.; Itoh, T.; Ihara, E., Fluorinated Poly(substituted methylene)s Prepared by Pd-Initiated Polymerization of Fluorine-Containing Alkyl and Phenyl Diazoacetates: Their Unique Solubility and Postpolymerization Modification. *Macromolecules* **2018**, 51 (2), 328-335.
17. Ihara, E.; Okada, R.; Sogai, T.; Asano, T.; Kida, M.; Inoue, K.; Itoh, T.; Shimomoto, H.; Ishibashi, Y.; Asahi, T., Pd-mediated polymerization of diazoacetates with aromatic ester group: Synthesis and photophysical property of poly(1-pyrenylmethoxycarbonylmethylene). *J. Polym. Sci., Part A: Polym. Chem.* **2013**, 51 (5), 1020-1023.
18. Shimomoto, H.; Shimizu, K.; Takeda, C.; Kikuchi, M.; Kudo, T.; Mukai, H.; Itoh, T.; Ihara, E.; Hoshikawa, N.; Koiwai, A.; Hasegawa, N., Synthesis of polymers with densely-grafted oligo(ethylene glycol)s by Pd-initiated polymerization of oxyethylene-containing diazoacetates. *Polym. Chem.* **2015**, 6 (47), 8124-8131.
19. Kryazhev, Y. G.; Petrinska, V. B.; Brodskaya, E. I., Synthesis of polyphenylmethine by dechlorination of benzene trichloride. *Pol. Sci. U.S.S.R.* **1969**, 11 (12), 2964-2970.

20. Holy, N. L., Reactions of the radical anions and dianions of aromatic hydrocarbons. *Chem. Rev.* **1974**, *74* (2), 243-277.
  
21. Bulychev, B. M.; Zvukova, T. M.; Sizov, A. I.; Aleksandrov, A. F.; Korobov, Y. A.; Kanzyuba, M. V.; Khomich, A. V., Poly(naphthalenehydrocarbyne): synthesis, characterization, and application to preparation of thin diamond films. *Russ. Chem. Bull.* **2010**, *59* (9), 1724-1728.
  
22. Quaternary is used here to refer to a carbon with no attached protons
  
23. Pell, A. J.; Pintacuda, G.; Grey, C. P., Paramagnetic NMR in solution and the solid state. *Prog. Nucl. Magn. Reson. Spectrosc.* **2019**, *111*, 1-271.
  
24. Klimov, V. I.; Raida, V. S.; Kryazhev, Y. G., Synthesis of polyenes from trichloromethyl derivatives. *Pol. Sci. U.S.S.R.* **1979**, *21* (1), 184-190.
  
25. Metz, G.; Wu, X. L.; Smith, S. O., Ramped-Amplitude Cross Polarization in Magic-Angle-Spinning NMR. *Journal of Magnetic Resonance, Series A* **1994**, *110* (2), 219-227.
  
26. Fung, B. M.; Khitrin, A. K.; Ermolaev, K., An Improved Broadband Decoupling Sequence for Liquid Crystals and Solids. *Journal of Magnetic Resonance* **2000**, *142* (1), 97-101.

# Chapter 4: Polymerization Mechanisms for Poly(carbyne)s

## 4.1 Introduction

As was shown previously, the polymeric structures of poly(carbyne)s differ based on the monomer used, with polymers containing carbonyl and phenyl side chains having a linear or branched backbone, respectively. This inherent difference could be caused by thermodynamic or kinetic differences and is possibly reflected in the polymerization mechanism. While polymers have been synthesized through the utilization of many different types of repeating chemical reactions (e.g. ATRP, ROMP, anionic, condensation, or even polyhomologation), the method in which a polymer grows, or polymerization mechanism, is always either chain-growth or step-growth. This can normally be determined by careful consideration of the polymerization's reactants and products, however, this is not always the case. Before discussing the experimental determination of the polymerization mechanism for poly(carbyne)s, its causes, and implications a brief introduction to step- and chain-growth will be given. This introduction will focus on the mechanism and kinetics of the two different pathways and their subclasses, with examples given for clarity.

Step-growth polymerizations can be thought of as a large number of independent reactions between multi-functional molecules, with each individual reaction leading to the linking of two molecules. Polymer growth, i.e. the increase of the average molecular weight of the solution, occurs through the repetition of this linking reaction, with monomers first reacting to form dimers, followed by dimers reacting with both monomers and dimers to form trimers and tetramers, respectively (Figure 1, a). This process continues, with random linking between molecules of different sizes, until oligomers and finally high molecular weight polymers form.

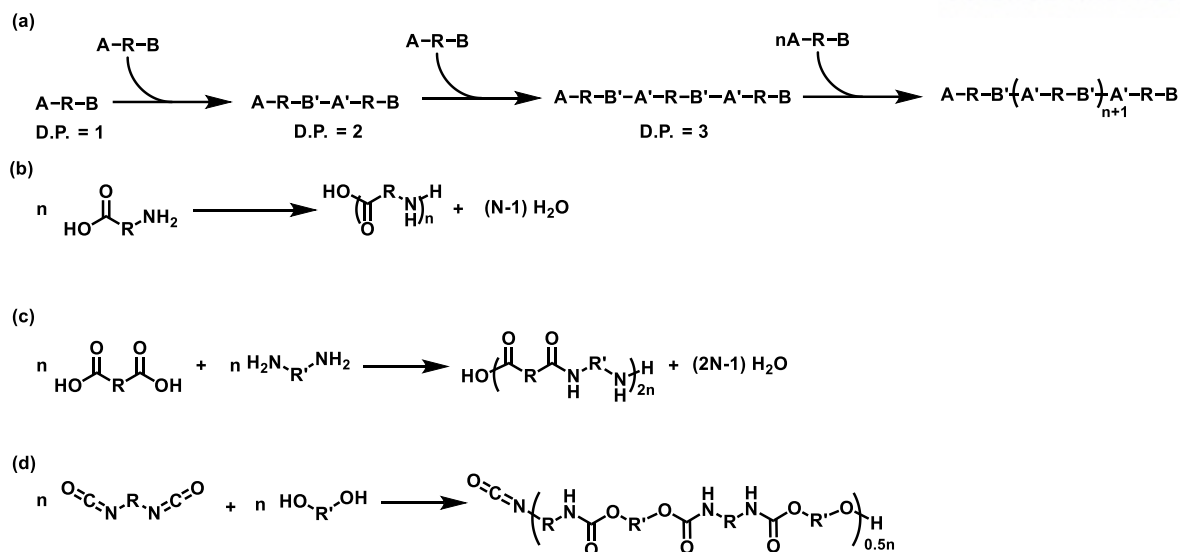


**Figure 1.** Reaction schemes for a generalized step-growth polymerization (a), poly(amides) from A-R-B (b) and A-R-A / B-R-B (c) type monomers, and poly(urethane) (d)

Bifunctional<sup>1</sup> monomers, the most common and simple monomers employed in step-growth polymerizations, can be divided into two groups. The A-R-B type monomer consists of an R group connecting two functionalities (A and B) which can undergo some bond-forming reaction (A'-B') (Figure 1, a). Each reaction creates a new molecule whose degree of polymerization (D.P.) is the sum of the two previous molecules D.P., which is the case for all polymerizations. Additionally, each molecule in solution will have one A and one B functionality on either end. This type of step-growth polymerizations can be seen in the polymerization of amino acids, where the repeated condensation of amine and carboxylic acid groups into amide linkages leads to the formation of a poly(amide) (Figure 1, b). Much more commonly, step-growth polymerizations occur between two different bifunctional molecules, A-R-A and B-R-B. In this case, polymerization proceeds in much the same manner, with a reaction between each monomer type leading to what is effectively an A-R-B species. For example, poly(amide)s can also be produced through this type of reaction, with diamines being reacted with diacids to produce a very similar (but not identical) polymer (Figure 1, c) to what was shown in figure 1b.

Both of the previous polymerization examples are accompanied by the production of a water molecule and are known as condensation polymerizations. Condensation polymerizations are defined as polymerizations in which small molecules are given off during polymer growth, and while this is oftentimes water, various other small molecules such as acids, salts, and organics can also be released from the process. Most step-growth polymerizations are condensation polymerizations, however, this is not always the case. Poly(urethane)s are polymerized in a step-growth manner by the reaction of alcohols with isocyanates to produce carbamate linkages with no small molecules being released



(Figure 1, d). Conversely, all condensation polymers do not necessarily grow in a step-growth manner, which will be examined later.

The kinetics of step-growth polymerizations are governed by the concept of “equal reactivity of functional groups,” and were worked out by Flory.<sup>2</sup> The principle of equal reactivity of functional groups states that the reactivity of all functional groups in solution, whether on a monomer, oligomer, or polymer all have essentially the same reactivity. Since the innate reactivity of all molecules in solution is the same, the probability of any two molecules (monomer, tetramer, octamer, etc.) reacting is based only on their relative concentrations in solution. Because monomer is the most abundant molecule in solution at the beginning of the polymerization, we see that monomer is consumed relatively quickly during a step-growth polymerization. At an extent of conversion, defined as

$$p = \frac{N}{N_0} \quad \text{Equation 1.}$$

where  $N$  is the number of functional groups reacted and  $N_0$  is the initial number of functional groups in solution, the amount of monomer remaining in solution ( $[M]/[M]_0$ ) is given by

$$\frac{[M]}{[M]_0} = (1 - p)^2 \quad \text{Equation 2.}$$

By plotting Eq. 2 (Figure 2, a), it is clear that monomer concentration decreases quickly at the beginning stages of the reaction, with the rate of consumption decreasing toward higher extents of conversion. It is expected that about 55% of the monomer is consumed one-third of the way to completion ( $p = 0.33$ ) and about 90% is consumed at  $p = 0.66$ .

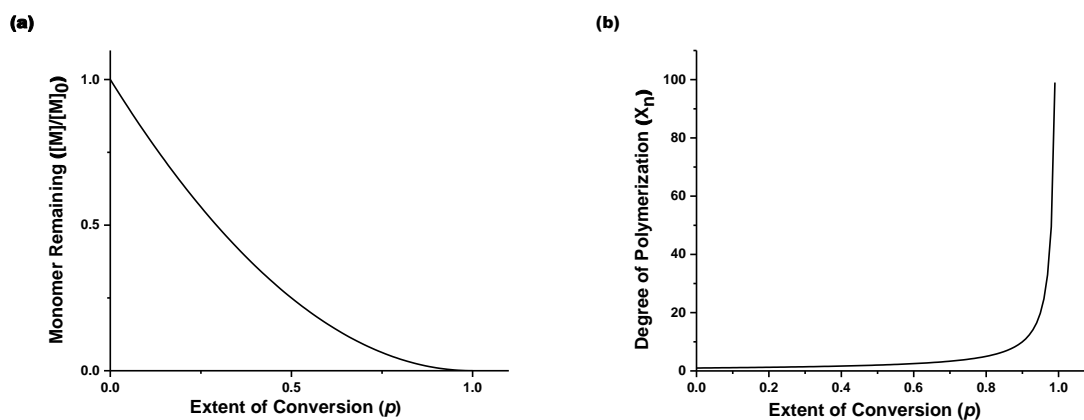


**Figure 2.** Graphs displaying the consumption of monomer (a) and degree of polymerization (b) versus the extent of conversion as predicted by theory.

Polymer D.P ( $\bar{X}_n$ ), and by extension molecular weight, initially increase very slowly, with primarily dimer and other small oligomers being formed at low values of  $p$ . It is not until  $p$  approaches one and the majority of functional groups in solution have been reacted, that high molecular weight polymer is formed. This process is described by the Carothers equation

$$\bar{X}_n = \frac{1}{(1-p)} \quad \text{Equation 3.}$$

From a plot of this equation (Figure 2, b), it is clear that a D.P. of two is not achieved until half of the functionalities have reacted and average chain lengths of ten are not seen until  $p = 0.9$ . The slow increase of average molecular weight and the quick consumption of monomer are perhaps the two most characteristic behaviors of a step-growth polymerization, and as we will see, differ substantially from what is observed in chain-growth polymerizations.

Unlike monomers in step-growth polymerizations, monomers (M) in chain-growth polymerizations are not all innately reactive toward each other under the conditions used in a normal polymerization. Instead, some initiator (I) is used to activate a small portion of the monomers in a process called initiation (Figure 3, a). This initiator can be a wide variety of chemicals including radical sources, anions, cations, or metallic catalysts or physical phenomena such as heat or light. An activated monomer ( $M^*$ ) is then able to react with other monomer molecules in solution (Figure 3, b). Upon reaction, the two monomers form a bond and the active center is passed from the initially activated monomer ( $M_1$ ) to the new “active chain end” ( $M_2$ ). The new chain end will react with another monomer ( $M_3$ ), forming another bond and again passing the active center on. This reaction repeats itself, in a process known as propagation, increasing the length of the growing polymer chain (P) by one structural unit every time. Propagation continues until either all of the monomer in solution is consumed or the growing chain is deactivated through what is called termination (Figure 3, c). Termination can occur through a reaction of two active centers, or in a reaction between the active center and some other molecule in solution (B). In the case of termination, B can either form a bond with the active chain end, forming a non-reactive endgroup, or generate a new species  $B^*$  that is not able to react with monomer. In some cases, the molecule (C) that terminates the growing chain can itself become an active center for propagation in what is known as chain transfer (Figure 3, d). A huge number of different types of chain-growth polymerizations exist, and while the exact details of these steps vary between the different types, the three fundamental steps of initiation, propagation, and termination are present in almost all cases.

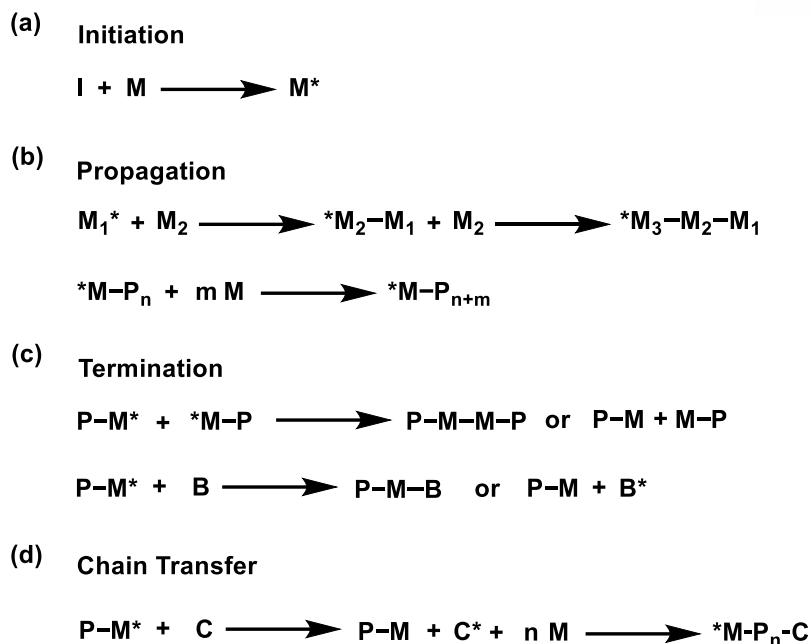


**Figure 3.** General steps in a chain-growth polymerization include initiation (a), which begins the polymerization reaction, propagation (b), which grows the polymer chains, termination (c), which ends the growth of chains, and chain transfer (d), which ends the growth of one chain while initiating another.

Perhaps the most well-known types of chain-growth polymerizations are those that employ vinyl monomers, which generally consist of a terminal alkene with one or two constituents on one carbon atom. Vinyl polymers are the most widely produced type of polymer, and include poly(ethylene), poly(propylene), poly(vinyl chloride), poly(styrene), and poly(acrylate)s. Based on the vinyl monomer choice, these polymers are often formed through propagation steps that utilize radical, cationic, or anionic active chain ends. In the case of ethylene and propylene, polymerization is most commonly catalyzed by various transition metal complexes in what is known as a coordination polymerization. Many non-vinyl chain-growth polymerizations are also catalyzed by metal complexes, including ring-opening metathesis polymerizations (ROMP), ring-opening polymerizations (ROP), and many of the polymerizations described in chapter one.<sup>3, 4</sup>

A general discussion of the kinetics of chain-growth polymerization is substantially more complex than a discussion of step-growth polymerization kinetics. This complexity arises from the number of different concurrent reactions occurring at once (initiation, propagation, termination, chain transfer) as well as the wide variety of different types of chain-growth polymerizations that try to maximize, minimize, or entirely remove certain reactions. Even the prototypical kinetic analysis of free radical polymerizations makes a number of assumptions including a steady-state concentration of

growing chains and the equal reactivity of active centers. Even with these assumptions in place, several important conclusions can be made about normal (non-controlled) chain-growth polymerizations. Firstly, monomer is consumed more slowly and consistently over the course of the polymerization in comparison to step-growth polymerizations. Secondly, the polymer's number average molecular weight ( $\bar{M}_n$ ) initially grows very quickly, plateauing at relatively low  $p$  values (Figure 4, a). This is because individual polymer chains are initiated, grow, and terminate very quickly relative to how long it takes all initiator or monomer to be consumed.

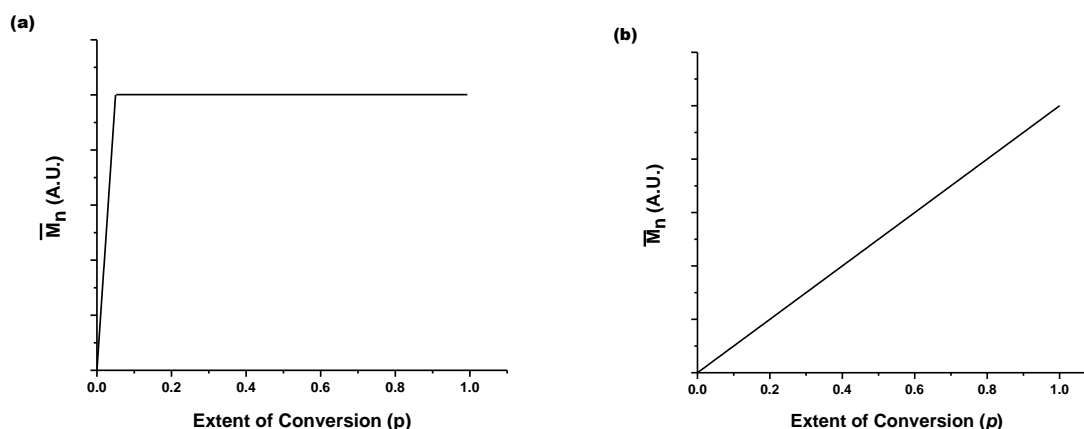


**Figure 4.** Graph of average molecular weight ( $\bar{M}_n$ ) versus the extent of conversion ( $p$ ) for normal (a) and living chain-growth polymerizations (b).

In some cases, termination and chain transfer can be greatly, if not entirely, suppressed in what are known as controlled and living polymerizations, respectively. Some vinylic monomers can be polymerized in a living manner through the use of ionic initiators. This causes the active chain ends to also be ionic, preventing termination from occurring between two chains. Szwarc first demonstrated this type of living polymerization in 1956 by polymerizing styrene using sodium naphthalenide as an initiator.<sup>5</sup> Initiation occurs as electrons are passed from the sodium naphthalenide to styrene, which subsequently dimerizes into a species with two active carbanions on each end (Figure 5, a). Since the anionic chain ends are unable to react with each other, subsequent polymerization from each side can continue until all monomer is consumed (Figure 5, b). The living nature of these polymerizations is only seen, however, if great care is taken in choosing correct monomers and reaction conditions. Stringent measures must be taken to ensure reactions are free from impurities such as water or oxygen, which rapidly cause termination with the highly reactive chain ends. In the case of metal-catalyzed chain-growth polymerizations, catalysts can be designed which do not undergo chain transfer or termination steps. For example, metal-catalyzed living polymerizations have been demonstrated for

cyclic olefins, diazoacetates, and isocyanides.<sup>3, 6, 7</sup> Because chain termination does not occur in living polymerizations, additional monomer can be added to reaction solutions to induce further polymer growth (chain extension) or to form copolymers. Additionally, when living polymerizations also undergo fast initiation (relative to propagation rates), number average molecular weights,  $\overline{M}_n$ , increase steadily as  $p$  increases (Figure 4, b), and incredibly narrow (1-1.5) PDI (polydispersity index) values are obtained. This also leads to controlled molecular weights, with the monomer to catalyst ratio dictating the expected D.P. These three properties (chain extension, low PDI, and controlled  $\overline{M}_n$ ) are not only incredibly useful for synthesizing high-quality polymers, but are generally used as experimental evidence of a living polymerization.

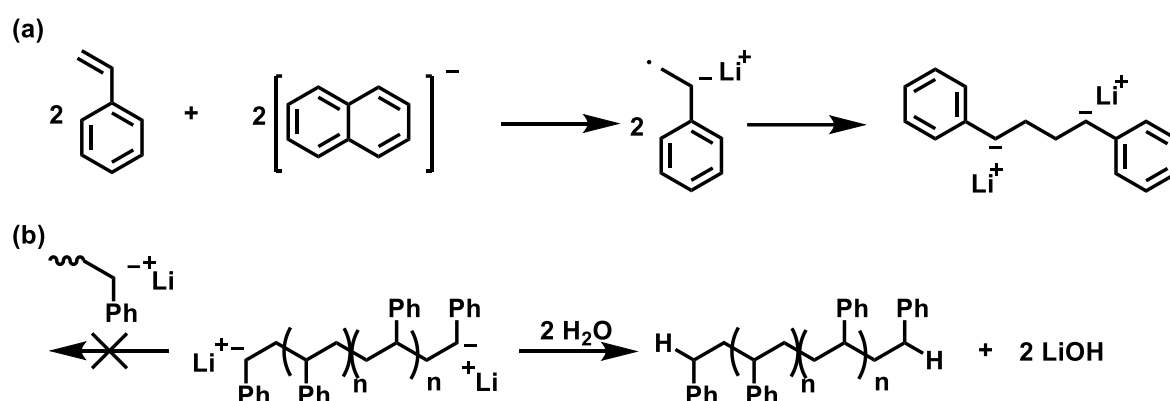


**Figure 5.** Initiation (a) and possible termination step (b) for the living anionic polymerization of styrene. While polymer chains cannot terminate with other active chains, reactions with impurities can cause termination.

If termination is effectively suppressed instead of being entirely absent, as is the case in controlled polymerizations, polymers can be synthesized with all of the benefits of a living polymerization. This is generally achieved through what is known as a “reversible-deactivation” radical polymerization (RDRP), which relies on a reversible reaction between active chain ends and some deactivating agent leading to the formation of dormant chain ends. The equilibria for these reactions lie heavily toward the dormant species, thus limiting the concentration of active chain carriers in solution at any time. Because the concentration of active chain ends is so low, the rate of termination reactions is greatly decreased, even though the rate constants of the associated reactions remain the same. If reversible-deactivation occurs concurrently with quick initiation, polymers with controlled molecular weights and low PDIs can be achieved. Additionally, on the right timescales, chain extension and copolymerization can be performed in a manner similar to living polymerizations. One example of RDRP which illustrates the method well is nitroxide-mediated radical polymerization (NMRP), which utilizes a stable nitroxide radical introduced through the initiator as the deactivating agent.<sup>8, 9</sup> The polymerizations are generally initiated thermally, with the decomposition of alkoxyamine initiator into

a stable nitroxide radical and another reactive fragment, for example, a benzylic radical (Figure 6, a). The reactive fragment acts as a traditional initiator for chain-growth polymerization, and a polymer chain begins to grow. At some point, the nitroxide radical can react with a growing chain, forming the relatively stable dormant alkoxyamine (Figure 6, b).<sup>10</sup> The dormant form can undergo homolysis, reforming the active chain end which is then free to continue growing, however, this is disfavored by the equilibrium so only small amounts of active chain exist in solution at any given time. A number of other RDRP methods including ATRP<sup>11</sup> and RAFT<sup>12, 13</sup> have been developed, and through similar mechanisms of deactivation, can display characteristics of living polymerizations.

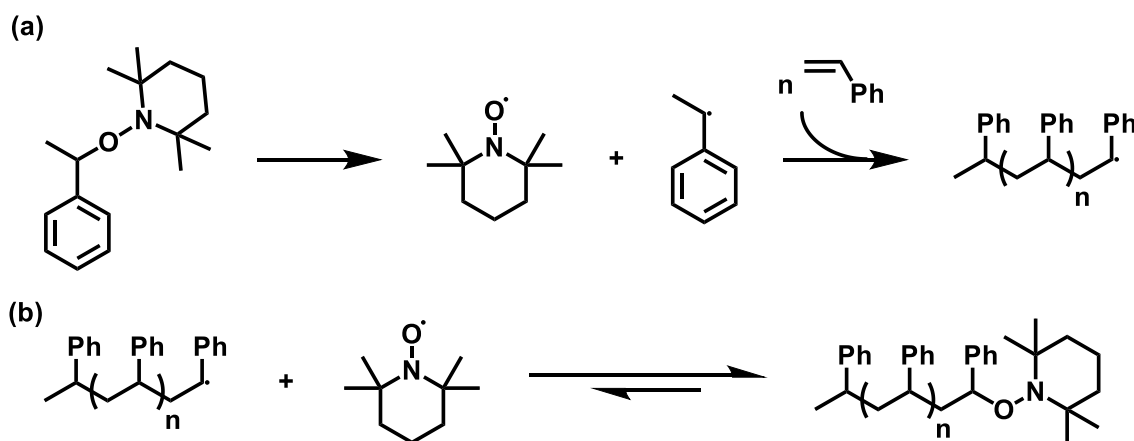


**Figure 6.** The initiation, propagation (a), and reversible deactivation (b) of a nitroxide-mediated radical polymerization of styrene

All of the aforementioned chain-growth polymerizations have been addition type polymerizations, propagating without the co-generation of small molecule byproducts. Chain-condensation polymerizations, however, both produce small molecule byproducts and grow through a chain-growth mechanism.<sup>14, 15</sup> Chain-condensation polymerizations still utilize reaction between two A-R-B type monomers but rely on either “change of substituent effects” or intramolecular catalyst transfer to insure that only activated chains can grow. Grignard Metathesis (GRIM) represents an example of the latter, where a large number of conjugated polymers can be synthesized through the polymerization of dihalo monomers using metal catalysts. For example, when 2-bromo-3-hexyl-5-iodothiophene is reacted with 1 equivalent of *i*-PrMgCl and catalytic amounts (0.4 mol %) of Ni(dppp)Cl<sub>2</sub> (dppp = 1,3-bis(diphenylphosphino)propane), a poly(thiophene) was formed in a manner consistent with chain-growth polymerization (Figure 7).<sup>16</sup> The initial step in the reaction is the formation of the Grignard reagent monomer, 2-bromo-5-chloromagnesio-3-hexylthiophene, which is not capable of self-polymerization. When Ni(II)(dppp)Cl<sub>2</sub> is present, two equivalents of the Grignard monomer complex to the catalyst and 2 equivalents of MgCl<sub>2</sub> are given off. Reductive elimination leads to coupling between the two monomers, and the zero-valent Ni complex is oxidatively added between one

of the remaining C-Br bonds. The Ni(II) catalyst is now primed for reaction with another monomer, and the repetition of this cycle makes up the propagation step. In some cases, controlled GRIM polymerizations can be performed which display narrow PDIs, controlled molecular weights, and active chain ends amenable to block co-polymerization.<sup>17, 18</sup>

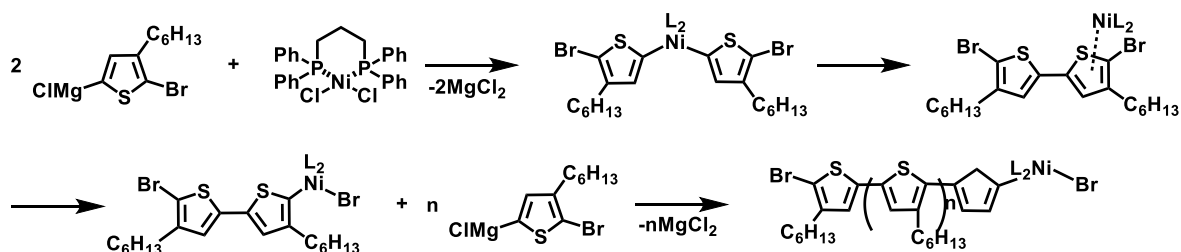


**Figure 7.** Mechanism of initiation and propagation for the GRIM polymerization of hexyl thiophene

Chain-condensation polymerizations that display a change of substituent effect do not utilize catalysts, but rather rely on an increased reactivity of the polymer end groups relative to the monomer.<sup>14, 15</sup> The increase in end group reactivity is caused by the change of electronic properties of the molecule induced by the transformation of the monomer (A-R-B) into the end group (P-B'-A'-R-B) (Figure 8, a). To date, this has only been observed in cases where R is conjugated between A and B and the change in electron withdrawing or donating effects between A and A' causes changes in the reactivity of B due to resonance effects. The first report of such an effect was in the polymerization of metallated p-halothiophenoxides, where less monomer was consumed at various extents of conversion in comparison to what was expected for a step-growth polymerization (Figure 8, b).<sup>19</sup> This effect was attributed to the transformation of the thiophenoxide anion, a strong electron donating group, into a much weaker electron donating sulfide group when polymerized. The decrease in electron density donated into the aromatic ring had the effect of increasing the reactivity of the halogen in the para position towards further condensation. This change in reactivity makes it more likely for monomers to condense with the activated halogen on a polymers endgroup than with each other, effectively breaking the assumption of equal reactivity. This leads to preferential growth of the polymer chains over dimerization and a polymerization that shows chain-growth character. Further studies were not conducted on the system to determine the extent that chain-growth was occurring over step-growth, however, many new condensation polymers utilizing the change of substituent effect have been shown to exclusively polymerize in a chain-growth manner.

Under basic conditions, phenyl 4-(octylamino)benzoate does not readily polymerize with itself, but when phenyl 4-nitrobenzoate is added as an initiator a chain-growth polymerization occurs (Figure 8, c).<sup>20</sup> Under basic conditions, the amine is deprotonated to form an aminyl anion, which strongly donates electron density into the aromatic ring and ester functionality. This has the effect of greatly

reducing the electrophilicity of the carbonyl carbon, rendering it unreactive towards nucleophilic attack by aminyl anions on other monomers. Nitro groups, on the other hand, are strongly electron withdrawing, rendering the ester on the initiator strongly electrophilic and prone to reaction with the aminyl anions on the monomers. When a monomer reacts with the initiator, the amide linkage formed is a much weaker electron donating group than the aminyl anion, resulting in an ester end group which is prone to nucleophilic attack. Subsequent reaction with another monomer leads to the formation of another amide linkage and the ester group of the terminal structural unit becomes the new active chain end. This process of amide formation and concurrent ester activation is the propagation step for this chain-growth polymer. The preference towards chain-growth is so strong that polymers with low ( $\leq 1.1$ ) PDIs and controlled molecular weights (up to 22 kDa) could be formed. A number of other chain-condensation techniques allow the polymerization of poly(amide)s, poly(ether)s, poly(thiophene)s, and more with high levels of control. Control over these typically uncontrolled condensation reactions greatly expands the utility of the polymer produced, however strict requirements on the potential monomers and reaction conditions potentially limit the utility of chain-condensation polymers.

With the various polymer growth mechanisms in mind, we devised several experiments to determine the polymerization mechanism for different poly(carbyne) precursors. The results of these experiments clearly show that different monomers polymerize through different mechanisms based on side chain functionality. Furthermore, we have shown that in addition to increasing polymer yields, the inclusion of naphthalene increases polymerization rate while not fundamentally altering the polymerization mechanism. While initial kinetic and thermodynamic analyses of the polymerizations did not reveal a clear cause for the differences in polymer structure and polymerization mechanism seen, some possible causes are discussed.



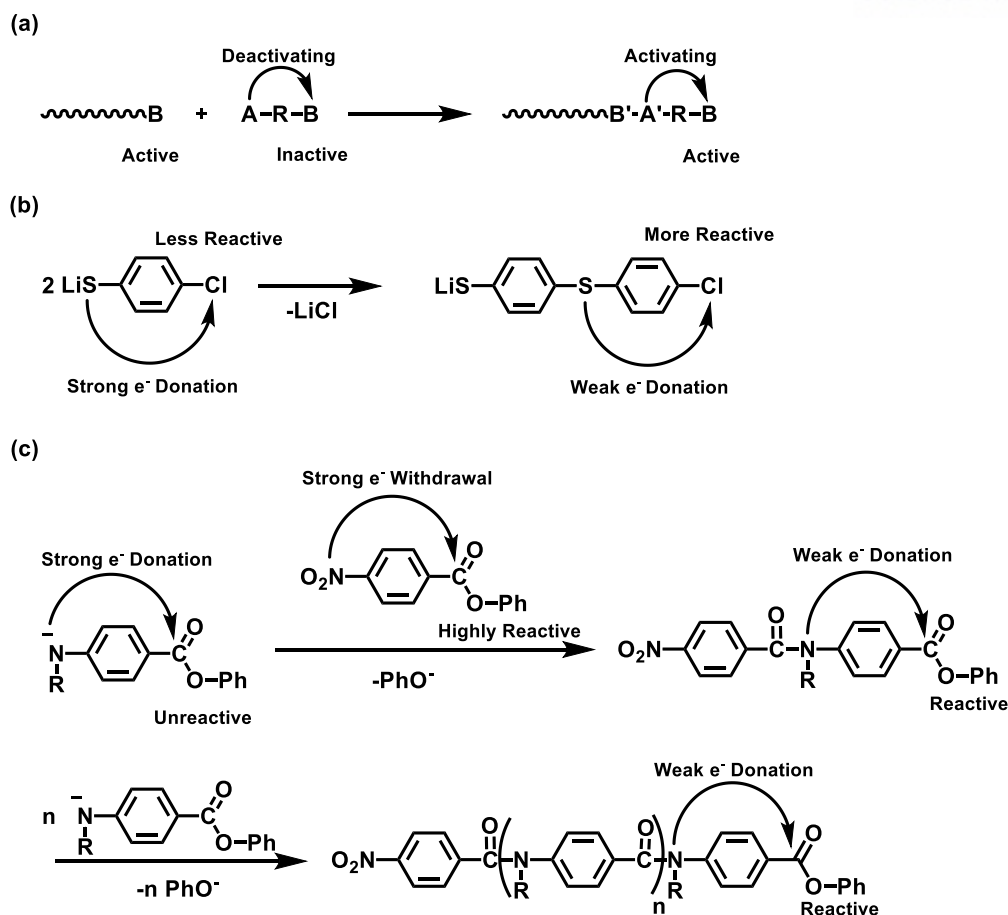


**Figure 8.** Chain-condensation polymerizations occur due to change of substituent effects when a functional group on the monomer is activated toward further polymerization upon incorporation into the polymer chain (a). The activation occurs due to the change in the electronic properties of the molecule, as is seen in the polymerizations of p-halothiophenoxides (b) and 4-(octylamino)benzoate (c). R = C<sub>8</sub>H<sub>17</sub>

## 4.2 Results and Discussion

The fundamental propagation step in Li driven poly(carbyne) synthesis consists of the transformation of two C-X bonds and two atoms of Li into one new C-C bond and 2 atoms of LiX (Figure 9, a). This is the case for the reaction of any two polymerizable species in solution, regardless of what other substituents are on the two reacting molecules. For example, both the reaction of a trifluorotoluene dimer with a structural unit of branched poly(phenyl carbyne) (Figure 9, b) and the reaction of a trichloro acetate monomer with the end group of a linear poly(ester carbyne) (Figure 9, c) both produce exactly one new C-C bond and 2 molecules of LiX. Because the fundamental coupling reaction always produces LiX as a byproduct, it is easy to classify this reaction as a condensation

polymerization. As was discussed above, however, condensation polymerizations can grow in both a step- and chain-growth manner. In order to elucidate the operant polymerization mechanism, a series of experiments that utilize some of the unique properties of poly(carbyne) synthesis were performed.

As mentioned previously, step-growth polymerizations generally obey the principle of equal reactivity of functional groups. When this is the case, the progress of the polymerization is dictated by probability and the amount of monomer remaining in solution should be governed by Equation 2. It then follows that if monomer concentration,  $[M]$ , and the extent of conversion,  $p$ , could accurately be measured at various points during the polymerization, then it should be possible to determine if a step-growth polymerization is operational by comparing a graph of the two. Measurements of monomer concentration during a polymerization are fairly common in the field of polymer chemistry and can be performed using a large variety of analytical techniques including nuclear magnetic resonance (NMR), high-performance liquid chromatography (HPLC), and gas chromatography (GC). Extent of conversion, or the amount of remaining reactive functional groups, can be more difficult to measure and depends strongly on the nature of the monomer. In the case of the chain-condensation of *p*-halothiophenoxides mentioned above,  $p$  was measured through elemental analysis of the amount of residual halogen remaining in polymer samples.<sup>19</sup> In much of the work Flory based his theories off of,  $p$  was measured in the polymerization of polyesters by titrating the remaining carboxylic acid in solution with base.<sup>21</sup> Aliquots had to be pulled out periodically as the fraction of conversion naturally moved toward 1 over time.

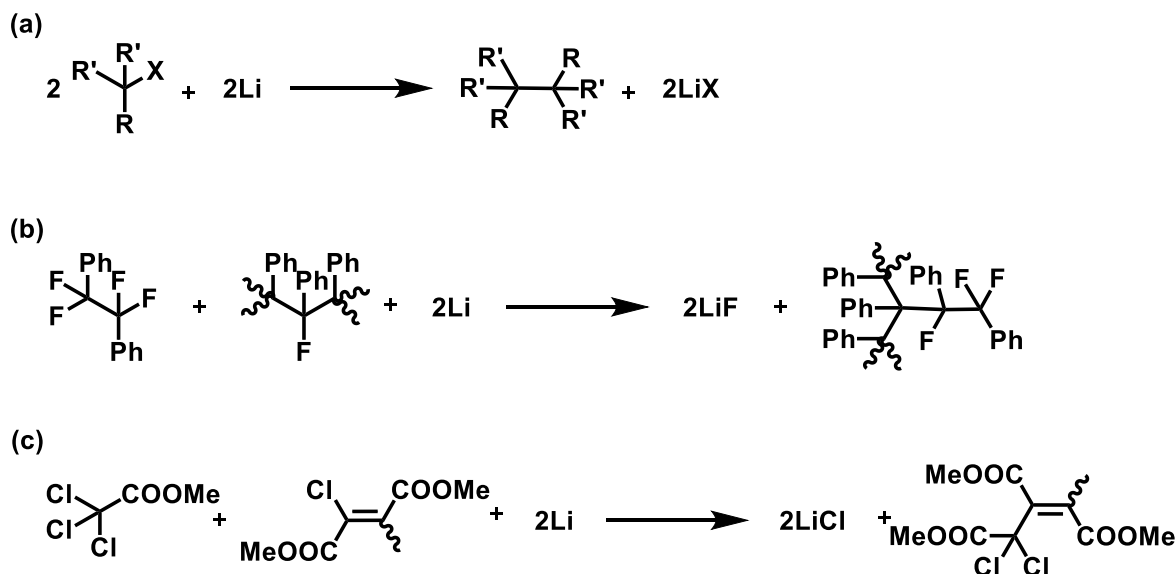


**Figure 9.** The fundamental coupling reaction present in poly(carbyne) synthesis (a) is seen in all examples of polymer growth, such as the addition of a dimer to branched poly(phenyl carbyne) (b) or the addition of a monomer to linear poly(ester carbyne) (c). R = phenyl, ester R' = structural unit, X X = leaving group

In the case of poly(carbyne)s, stoichiometric amounts of reductant are required to drive the reaction forward and thus increase  $p$ . This can easily be seen in the first paragraph of the discussion. From the chemical equation of the polymerizations, it is clear that 3 equivalents of Li are required to fully polymerize a poly(carbyne) monomer, assuming a complete reaction between the two. As we have previously shown, near complete dechlorination ( $p = 1$ ) of trichlorotoluene and pentyl trichloroacetate is in fact achieved when stoichiometric amounts (3 eq.) of Li are added. Since we can directly relate the equivalents of Li added to the extent of conversion, Equation 1 can be rewritten as

$$p = \frac{[Li]_0}{[M]_0} \quad \text{Equation 4.}$$

By performing the polymerizations with varying substoichiometric amounts of Li, it is possible to measure monomer consumption at varying values of  $p$ , and thus determine whether a step-growth or chain-condensation mechanism is active. If monomer is consumed in a fashion predicted by Flory (Figure 10 a), a step-growth polymerization must be active. However, if the poly(carbyne) were to form according to a chain-condensation mechanism, monomer should be consumed more slowly and be present at late stages of the reaction (Figure 10 b).

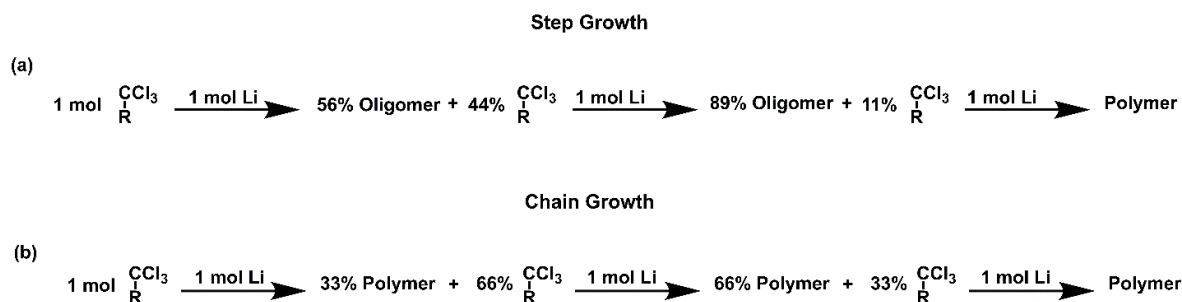


**Figure 10.** Comparison of monomer remaining after various equivalents of Li are added to carbyne precursors if an ideal step-growth (a) or chain-growth (b) polymerization is active.

In practice, the experiments were performed by charging solutions of either  $\alpha,\alpha,\alpha$ -trichlorotoluene (TCT) or pentyl 2,2,2-trichloroacetate (PTCA) with varying quantities of Li (0.5 – 3.5 equiv. relative to monomer) in THF and measuring the remaining monomer by gas chromatography. The percentage of monomer remaining ( $([M] / [M]_0) \cdot 100$ ) versus the equivalents of Li added ( $[Li]_0 / [M]_0$ ) was then plotted. As shown in Figure 11a, TCT (red squares) was detected in solution even after several equivalents of Li were added. Linear regression of the data showed that approximately 34% of monomer was consumed for each equivalent of Li added which agreed with the value (33%) expected for an ideal chain-growth polymerization. This suggests that 2/3 of the monomer remains while 1/3 is fully dechlorinated a third of the way through the reaction, showing a stark difference to what is expected in a step-growth polymerization. In contrast, linear regression of the data recorded for analogous experiments performed with PTCA (Figure 11a, blue circles) indicated that approximately 56% of the

monomer was consumed per equivalent of Li added, much closer to what would be expected in a step-growth polymerization.

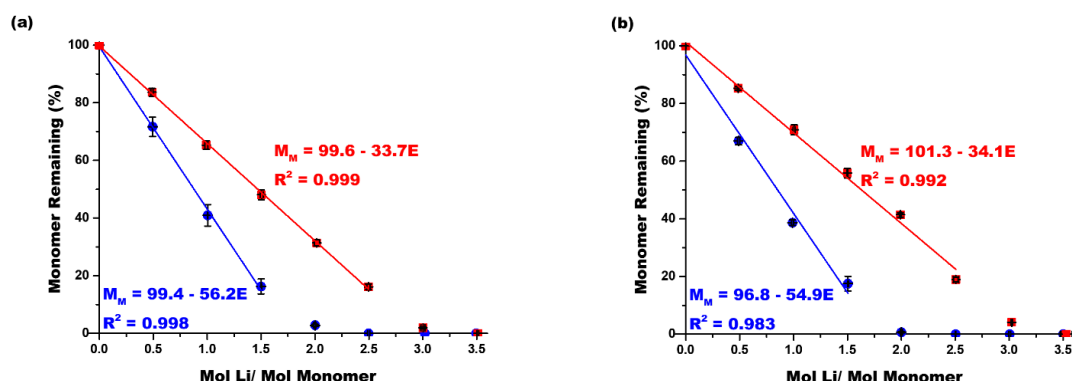


**Figure 11.** (a) Monomer (TCT, red squares or PTCA, blue circles) remaining as a function of equivalents of Li added. (b) Monomer (TCT, red squares or PTCA, blue circles) remaining as a function of equivalents of Li added and in the presence of naphthalene.

The potential effects of the added electron transfer agent on the polymerization mechanisms were also investigated. The aforementioned monomer consumption experiments were repeated in the presence of 0.25 equiv. of naphthalene and key results are shown in Figure 11b. In the presence of naphthalene, the amount of monomer consumed per equivalent of Li added was calculated to be approximately 34% and 55% for TCT and PTCA, respectively (red squares and blue circles, respectively). Kinetics data were also recorded and revealed that the monomers were consumed relatively rapidly when naphthalene was added. For example, the amount of TCT consumed after 1 h was determined to be 28% in the presence of naphthalene and 16% in the absence. Likewise, conversions of 76% and 34%, respectively, were measured for experiments that involved PTCA. More in-depth kinetic experiments were attempted, however consistent results were difficult to obtain due to the heterogeneous nature of the reaction as well as the extremely fast initial reaction rate. Regardless, the basic kinetic observations, along with the results from figure 11, indicated that higher reaction rates were observed when PTCA was polymerized in comparison to TCT and that the charge transfer agent accelerated the polymerization without affecting the underlying mechanism.

If the results from Figure 11a are plotted against Equation 2, we see further evidence that different growth mechanisms are operant based on monomer choice (Figure 12). The amount of TCT consistently falls above the theoretical predictions, suggesting an increased reactivity of structural units in the polymer when compared to monomer.<sup>19</sup> This is indicative that, at least by monomer consumption studies, the polymerization of TCT displays some chain-condensation character. Alternatively, while concentrations of PTCA initially lie close to the theoretical predictions for a step-growth mechanism,

they deviate to lower than expected values as the extent of conversion increases. This could potentially indicate some degree of deactivation of the structural units in the polymer versus the monomer.

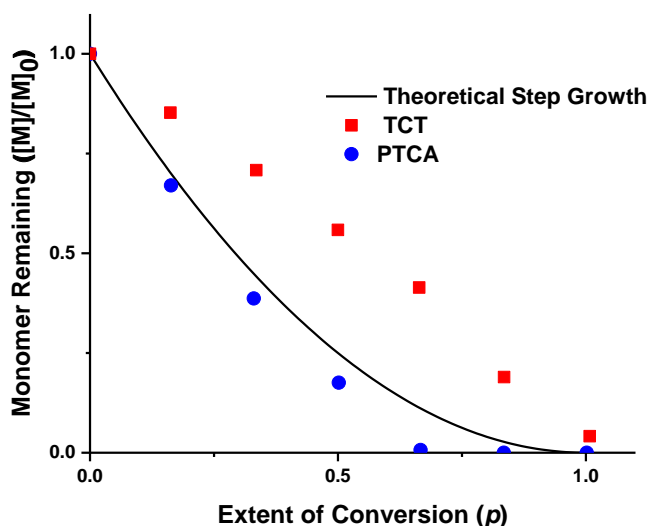


**Figure 12.** Data from Figure 11a plotted as fraction of monomer remaining vs extent of conversion for TCT (red squares) and PTCA (blue circles), as well as the theoretical curve for a step-growth polymerization according to *Eq. 2*.

While the exact mechanism of activation and deactivation observed in the growing polymer chains is not readily apparent, its presence in the formation of poly(carbyne)s is not entirely unexpected. While change of substituent effects have only been observed in conjugated polymers, there is no reason to think that they cannot occur in other polymer systems. In the case of poly(carbyne)s, all reactive functionalities in a monomer are located on the same carbon atom. Because of this, it is not unexpected that the conversion of a germinal C-Cl bond to a C-C bond would have an effect on the reactivity of the remaining reactive functionalities (C-Cl) (Figure 13, a). The change of the C-Cl to C-C bond could be considered analogous to the “change of substituent effect” in this case. In the cases reported, we see both an increase in reactivity (TCT) as well as a decrease in reactivity (PTCA) as the C-Cl bonds are replaced, which likely arise from the steric and electronic effects of the side chains of both the structural unit in question as well as its neighbors (Figure 13, b).

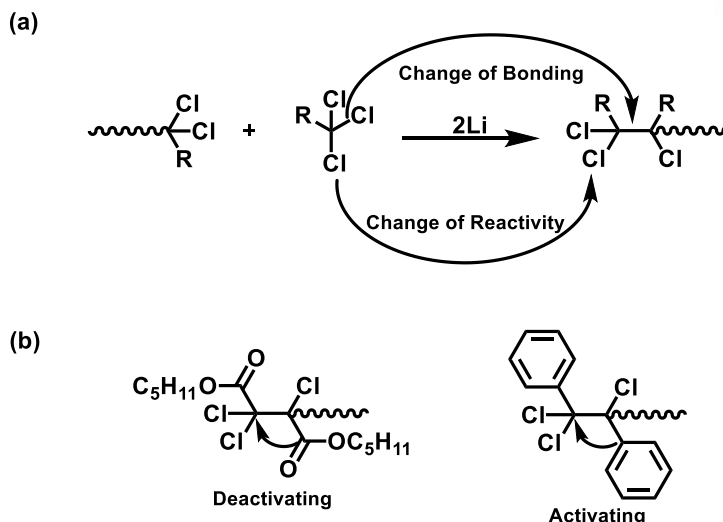


**Figure 13.** The change in bonding (C-Cl to C-C) at the reactive carbon of a carbyne structural unit can lead to a change in reactivity of the remaining leaving groups (a), leading to either activation or deactivation in relation to the monomer (b).

A study into the thermodynamics of the monomers and their dimers was designed to further probe the cause of these increased and decreased reactivities. It was hypothesized that differences in reduction potentials,  $V$ , between the monomers and their respective dimers could be the cause of the observed activation and deactivation, and would explain the differing mechanisms seen. Specifically, we expected the dimer of TCT to have a lower absolute (less negative) reduction potential ( $V_2$ , Figure 14) than TCT ( $V_1$ ). If this were true, it would suggest that partially dechlorinated poly(phenyl carbyne) chains are more easily reduced into reactive intermediates than TCT. Under the strongly reducing conditions present during polymerization, this would equate to growing polymer chains that are activated toward further polymerization in comparison to their monomers, and explain the chain-condensation behavior observed. We expected to see the opposite in the case of PTCA ( $V_4$ ), with a slightly higher absolute (more negative) reduction potential deactivating the polymer chains ( $V_3$ ) and leading to the higher than expected monomer consumption. The reduction potentials of each molecule could easily be determined by cyclic voltammetry, however, the two dimers needed to be synthesized first.

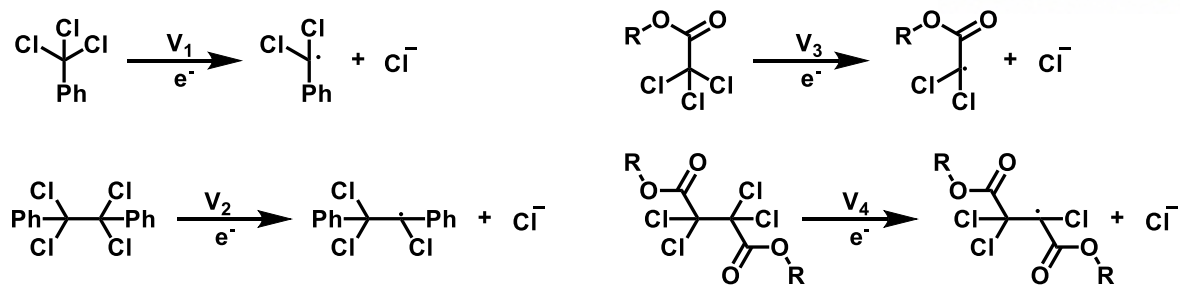
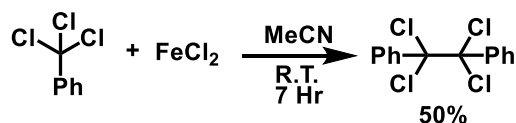


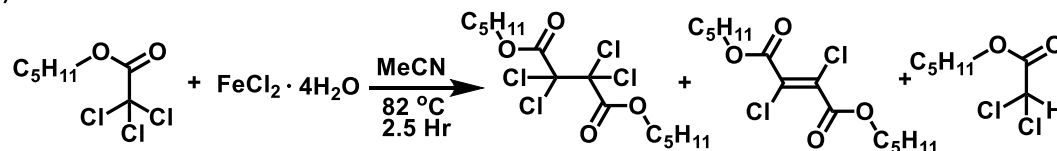
**Figure 14.** The electrochemical reduction of TCT, PTCA, and their dimers. If  $V_2 > V_1$  then growing chains are more easily reduced than the monomer and could be thought of as “activated” toward further polymerization leading to chain-growth. If  $V_4 \leq V_3$  then no activation is seen in the growing polymer chains and step-growth would be observed.  $R = C_5H_{11}$

The dimer of TCT was relatively easy to synthesize and purify, with TCT being coupled using stoichiometric amounts of  $FeCl_2$  as a reductant (Figure 15, a). The reaction was performed by adding 2 equivalents of  $FeCl_2$  to a solution of TCT in acetonitrile.<sup>22, 23</sup> After stirring for 2 hours at room temperature, a simple series of extractions easily removed the benzoic acid byproduct. The remaining mixture was then run on a silica column to effectively remove remaining starting material to give a 50% yield of the pure dimer. Unfortunately, this same chemistry is not as effective with trichloroacetates. Strong complexation between the carbonyl and iron arrest coupling reactions and at best 28% yields of the desired compound can be produced in a multi-component mixture of products (Figure 15, b).<sup>23</sup> The other byproducts are the dichloroacetate, formed through hydrolysis of the Fe-C bond, and dichloro fumarate and maleate derivatives, formed through over reduction of the compound. The identities of these compounds were confirmed through  $^1H$  and  $^{13}C$  NMR, but the exact quantification of each product was made difficult due to overlapping peaks. Separation of the desired tetrachloro succinate from the two dichloro alkene isomers was not successful and another synthetic strategy was devised.

(a)



(b)



(c)

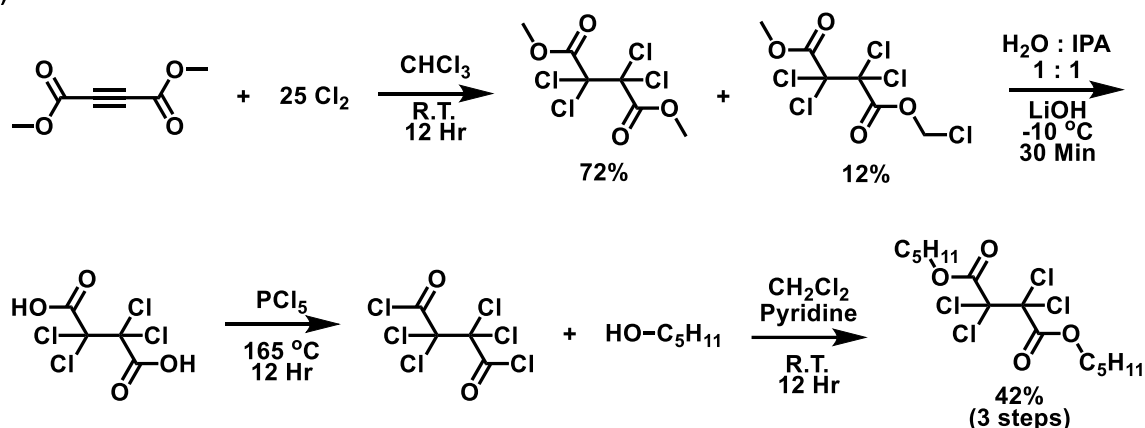


**Figure 15.** The synthetic scheme for the synthesis of TCT dimer (a) using  $\text{FeCl}_2$  produces an inseparable mixture when trichloro acetates are used (b). Instead, the chlorination, hydrolysis, and esterification of DMAD were used to produce the PTCA dimer (c).

Several methods utilizing the chlorination and transesterification of dimethyl acetylenedicarboxylate (DMAD) and related derivatives were attempted, and successful synthesis of the PTCA dimer, dipentyl 2,2,3,3-tetrachlorosuccinate, was finally achieved (Figure 15, c). The synthesis began with the chlorination of DMAD, which was performed by bubbling 25 eq. of  $\text{Cl}_2$  through a 0.25 M solution of DMAD in  $\text{CHCl}_3$ . After reacting overnight, washing with sodium thiosulfate and brine, and removing solvent under vacuum, a mixture of dimethyl tetrachlorosuccinate and the asymmetric ester chloromethyl methyl tetrachlorosuccinate was obtained in 72% and 12% yields, respectively. This mixture was subsequently hydrolyzed at  $-10\text{ }^\circ\text{C}$  in a 1 : 1 mixture of isopropyl alcohol and 1.5 M LiOH in water. After 30 minutes 10% HCl was added to the solution until acidified, and tetrachlorosuccinic acid was extracted into DCM and subsequently dried. Without further purification, the diacid (4.7 mmol) was added under  $\text{N}_2$  to  $\text{PCl}_5$  (9.4 mmol) in a Schlenk flask with an attached condenser column. The reaction was heated to  $165\text{ }^\circ\text{C}$ , upon which the  $\text{PCl}_5$  liquefied. After allowing to react overnight, the flask was cooled to room temperature, and 12.5 mL of DCM, 0.5 mL of pyridine, and 3.4 g of 1-pentanol were added to the flask and allowed to react for 12 hrs. Subsequent



extraction of the compound yielded 2 mmol (42 % over 3 steps) of the desired dipentyl 2,2,3,3-tetrachlorosuccinate.

With the required compounds successfully synthesized, electrochemical analysis could be performed. Cyclic voltammograms were taken for TCT, its dimer, PTCA, and its dimer in 0.01 M TBAPF (tetra-*n*-butylammonium fluoride) solution in dimethylformamide (DMF). Unexpectedly, the first reduction peak for the TCT dimer (-2.50 V, Figure 15, b) is slightly more negative than that of TCT (-2.42 V, Figure 15, a). While a difference of only 0.08 V is quite small, it was expected that the reduction potential of the dimer would be considerably less negative than that of TCT to facilitate the chain-condensation mechanism. Even more surprising was that the first reduction peak for the PTCA dimer (-2.12 V, Figure 15, d) was 0.2 volts less negative than the monomer (-2.34 V, Figure 15 c), suggesting it is more prone to reduction than the monomer. If the initial reduction of the compound was the reaction step causing increased reactivity in the polymer chain, and thus chain-condensation, we would expect PTCA to grow in a chain-growth manner. Since the differences in monomer-dimer reduction potentials do not line up with the expected values, we cannot say that the removal of chlorine to form the reactive carbon center is the process leading to the observed mechanistic differences.

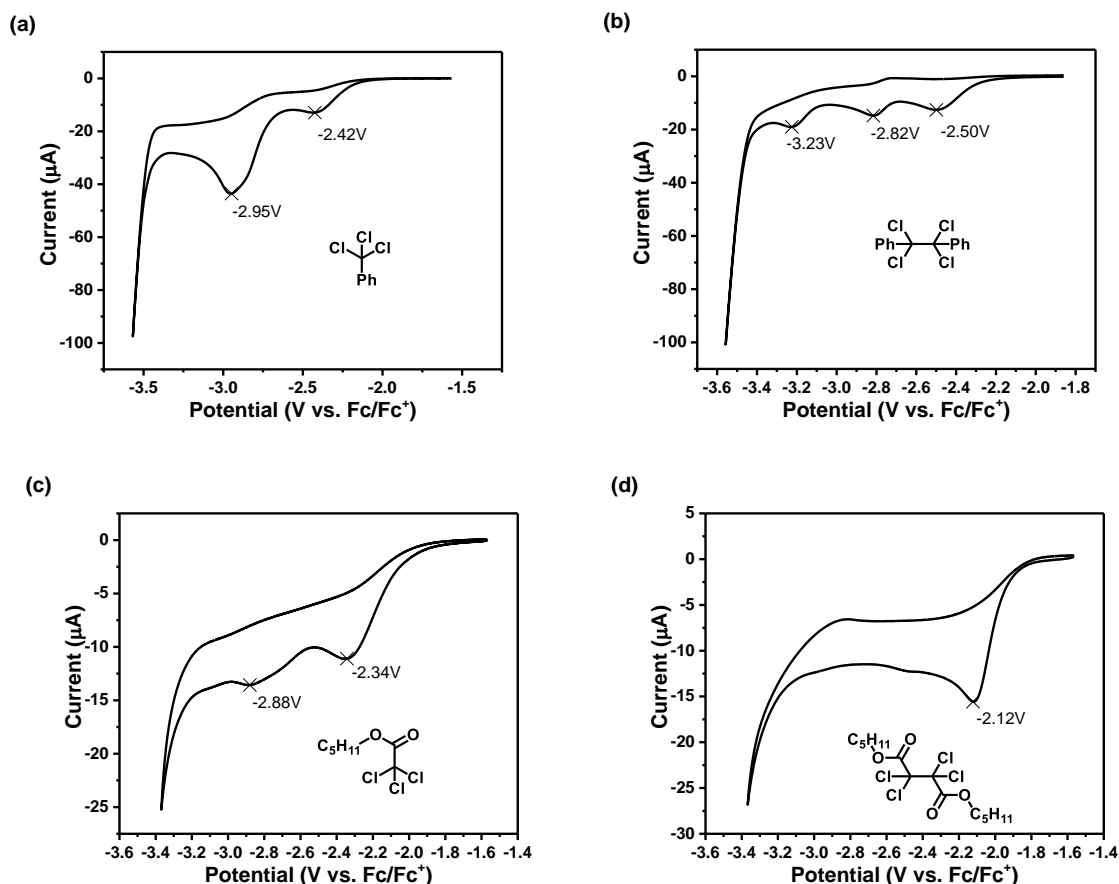


**Figure 16.** Cyclic voltammograms for TCT (a), its dimer (b), PTCA (c), and its dimer (d).

If the formation of the reactive carbon center is not the step leading to chain-condensation, then the observed differences in polymerization mechanism must arise from the coupling reaction, where linking of structural units occurs. The coupling reactions can occur through one of two pathways, either radical or anionic. Both pathways begin with the single electron transfer from Li (or Li Naphthalenide) to a chlorine atom on the polymerizing species, leading to homolytic cleavage of the C-Cl bond (Figure 16, a). It was this step that was investigated in the electrochemical study. In the case of a radical coupling, as the name implies, the generated radical reacts with another radical species (monomer or other polymer) in solution to form a new C-C bond (Figure 16, b). Alternatively, the radical can be further reduced into an organo-lithium compound through another single electron transfer (Figure 16, c). Subsequent nucleophilic attack by the anion on the electron-deficient carbon of another monomer or polymer leads to the coupling reaction. These potential pathways are similar to what are seen in Wurtz-like polymerizations, where it has been shown that both radical and ionic pathways are operant at any given time.<sup>24</sup> In the case of poly(carbyne) synthesis, polymerizations have been performed in both the presence of radical traps (TEMPO) and electrophiles (p-trifluormethylbenzaldehyde) and in both cases incorporation of the traps into the polymer have been observed. This suggests that similar to the Wurtz polymerization, both pathways are active.

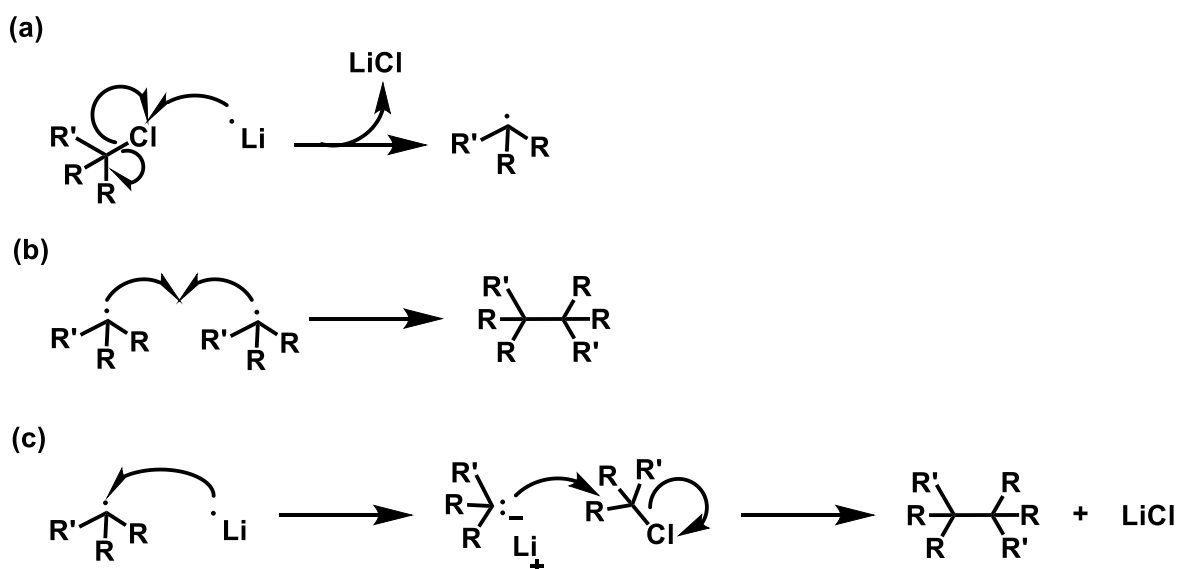


**Figure 17.** The steps in poly(carbyne) formation consist of monomer activation through reduction (a) followed by either radical coupling (b) or further reduction into an organo-lithium compound and subsequent nucleophilic attack (c). R = phenyl, ester R' = Cl, polymer

Identifying the specific cause of chain-condensations in the coupling step is quite difficult, both because of the two possible coupling pathways as well as the innately reactive nature of the molecules involved. We can, however, make some general statements about what to expect (and potentially look

for) in a system that is thermodynamically prone to chain-condensation. In the case of a radical coupling, chain-growth would be expected if a monomer radical was substantially more stable than a radical located on a polymer chain. While we can say that benzylic radicals are generally more stable than acetyl radicals, bond dissociation energies for the specific monomers and polymers (or dimers) would have to be determined experimentally or computationally and then compared.<sup>25,26</sup> Alternatively, if the ionic pathway was responsible for the chain-growth observed, it could stem from properties of the nucleophile or electrophile. If the dimer (or oligomer) was substantially more electrophilic than its monomer, it would be more prone towards attack by anionic species, which would lead to a relative activation. Conversely, if an activated anionic dimer was substantially more nucleophilic than activated monomer, a similar, though reversed, explanation of activation could be made. Again, testing of the hypothesis is made difficult due to the highly reactive nature of the intermediates, though perhaps carefully performed test reactions or computational calculations could probe whether chain-condensation is seen due to the thermodynamics of the coupling step.

### 4.3 Conclusions

We have demonstrated that the polymerization of carbyne precursors follow either a chain- or step-growth mechanisms based on the choice of monomer. Interestingly, the difference in mechanism aligns with the dichotomy seen in the structure of the polymer backbone. The carbonyl-containing monomers were found to polymerize primarily in a step-growth manner and afforded unsaturated, linear polymers. In contrast, the reductive C1 polymerization of arylated monomers afforded branched polymers and proceeded in a manner that was consistent with a chain-growth process. Additionally, it was found that while naphthalene increased the reaction rates, it did not fundamentally alter the polymerization mechanism.

The cause for these mechanistic differences likely arises due to the activation or deactivation of structural units as they are incorporated into the polymer, in a manner similar to change of substituent chain-condensation polymerizations. This likely occurs due to electronic and steric differences in the structural unit when the C-Cl bond of a monomer is converted into a C-C bond in the polymer. Electrochemical analysis revealed this activation is not from the initial reduction step but is likely caused by differences in the active radical or anionic intermediates. Further experimental or computational studies to better understand the exact source of the activation causing chain-growth could lead to further enhancement of the effect, and potentially lead to the controlled polymerization of poly(carbyne)s.

## 4.4 Experimental

*General Considerations.* All solvents were dried using a Vac Atmospheres solvent purification system. Monomer syntheses were performed under an atmosphere of nitrogen using standard Schlenk techniques unless otherwise noted. Since lithium nitride can form when lithium is exposed to nitrogen, the polymerization reactions were set up under an atmosphere of argon and run in sealed vials. All reagents were purchased from commercial sources and used as received unless otherwise noted.  $\alpha,\alpha,\alpha$ -trichlorotoluene was purchased from Alfa Aesar. Solution-state  $^1\text{H}$  and  $^{13}\text{C}$  NMR spectra were recorded at room temperature on a Bruker Avance III HD spectrometer operating at 400 MHz for  $^1\text{H}$ , in  $\text{CDCl}_3$  (internal standard: 7.26 ppm,  $^1\text{H}$ ; 77.16 ppm,  $^{13}\text{C}$ ),  $\text{CD}_2\text{Cl}_2$  (internal standard: 5.32 ppm,  $^1\text{H}$ ; 53.84 ppm,  $^{13}\text{C}$ ) or  $\text{THF}-d_8$  (internal standard: 3.58 ppm,  $^1\text{H}$ ; 67.21 ppm,  $^{13}\text{C}$ ). Splitting patterns are denoted as follows: br, broad; s, singlet; d, doublet; t, triplet; q, quartet; m, multiplet. Infrared spectra were collected either by attenuated total reflectance (ATR) on an Agilent Cary-630 spectrometer using a germanium crystal for liquid samples or via transmission through a KBr pellet on a Perkin-Elmer Frontier spectrometer for solid samples. Gas chromatography was performed on an Agilent Technologies 6850 system fitted with an FID detector using *n*-dodecane as an internal reference. Method details: 30 m, 0.32 mm ID, 0.25  $\mu\text{m}$  coating HP-1 column, 100 : 1 split ratio, 1.5 mL  $\text{min}^{-1}$  flow of He, 100  $^\circ\text{C}$  for 1.5 min, ramp to 200  $^\circ\text{C}$  at 20  $^\circ\text{C min}^{-1}$ . Cyclic voltammetry was performed on 10 mg of the compound in a 0.01 M TBAF (tetra-*n*-butylammonium fluoride) solution in DMF. A 1.6 mm platinum disk working electrode and non-aqueous  $\text{Ag}/\text{Ag}^+$  (acetonitrile) reference electrode were used, with voltages being referenced to a saturated calomel electrode (SCE) by shifting  $\text{Fc}/\text{Fc}^+$ .

*n-Pentyl Trichloroacetate.* A dry 250 mL flask was charged with 100 mL of anhydrous  $\text{CH}_2\text{Cl}_2$  and 4.176 g (47.4 mmol) of 1-pentanol. The flask was cooled to 0  $^\circ\text{C}$  and then charged with 10.306 g (54.7 mmol) of trichloroacetyl chloride. After adding 4 mL of pyridine in a dropwise manner to the flask, the resulting mixture was slowly warmed to room temperature and stirred overnight. The mixture was then washed with 100 mL of an aqueous solution of HCl (10%) followed by 100 mL of brine before being dried over  $\text{MgSO}_4$ . After filtration, the solvent was evaporated to afford 10.096 g (91% yield) of the desired compound as a straw-colored liquid.  $^1\text{H}$  NMR (400 MHz,  $\text{CDCl}_3$ ):  $\delta$  4.32 (t, 2H), 1.73 (m, 2H), 1.34 (m, 4H), 0.88 (t, 3H).  $^{13}\text{C}$  NMR (100 MHz,  $\text{CDCl}_3$ ):  $\delta$  161.86, 90.00, 69.43, 27.84, 27.67, 22.10, 13.80. FT-IR (Ge-ATR): 2960, 2932, 2863, 1763, 1457, 1379, 1236, 1042, 980, 885, 827, 751, 680  $\text{cm}^{-1}$ .

*Monomer Consumption Analyses.* A total of eight 30 mL vials equipped with glass-coated stir bars were each charged with 4 mmol of monomer, 4 mmol of *n*-dodecane, 4 mL of anhydrous THF, and in some cases 1 mmol of naphthalene. Seven of the vials were charged with 13 mg (2 mmol) of lithium. After 5

min, additional lithium (13 mg) was added to six of the vials. This process was repeated every 5 minutes until samples were created with lithium to monomer molar ratios of 0.5, 1.0, 1.5, 2.0, 2.5, 3.0, and 3.5. Other reaction conditions and work-up procedures are described above. Aliquots (50  $\mu$ L) were withdrawn from the vials, diluted with a 4:1 (v/v) mixture of THF and methanol (1 mL) and then analyzed by gas chromatography (GC). Monomer consumption was determined by comparing the area of the GC signal assigned to the monomer to that of an internal standard (*n*-dodecane). Each analysis was performed in triplicate.

*Kinetics Analyses.* Under an atmosphere of argon, 5 mL of anhydrous THF, 5 mmol of *n*-dodecane, and 208.2 mg (30 mmol) of lithium were added to a 30 mL vial equipped with a glass-coated stir bar. In some cases, 160.2 mg (1.25 mmol) of naphthalene was added. The vial was sealed and 5 mmol of monomer was added dropwise via syringe before heating the resulting mixture to 70  $^{\circ}$ C. After 1 h, an aliquot (50  $\mu$ L) was withdrawn from the reaction mixture, diluted with a 4:1 (v/v) mixture of THF and methanol (1 mL) and then analyzed by gas chromatography (GC) as described above.

*1,1,2,2-tetrachloro-1,2-diphenylethane.* 2 g (10 mmol) of  $\alpha,\alpha,\alpha$ -trichlorotoluene was added to a dry 500 mL flask with 300 mL of acetonitrile followed by 2.5 g (20 mmol) of  $\text{FeCl}_2$ . The reaction was run for 2 hours at R.T. before the solvent was removed under vacuum. Extraction of the desired compound into ethyl acetate followed by removal of the solvent under vacuum and subsequent running on a column using hexane as an eluent led to isolating the target compound in a 50% yield.  $^1\text{H}$  NMR (400 MHz,  $\text{CDCl}_3$ ):  $\delta$  7.43 (b, 2H), 7.35 (m, 1H), 7.22 (2, 2H).  $^{13}\text{C}$  NMR (100 MHz,  $\text{CDCl}_3$ ):  $\delta$  130.80, 129.84, 126.64. FT-IR (Ge-ATR):  $\text{cm}^{-1}$ .

*Dimethyl 2,2,3,3-tetrachlorosuccinate (mixture with methyl chloromethyl 2,2,3,3-tetrachlorosuccinate).* 50 mL of chloroform and 1.7 g (12 mmol) of dimethyl acetylenedicarboxylate was added to a 3 neck round bottom flask. 300 mmol of  $\text{Cl}_2$ , generated through the reaction of  $\text{Ca}(\text{ClO})_2$  and HCl were bubbled through the reaction at room temperature. After chlorine addition was completed, the reaction was allowed to react overnight before being washed with sodium thiosulfate and brine and removal of solvent under vacuum. This produced 72% and 12% yields of the dimethyl and methyl chloromethyl esters, respectively, which were subsequently used without further purification.  $^1\text{H}$  NMR (400 MHz,  $\text{CDCl}_3$ ):  $\delta$  5.85 (s, 2H), 3.95 (s, 3H), 3.94 (s, 6H).  $^{13}\text{C}$  NMR (100 MHz,  $\text{CDCl}_3$ ):  $\delta$  163.18, 163.00, 161.03, 87.38, 86.97, 86.87, 71.25, 55.39, 55.29. FT-IR (Ge-ATR):  $\text{cm}^{-1}$ .

*Dipentyl 2,2,3,3-tetrachlorosuccinate.* 3.4 g of the diester mixture was added to 24 mL of IPA and cooled to -10  $^{\circ}$ C before 24 mL of 1.5 M LiOH in water was added with stirring. The mixture was allowed to react for 15 minutes at the lowered temperature before 20 mL of 10% HCl was added. The mixture was extracted with 50 mL of DCM two times before the organic layer was dried with  $\text{MgSO}_4$  and solvent was removed. The isolated product (4.7 mmol) was added to a 50 mL Schlenk flask with 2 g (9.5 mmol)

of  $\text{PCl}_5$ . The flask was fitted with a reflux condenser and a  $\text{N}_2$  filled balloon before it was heated to  $165^\circ\text{C}$  overnight. The flask was subsequently cooled to room temperature before 12.5 mL of DCM, .5 mL of pyridine, and 3.418 g of 1-pentanol were added and allowed to react overnight. The reaction was worked up in a manner similar to that used in the synthesis of pentyl trichloroacetate to give a 42% yield of the desired product.  $^1\text{H}$  NMR (400 MHz,  $\text{CDCl}_3$ ):  $\delta$  4.31 (t, 4H), 1.74 (m, 4H), 1.37 (m, 8H), 0.92 (t, 6H).  $^{13}\text{C}$  NMR (100 MHz,  $\text{CDCl}_3$ ):  $\delta$  162.47, 87.60, 68.93, 27.81, 27.78, 22.13, 13.86. FT-IR (Ge-ATR):  $\text{cm}^{-1}$ .

## 4.5 Additional Data

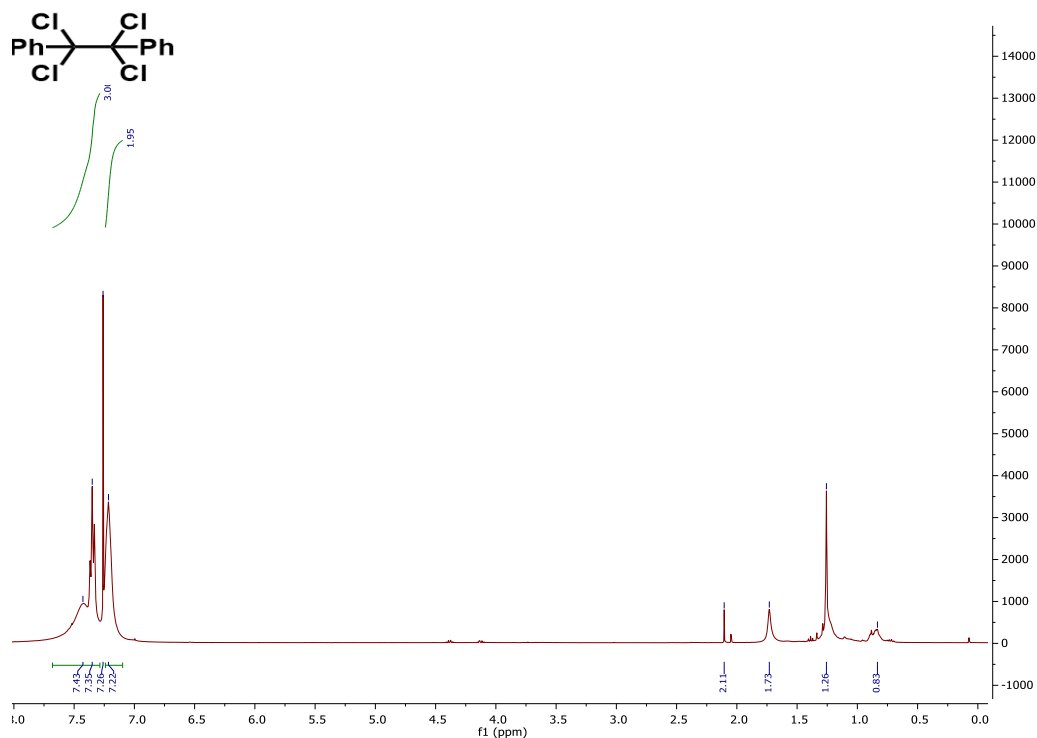


**Figure S1.** <sup>1</sup>H NMR spectrum of 1,1,2,2-tetrachloro-1,2-diphenylethane (400 MHz, 298 K, CDCl<sub>3</sub>).

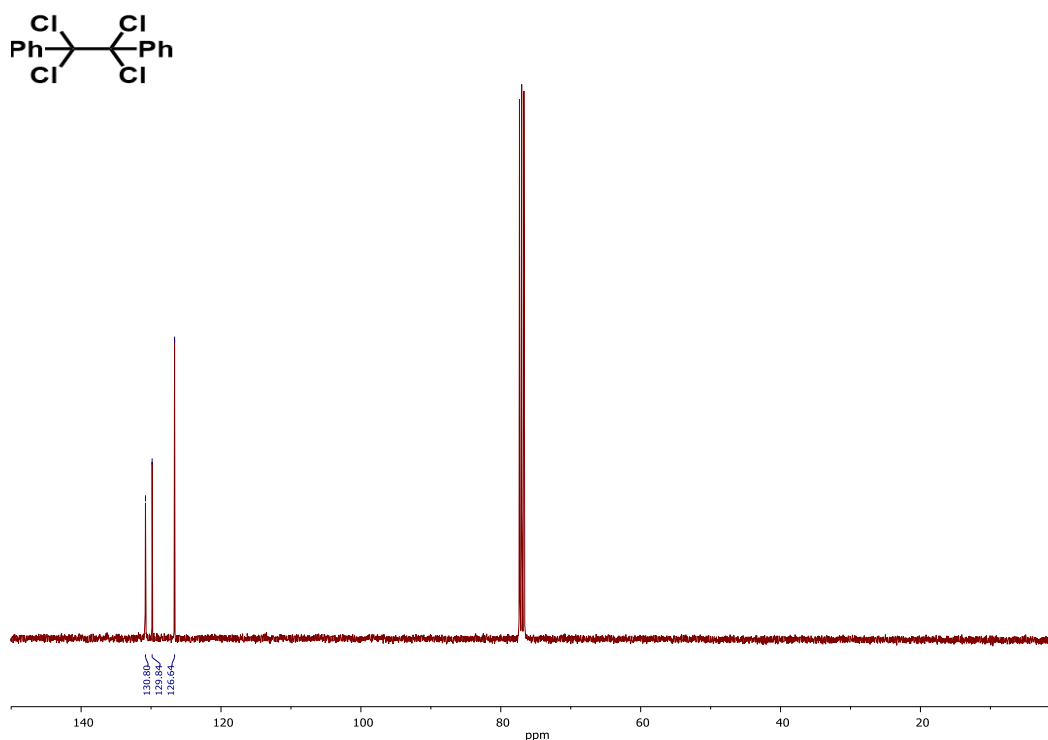


**Figure S2.** <sup>13</sup>C NMR spectrum of 1,1,2,2-tetrachloro-1,2-diphenylethane (100 MHz, 298 K, CDCl<sub>3</sub>).

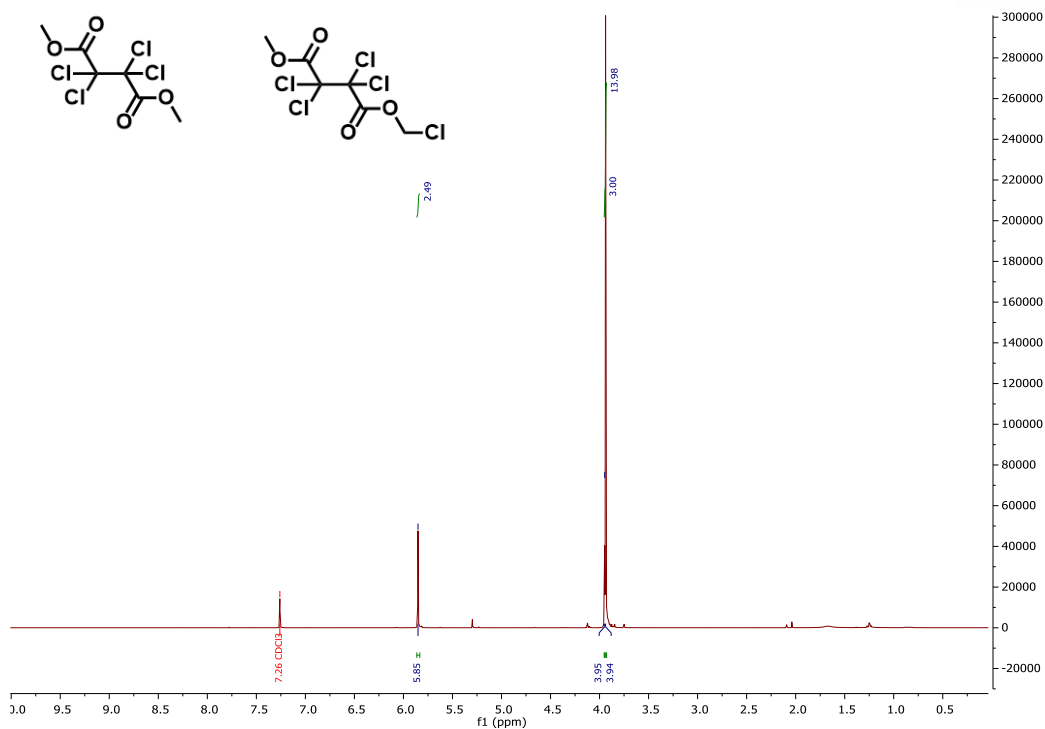


**Figure S3.**  $^1\text{H}$  NMR spectrum of Dimethyl 2,2,3,3-tetrachlorosuccinate (400 MHz, 298 K,  $\text{CDCl}_3$ ).

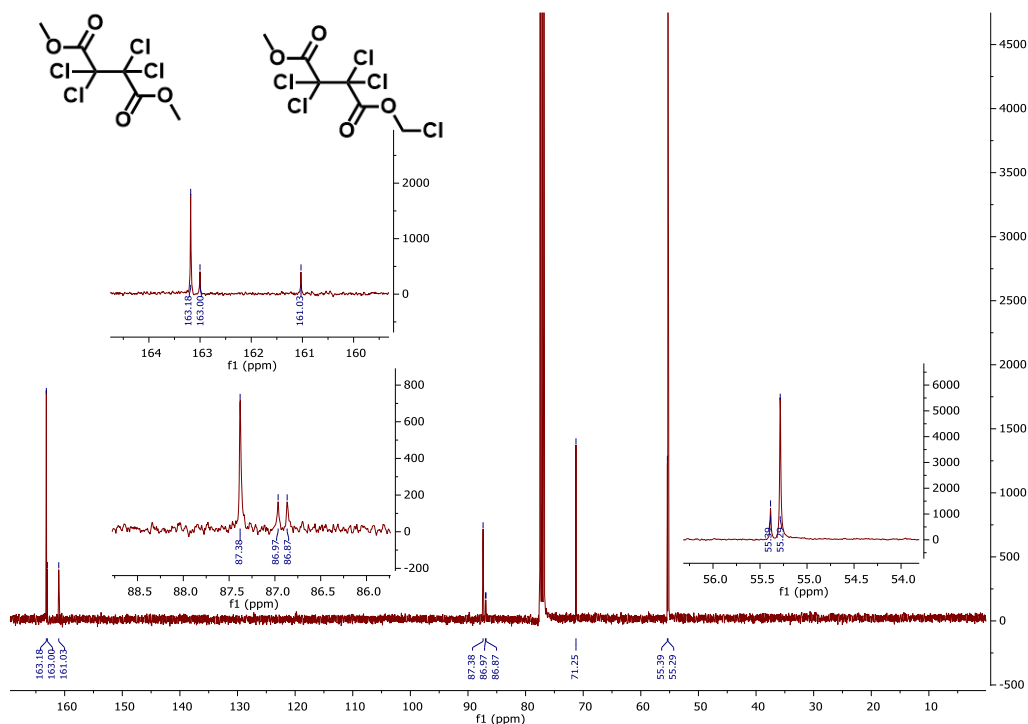


**Figure S4.**  $^{13}\text{C}$  NMR spectrum of Dimethyl 2,2,3,3-tetrachlorosuccinate (100 MHz, 298 K,  $\text{CDCl}_3$ ).



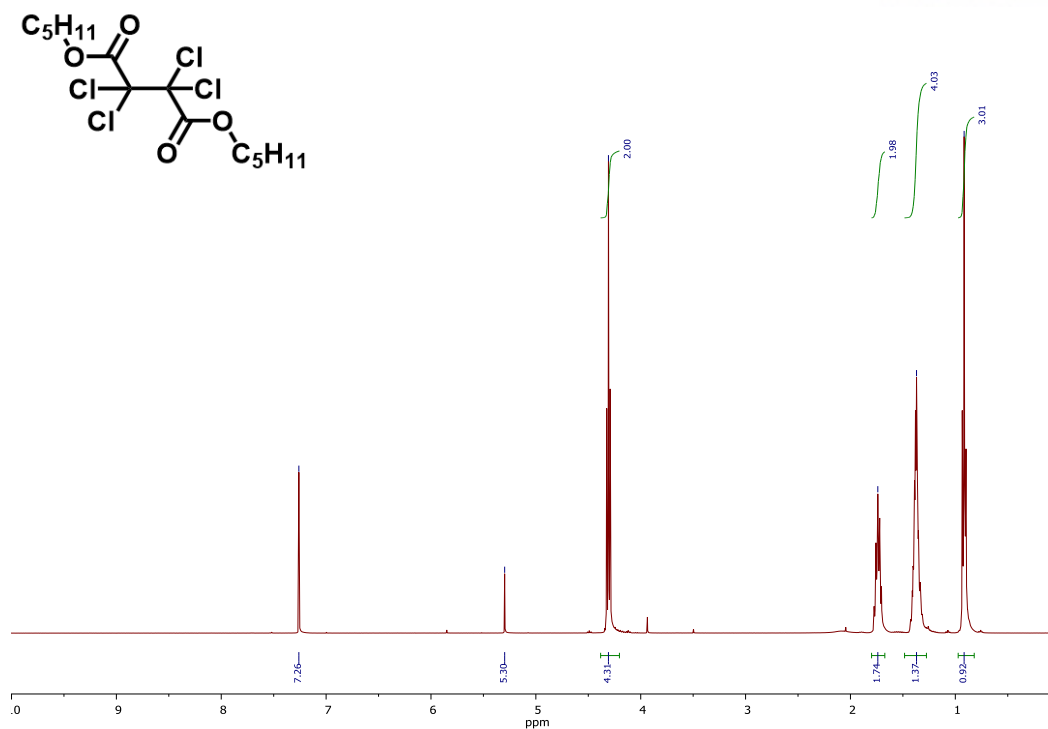


**Figure S5.** <sup>1</sup>H NMR spectrum of Dipentyl 2,2,3,3-tetrachlorosuccinate (400 MHz, 298 K, CDCl<sub>3</sub>).

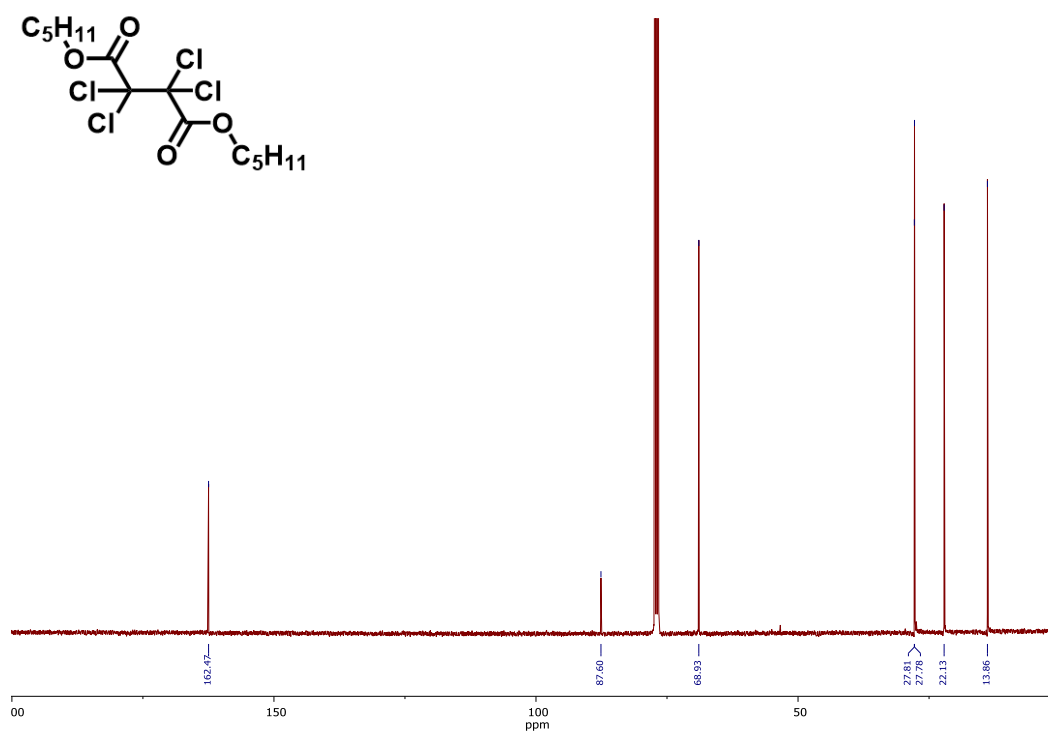


**Figure S6.** <sup>13</sup>C NMR spectrum of Dipentyl 2,2,3,3-tetrachlorosuccinate (100 MHz, 298 K, CDCl<sub>3</sub>).

## 4.6 References

1. Here, bifunctional mean "containing two functional groups," as opposed to "containing two different functional groups" which is sometimes, but not always the case.
2. Flory, P. J., Principles of Polymer Chemistry. Ithaca : Cornell University Press: Ithaca, 1953; p 319.
3. Bielawski, C. W.; Grubbs, R. H., Living ring-opening metathesis polymerization. *Prog. Polym. Sci.* **2007**, *32* (1), 1-29.
4. Dechy-Cabaret, O.; Martin-Vaca, B.; Bourissou, D., Controlled Ring-Opening Polymerization of Lactide and Glycolide. *Chem. Rev.* **2004**, *104* (12), 6147-6176.
5. Szwarc, M., 'Living' Polymers. *Nature* **1956**, *178* (4543), 1168-1169.
6. Chu, J.-H.; Xu, X.-H.; Kang, S.-M.; Liu, N.; Wu, Z.-Q., Fast Living Polymerization and Helix-Sense-Selective Polymerization of Diazoacetates Using Air-Stable Palladium(II) Catalysts. *J. Am. Chem. Soc.* **2018**, *140* (50), 17773-17781.
7. Lee, J.; Shin, S.; Choi, T.-L., Fast Living Polymerization of Challenging Aryl Isocyanides Using an Air-Stable Bisphosphine-Chelated Nickel(II) Initiator. *Macromolecules* **2018**, *51* (19), 7800-7806.
8. Kreutzer, J.; Yagci, Y., Metal Free Reversible-Deactivation Radical Polymerizations: Advances, Challenges, and Opportunities. *Polymers* **2018**, *10* (1).
9. Nicolas, J.; Guillaneuf, Y.; Lefay, C.; Bertin, D.; Gimes, D.; Charleux, B., Nitroxide-mediated polymerization. *Prog. Polym. Sci.* **2013**, *38* (1), 63-235.
10. Hawker, C. J.; Barclay, G. G.; Dao, J., Radical Crossover in Nitroxide Mediated "Living" Free Radical Polymerizations. *J. Am. Chem. Soc.* **1996**, *118* (46), 11467-11471.
11. Matyjaszewski, K., Atom Transfer Radical Polymerization (ATRP): Current Status and Future Perspectives. *Macromolecules* **2012**, *45* (10), 4015-4039.
12. Moad, G.; Rizzardo, E.; Thang, S. H., Radical addition-fragmentation chemistry in polymer synthesis. *Polymer* **2008**, *49* (5), 1079-1131.
13. Perrier, S., 50th Anniversary Perspective: RAFT Polymerization—A User Guide. *Macromolecules* **2017**, *50* (19), 7433-7447.

14. Yokozawa, T.; Yokoyama, A., Chain-Growth Condensation Polymerization for the Synthesis of Well-Defined Condensation Polymers and  $\pi$ -Conjugated Polymers. *Chem. Rev.* **2009**, *109* (11), 5595-5619.
15. Yokozawa, T.; Ohta, Y., Chain-Growth Condensation Polymerization. In *Encyclopedia of Polymeric Nanomaterials*, Kobayashi, S.; Müllen, K., Eds. Springer Berlin Heidelberg: Berlin, Heidelberg, 2021; pp 1-10.
16. Yokoyama, A.; Miyakoshi, R.; Yokozawa, T., Chain-Growth Polymerization for Poly(3-hexylthiophene) with a Defined Molecular Weight and a Low Polydispersity. *Macromolecules* **2004**, *37* (4), 1169-1171.
17. Iovu, M. C.; Sheina, E. E.; Gil, R. R.; McCullough, R. D., Experimental Evidence for the Quasi-“Living” Nature of the Grignard Metathesis Method for the Synthesis of Regioregular Poly(3-alkylthiophenes). *Macromolecules* **2005**, *38* (21), 8649-8656.
18. Zhang, Y.; Tajima, K.; Hirota, K.; Hashimoto, K., Synthesis of All-Conjugated Diblock Copolymers by Quasi-Living Polymerization and Observation of Their Microphase Separation. *J. Am. Chem. Soc.* **2008**, *130* (25), 7812-7813.
19. Lenz, R. W.; Handlovits, C. E.; Smith, H. A., Phenylene sulfide polymers. III. The synthesis of linear polyphenylene sulfide. *Journal of Polymer Science* **1962**, *58* (166), 351-367.
20. Yokozawa, T.; Asai, T.; Sugi, R.; Ishigooka, S.; Hiraoka, S., Chain-Growth Polycondensation for Nonbiological Polyamides of Defined Architecture. *J. Am. Chem. Soc.* **2000**, *122* (34), 8313-8314.
21. Flory, P. J., Kinetics of Polyesterification: A Study of the Effects of Molecular Weight and Viscosity on Reaction Rate. *J. Am. Chem. Soc.* **1939**, *61* (12), 3334-3340.
22. Cornia, A.; Folli, U.; Sbardellati, S.; Taddei, F., Electron transfer in the reactions of organic trichloromethyl derivatives with iron(II) chloride. *Journal of the Chemical Society, Perkin Transactions 2* **1993**, (10), 1847-1853.
23. Folli, U.; Goldoni, F.; Iarossi, D.; Sbardellati, S.; Taddei, F., Selectivity towards hydrodehalogenation and dehalo-coupling in the reduction of trichloromethyl derivatives with iron(II) chloride. *Journal of the Chemical Society, Perkin Transactions 2* **1995**, (5), 1017-1020.
24. Jones, R. G.; Holder, S. J., High-yield controlled syntheses of polysilanes by the Wurtz-type reductive coupling reaction. *Polym. Int.* **2005**, *55* (7), 711-718.
25. Luo, Y.-R.; Cheng, J.-P., Bond Dissociation Energies. In *CRC handbook of chemistry and physics : a ready-reference book of chemical and physical data*, Haynes, W. M.; Lide, D. R.; Bruno, T. J., Eds. CRC Press: Boca Raton, Florida, 2013.
26. Based on the bond dissociation energies reported (ref. 22) for H-CH<sub>2</sub>C<sub>6</sub>H<sub>5</sub> (375.5 kcal/mol) and H-CH<sub>2</sub>C(O)OCH<sub>2</sub>CH<sub>3</sub> (401.7 kcal/mol).

# Chapter 5. Conclusions and Future Outlooks

C1 polymerizations provide a unique synthetic pathway towards persubstituted polymers, which can possess enhanced physicochemical properties over their conventional C2 analogs. Much of the work to date on C1 polymers has focused on using carbene precursors as monomer sources, and in some cases, these polymerizations have been shown to be living or controlled. In comparison, the field of poly(carbyne)s is relatively unexplored, with only a handful of monomers being used in their synthesis. Additionally, no in-depth study of the polymerization mechanism of poly(carbyne)s had previously been undertaken. We have addressed both of these deficiencies by greatly expanding the scope of known carbyne precursors which polymerize under reductive conditions as well as conducting the first investigation into the polymerization mechanism of some of these monomers. Interestingly, we have found both the polymer structure and polymerization mechanism to be dependent on the monomer used. Of particular interest are the polymers which form via a chain-condensation polymerization. Future work should be directed at understanding the cause of activation in these chain-condensation polymerizations and subsequently utilizing new monomers and reductants to achieve a controlled or living poly(carbyne) polymerization.

Initial experimentation was directed at optimizing the Li promoted synthesis of poly(phenyl carbyne) and subsequent characterization of the polymer. Maximum molecular weights and yields were seen when 6 Eq. (relative to monomer) of Li were added to a 1 M solution of trichlorotoluene. Heating of the solution at 70 °C for 12 hours led to the formation of a polymer with a number average molecular weight of 4.1 kDa ( $\bar{D} = 2.8$ ) which was isolated in 85% yield. Structural analysis of the poly(phenyl carbyne) through NMR and IR spectroscopy showed strong evidence that it had a branched structure and contained only  $sp^3$  hybridized carbons along the backbone. This is consistent with the structural characterization of poly(phenyl carbyne) as well as other poly(carbyne)s from recent literature.

With a firm grasp on the experimental methods used in reductive poly(carbyne) synthesis and characterization, a number of new potential monomers were envisioned and prepared. Carbyne precursors containing fluorine as well as other non-halogen leaving groups were investigated, and while germinal trifunctionalized molecules such as methyl orthobenzoate or trifluorotoluene readily polymerized, molecules with  $sp$  and  $sp^2$  carbons in a similarly electron deficient state did not undergo reductive polymerization. Monomers containing several polar side chains were also investigated as poly(carbyne) precursors. The polar monomers, including those containing an ester functionality, were successfully polymerized into the first poly(carbyne)s with carbonyl-containing side chains.

Surprisingly, these polar poly(carbyne)s had a linear structure, possessing alternating single and double bonds along the backbone, in contrast to the reported branched structure in all other poly(carbyne)s.

To better understand why a dichotomy was seen in polymer structure based on monomer choice, a number of experiments were performed to investigate the polymerization mechanism. According to monomer consumption studies, polar poly(carbyne)s, such as those made from pentyl trichloroacetate (PTCA), undergo step-growth polymerization while poly(carbynes) containing phenyl side chains, such as those made from trichlorotoluene (TCT), undergo a chain-growth polymerization. While the addition of an electron transfer agent, such as naphthalene, was found to catalyze the reaction and increase molecular weights and yields of many poly(carbyne)s, it was not found to alter the underlying polymerization mechanism. When compared to theoretical predictions of monomer consumption in a step-growth polymerization, clear deviations are seen in both the polymerization of TCT and PTCA. This is likely caused by the increased (TCT) or decreased (PTCA) reactivity of growing polymer chains caused by the conversion of C-Cl bonds in the monomer to C-C bonds after a coupling reaction. Electrochemical analysis suggests that this activation does not stem from the initial reduction step, and therefore must come from the bond formation step, which can potentially occur through either radical coupling or nucleophilic substitution.

Further investigation into the polymerization mechanism of carbyne precursors is essential to the maturation of the field. Currently, the reductive polymerization of carbyne precursors relies on harsh conditions and produces relatively low molecular weight polymers in varying yields. The discovery of chain-condensation character in the polymerization of trichlorotoluene suggests that perhaps many of these issues could be remedied, as several living and controlled polymerizations exist which take advantage of similar change of substituent effects. The first step to achieving this goal, however, is obtaining a better understanding of the fundamental step leading to the activation (or even deactivation) of poly(carbyne) chains versus their monomers. Test reactions as well as computational studies could likely elucidate the exact thermodynamic, kinetic, or steric reason activation is seen in some cases. From there, further chemistry can be designed to enhance this activation. This can happen through the use of specifically chosen monomers, either with entirely new pendant groups or those altered electronically (e.g. substituted aryl rings), which further amplify this activating effect. Alternatively, different potentially milder reducing agents (or even electrochemical methods) could be used which might selectively react with the activated chain ends, leading to a more pronounced chain-condensation. When some degree of control is seen in the polymerization, likely resulting in substantially increased molecular weights, focus can be shifted to the preparation of poly(carbyne)s that possess useful properties. Incorporation of various functionalities (particularly as ester side chains) into well-

controlled poly(carbyne)s could lead to densely functionalized persubstituted polymers which contain different polymer architectures than other C1 polymers generated from carbene precursors.

Overall, we have made considerable contributions to the field of poly(carbyne)s as well as C1 polymerizations in general. This work has more than doubled the number of reported monomers used in the reductive synthesis of poly(carbyne)s and provided a groundwork to prepare poly(carbyne)s from an even larger number of other monomers. These include monomers with ester side chains, which in addition to forming the first polar poly(carbyne)s, also provide a potent handle for further functionalization of the polymers. We have also reported the first mechanistic investigation of the reductive polymerization of carbyne precursors, and shown that certain monomers undergo a chain-condensation polymerization, presumably due to change of substituent effects. If this change of substituent effects can be enhanced and controlled, then it is likely that a living polymerization of carbyne precursors could be developed, leading to a new source of high quality, unique, persubstituted polymers.

# Acknowledgements

I want to take this space to extend my deepest thanks to family, friends, and colleagues, both in Korea, the U.S., and abroad. Without your constant support, I would not have made it to graduation, let alone to Korea.

Firstly, I would like to thank my wife, Jiyoung Lee. Since we've been together, you've always been there for me, to enjoy the good times with me and help me through tough times. My life has been so much better since you've been in it these last years, and I love you so much. It's so strange to think that I've been in graduate school throughout our whole time together, but I am so excited to see what the future will hold for us.

Secondly, I'd like to thank my family for always supporting me and my interests, especially my parents, who have always fostered my love for science and chemistry. Who would have thought that watching Beakman's World and mixing various things from the spice cabinet would lead to a lifelong passion and career? It's been difficult being so far apart for these last 6 years, and I've truly cherished every visit or conversation we've been able to have. I love you both and can't wait to be closer to you guys in the states.

I would also like to acknowledge all of my friends, graduate school has been a lot of hard work, and without such a great group of people to relax and socialize with, I don't think it would have been possible to make it here today. I'd specifically like to thank Eric Larsen, Yeonkyeong Ryu, Dr. Guillermo Ahumada, Dr. Benjamin Cuning, and Kyeongnam Kang for making my time in Korea particularly pleasant.

I'd like to thank the Center for Multidimensional Carbon Materials, UNIST, and IBS for providing me the amazing opportunity and financial support to obtain my PhD. I've greatly enjoyed conducting research here and being able to utilize such state of the art facilities. While the facilities are amazing, my coworkers in research, administrative, and support roles are what have made working here truly special. I would like to specifically acknowledge Dr. Karel Goossens, Dr. Prakash Sultane, Dr. Guillermo Ahumada, Dr. Jinwon Seo, and Hyeonmyeong Seo for their academic support.

Finally, I would like to express my deepest gratitude to Dr. Christopher Bielawski. If it weren't for your excellent teaching and passion for chemistry during my undergraduate polymer chemistry class, I would certainly not be here today. Since joining the lab, I have grown so much as a scientist thanks to your mentorship, and I'm so thankful for the knowledge you have shared.

